U.PORTO
FACULDADE DE CIÊNCIAS
UNIVERSIDADE DO PORTO

MSc

2.º
CICLO

FCUP
2021

U.PORTO

Cell wall rhamnosylation: an original target for innovative antimicrobial strategies against *Listeria monocytogenes*

Rui Pedro da Silva Ferreira Macedo

FC

U.PORTO
FACULDADE DE CIÊNCIAS
UNIVERSIDADE DO PORTO

Cell wall rhamnosylation: an original target for innovative antimicrobial strategies against *Listeria monocytogenes*

Rui Pedro da Silva Ferreira Macedo

Dissertação de Mestrado apresentada à
Faculdade de Ciências da Universidade do Porto em
Aplicações em Biotecnologia e Biologia Sintética

2021

MSc

2.º CICLO

Cell wall rhamnosylation: an original target for innovative antimicrobial strategies against *Listeria monocytogenes*

Rui Pedro da Silva Ferreira Macedo
Mestrado em Aplicações em Biotecnologia e Biologia Sintética
Departamento de Biologia e Departamento de Química e Bioquímica
2021

Orientador
Didier Cabanes, Investigador Principal, i3S - Instituto de Investigação e Inovação em Saúde

Coorientador
Fernando Tavares, Professor Associado, Faculdade de Ciências da Universidade do Porto

U.PORTO

FACULDADE DE CIÊNCIAS
UNIVERSIDADE DO PORTO

Todas as correções determinadas pelo júri, e só essas, foram efetuadas.

O Presidente do Júri,

Porto, _____/_____/_____

Agradecimentos

A presente dissertação de mestrado não poderia ter sido possível sem o valioso apoio de várias pessoas. Assim sendo, gostaria de agradecer a todos aqueles que, de forma direta ou indireta, contribuíram para a realização da mesma.

Em primeiro lugar, gostaria de agradecer ao meu orientador, Doutor Didier Cabanes, pela oportunidade que me concedeu em desenvolver a minha dissertação de mestrado na sua equipa de investigação. Quero agradecer o voto de confiança, a disponibilidade, os ensinamentos e a sabedoria que me transmitiu.

Ao Doutor Ricardo Monteiro, deixo o meu mais sincero obrigado por toda a ajuda, paciência e orientação prestada para que este trabalho se realizasse.

À Doutora Sandra Sousa, por todas as críticas construtivas e preciosos conhecimentos que me transmitiu.

A todos os meus colegas de laboratório (Alexandra, Ângela, Catarina, Chiara, Diana, Joana, Lua, Mariana, Rita e Sara), pelo ambiente de trabalho fantástico que me proporcionaram. Um especial obrigado à Diana Meireles, não só por ter estado sempre disponível para me ajudar, mas também pela amizade e companheirismo. Um especial obrigado também à Joana pela ajuda prestada sempre que necessitei.

Aos meus colegas de faculdade, Rui, Inês, Beatriz Cruz, Beatriz Nogueira e Raquel por todo o incentivo e por me terem dado os melhores anos da minha vida.

Ao André Rodrigues, por ser o melhor amigo que podia ter. Obrigado por todo o apoio, motivação e encorajamento ao longo destes anos.

Por fim, à minha mãe, por ser a razão de tudo isto ser possível. Obrigado pelo amor incondicional, apoio, e sacrifício que me permitiu levar avante este marco na minha formação académica e pessoal.

Resumo

A descoberta de substâncias antimicrobianas representa um dos avanços mais importantes na saúde pública. Infelizmente, o uso massivo destes compostos e a falta de desenvolvimento de novos medicamentos pela indústria farmacêutica têm promovido a seleção de patógenos resistentes. A identificação de novos antibióticos permanece assim essencial. No entanto, o uso de antibióticos convencionais para matar ou inibir o crescimento de estirpes sensíveis induz uma alta pressão para a seleção de mecanismos de resistência aos antibióticos. Uma estratégia alternativa é desarmar os patógenos, utilizando fármacos que atuem diretamente nos fatores de virulência, sem matar as bactérias ou inibir o seu crescimento.

Listeria monocytogenes é um importante patógeno Gram+ de origem alimentar, responsável pela maior taxa de pacientes hospitalizados e pelo maior número de mortes na Europa. A parede celular dos microrganismos Gram+ é densamente decorada com glicopolímeros, conhecidos como os ácidos teicóicos de parede (WTAs), que apresentam substituintes não-essenciais de açúcar. A ausência de ramnose nos WTAs de *L. monocytogenes* mostrou reduzir a ancoragem de fatores de virulência à superfície da bactéria e aumentar a sensibilidade da mesma a peptídeos antimicrobianos e antibióticos, sem afetar o crescimento bacteriano. A ramnosilação da parede celular aparece, deste modo, como um novo alvo para o desenvolvimento de estratégias de antivirulência contra *L. monocytogenes*.

O objetivo deste trabalho foi procurar 1- novos compostos antimicrobianos contra *L. monocytogenes*, e 2- novos fármacos que inibam a presença de ramnose na superfície bacteriana como uma estratégia complementar para combater infeções provocadas por *L. monocytogenes*. Com este propósito, foi realizada uma Triagem de Alto Rendimento (HTS) para encontrar possíveis hits, confirmar através de experiências de dose-resposta os candidatos mais promissores e validar o uso desses fármacos em estudos *in vitro*.

O HTS implementado neste trabalho não permitiu a descoberta de compostos com ação contra a ramnosilação dos WTA. Contudo, fomos capazes de identificar com sucesso 2 compostos promissores (DC001 e DC002) com alta atividade antimicrobiana contra *L. monocytogenes*. Investigação adicional é agora necessária para demonstrar a atividade bactericida destes compostos contra *Listeria* intracelular *in vitro* e *in vivo*, bem como a sua capacidade de atuar contra outros patógenos bacterianos.

Palavras-chave: *Listeria monocytogenes*, Glicolisações dos WTA, Antimicrobianos, Triagem de Alto Rendimento, Descoberta de fármacos

Abstract

The discovery of antimicrobials represents one of the most important advances in public health. Unfortunately, the massive use of these compounds and the lack of new drug development by the pharmaceutical industry has promoted the selection of resistant pathogens. The identification of new antibiotics remains thus vital. However, the use of conventional antibiotics to kill or inhibit the growth of sensitive strains induces a high selection pressure for antibiotic resistance mechanisms. An alternative strategy is to disarm pathogens by directly targeting virulence factors using antivirulence drugs, without killing bacteria or halting their growth.

Listeria monocytogenes is a major foodborne Gram+ pathogen that accounts for the highest proportion of hospitalized cases and the highest number of deaths in Europe. The cell wall of Gram+ microorganisms is densely functionalized with glycopolymers, known as wall teichoic acids (WTAs), that display non-essential sugar substituents. The absence of rhamnose in the *L. monocytogenes* WTAs was shown to reduce virulence factor surface anchoring and to increase bacterial sensitivity to antimicrobial peptides and antibiotics, without affecting bacterial growth. The cell wall rhamnosylation appears thus as an original target for innovative anti-virulence strategies against *L. monocytogenes*.

The aim of this work was therefore to screen for 1- new antimicrobial compounds against *L. monocytogenes*, and 2- new drugs inhibiting the presence of rhamnose at the bacterial surface as a complementary strategy to fight *L. monocytogenes* infections. For this purpose, a High-Throughput Screening (HTS) was performed to find potentials hits, confirm by dose-response experiments the more promising candidates, and validate the use of these candidate drugs in *in vitro* studies.

The HTS here implemented did not allow the discovery of compounds with action against WTA rhamnosylation. Nonetheless, we were able to successfully identified 2 promising compounds (DC001 and DC002) with high antimicrobial activity against *L. monocytogenes*. Further investigation is now necessary to demonstrate the bactericidal activity of these compounds against intracellular *Listeria in vitro* and *in vivo*, as well as their capacity to act against other bacterial pathogens.

Keywords: *Listeria monocytogenes*, WTA glycosylations, Antimicrobials, High-Throughput Screening, Drug Discovery

Index

List of Tables

List of Figures

Abbreviation List

ActA	Actin assembly-inducing protein
Amp	Ampicillin
AMPs	Antimicrobial peptides
Arp2/3	Actin-related proteins 2 and 3
BHI	Brain heart infusion
c-Met	Tyrosine-protein kinase (receptor)
CC	Clonal complexes
CDCs	Cholesterol-dependent pore-forming cytolysins
CFUs	Colony forming units
CNS	Central nervous system
CRISPR-Cas9	Clustered regularly interspaced short palindromic repeats
CV	Column volumes
CWA	C-terminal cell wall-anchoring
DMEM	Dulbecco's modified Eagle medium
DMSO	Dimethyl sulfoxide
DNA	Deoxyribonucleic acid
Ecad	E-cadherin
FBS	Fetal bovine serum
GAGs	Glycosaminoglycans
GC	Guanine-cytosine content
gC1qR	Receptor for the globular component of complement c1q
GFP	Green fluorescent protein
GlcNAc	N-acetylglucosamine
Gram+	Gram-positive
GroP	1,3-L-α-glycerol-phosphate
GW	Glycine-tryptophan
HGF	Hepatocyte growth factor
Hpt	Hexose phosphate transporter
HTS	High-throughput screening
IMAC	Immobilized metal affinity chromatography
InlA	Internalin A
InlB	Internalin B
InlF	Internalin F
IPTG	Isopropyl β-D-1-thiogalactopyranoside

IR	Inter-repeat
kDa	Kilodalton
LAP	*Listeria* adhesion protein
LB	Lysogeny broth
LIPI-1	Pathogenicity island 1
LLO	Listeriolysin O
LRR	Leucine-rich repeats
LTAs	Lipoteichoic acids
MIC	Minimum inhibitory concentration
MLST	Multi locus sequence typing
MOI	Multiplicity of infection
MurNAc	N-acetylmuramic acid
nm	Nanometres
PBS	Phosphate buffer solution
PCR	Polymerase chain reaction
PGN	Peptidoglycan
PI	Propidium iodide
PI-PLC	Phosphatidylinositol-specific phospholipase C
PlcA	Phosphatidyl-inositolphospholipase
PlcB	Phosphatidyl-choline-phospholipase C
PrfA	Positive regulatory factor A
RboP	1,5-D-ribitol-phosphate
rRNA	Ribosomal ribonucleic acid
RybP	Nuclear host regulatory protein
SDS-PAGE	Sodium dodecyl sulfate polyacrylamide gel electrophoresis
Sec	General secretion system
SrtA	Sortase A
STs	Sequence types
TALENs	Transcription activator-like effector nucleases
TAs	Teichoic acids
WTA-rha	WTA rhamnosylation
WTAs	Wall teichoic acids

1. Introduction

1.1. Gram-positive pathogens

Gram-positive (Gram+) bacteria are among the most common causes of infection in humans, usually related to increasing clinical infections. This is predominantly due to their association with a varied spectrum of pathologies, extending from soft tissue and mild skin infections to life-threatening meningitis and sepsis. There are several drugs to treat these diseases, however the emergence of new infections and the acquisition of new virulence or antimicrobial resistance properties by microorganisms is a worrying public health problem and a major medical challenge nowadays. Consequently, it is essential to develop new antivirulence strategies to neutralize pathogens and enable the host's natural protections to combat infections. Understanding the molecular mechanisms behind the bacterial infection is of great scientific interest and offers crucial information for the development of novel therapeutic strategies.

This study focuses on the discovery of new compounds against *Listeria monocytogenes* (*L. monocytogenes*), the deadliest food-borne Gram+ pathogen. Our approach is based on a disarm/sensitize strategy that, without killing or inhibiting the growth of sensitive strains, renders *L. monocytogenes* less virulence and more susceptible to the natural host immunity.

1.2. *Listeria monocytogenes*

1.2.1. Historical overview and taxonomy

L. monocytogenes is an outstanding model organism to study new molecular facets of host-pathogen interactions and cell biology [1]. In 1926, E.G.D. Murray isolated Gram+ rods from rabbit blood and guinea pigs. At the time, he was unable to assign these pathogenic microorganisms to any recognized bacterial genus, thus naming these new agents *Bacterium monocytogenes* [2]. The next year, J. Harvey Pirie, in honor of Lord Joseph Lister, the father of antiseptic surgery, renamed it *Listerella hepatolytic*, after he isolated the same species from South Africa's rodent liver [3]. Yet, since the generic name *Listerella* had previously been used for protozoa, the International Committee for Systematic Bacteriology did not accept it. Therefore, in 1940, the organism was given its definitive name *Listeria monocytogenes* [4].

L. monocytogenes is widely acknowledged as a cause of several clinical syndromes such as bacteremia, gastroenteritis, endocarditis, pericarditis, central nervous system (CNS), and perinatal infections [5], but the infectious disease, listeriosis, caused by *L. monocytogenes* was only recognized as a foodborne human disease in 1981, when an austere outbreak of the illness happened in Canada [6-8].

This microorganism fits in the phylum Firmicutes, class Bacilli, order Bacillales, family Listeriaceae, and the genus *Listeria*. Presently, the *Listeria* genus is composed of 20 species, including *L. monocytogenes*, which is pathogenic for humans and animals, and *L. ivanovii*, an entirely animal pathogen. The remaining species are non-pathogenic and they survive in nature as saprophytes (*L. marthii, L. innocua*, *L. weihenstephanensis, L. welshimeri*, *L. grayi*, *L. seeligeri, L. fleichmannii*, *L. riparia*, *L. aquatica*, *L. newyorkensis*, *L. rocourtiae*, *L. floridensi*s, *L. thailandensis, L. grandensis*, *L. costaricensis, L. booriae*, *L. goaensis* and *L. cornellensis*) [9-12].

The genus can be divided into two groups, *Listeria sensu stricto* and *Listeria sensu lato*, being this separation based on shared genomic and phenotypic characteristics among species [11, 13]. The group *Listeria sensu stricto* contains the most studied and important species in the genus, *L. monocytogenes*.

The first complete genomes of *L. monocytogenes* EGD-e and *L. innocua* CLIP 11262 were published in 2001 and, in the next years, other *Listeria* species also had their genomes published [14]. The analysis of *Listeria* genomes demonstrated high stability of genome organization and robust conservation among the different species of *Listeria*, where *L. innocua*, a non-pathogenic, have evolved from *L. monocytogenes* ancestor, losing its virulence gene cluster [14].

Serotyping is the standard subtyping technique for analyzing *Listeria* phenotypic characteristics and is commonly used in the epidemiological surveillance of human and food isolates, as it is an effective diagnostic method [15-18]. *L. monocytogenes* is a highly heterogeneous species, separated into 13 serotypes because of their somatic (O) and flagellar (H) antigens: 1/2a, 1/2b, 1/2c, 3a, 3b, 3c, 4a, 4b, 4c, 4d, 4e, 5, 7 (Table 1) [15, 19]. Thanks to differences in their ecology, recombination rates, and genomic content, serotypes of *L. monocytogenes* are divided into four evolutionary lineages: I, II, III, and IV (Table 1) [20]. Lineages I and II are usually linked to human clinical cases of listeriosis, while lineages III and IV are uncommon and related to animals [19]. Serotyping has limited usefulness since there is a limited range of serotypes involved in the development of human listeriosis (where serotypes 1/2a, 1/2b, and 4b are responsible for about 95% of infections worldwide) and exists a small number of serotypes detected in edibles [21]. Consequently, ribotyping has been used routinely in the last few years to type various microorganisms, including *L. monocytogenes* [22].

Table 1 - Summary of *Listeria monocytogenes* lineages (adapted from [19]).

	***Listeria monocytogenes* lineages**			
	I[1]	**II[1]**	**III**	**IV**
Serotype[1]	1/2b[2], 3b, 3c, 4b[2]	1/2a[2], 1/2c[2], 3a	4a, 4b, 4c	4a, 4b, 4c

[1] Not all known serotypes present.
[2] Relevant lineages and serotypes in foodborne listeriosis infection.

The rising application of new and more complex genomic analyzes brought more knowledge about *L. monocytogenes* population structure [23, 24]. Using Multi Locus Sequence Typing (MLST) provided an understanding of the evolution of the species and acknowledged associations of subgroups to certain environment niches and clinical diseases [25]. MLST allowed as well the identification of dominant sequence types (STs) and clonal complexes (CC) in terms of sources and geography. It is known that exists a prevalence of CC1, CC2, CC3, CC4, and CC6 isolates in systemic disorders in individuals with neurological types of listeriosis [25, 26].

1.2.2. General features

L. monocytogenes is a small rod-shaped (0.5 x 1-2 μm) Gram+ bacterium usually found in chains or as single cells. It is a facultative anaerobic and facultative intracellular, catalase positive and oxidase negative pathogenic bacilli that is unable to form spores or capsule. *Listeria* is motile at 20-30 ºC thanks to the expression of peritrichous flagella, however it loses its motility at temperatures above 37 ºC, due to the transcriptional suppression of the flagellar assembly system [27-29].

Growth of the organism in culture medium is stimulated by the availability of glucose or other fermentable sugars, but the temperature and atmosphere at which it is cultivated also play a major role. This bacillus can survive in large shifts of temperature (<0 to 45º, with optimal growth at 30-37 ºC), osmotic pressure (up to 10% NaCl), and pH (4.3 to 9, optimal at 7) [30, 31]. This makes *L. monocytogenes* a ubiquitous microorganism especially capable to proliferate in refrigerated foods with high salinity and low humidity, and therefore challenging to remove by traditional food decontamination methods [32, 33].

The natural habitat of *L. monocytogenes* consists of soil surface rich in putrefying plant matter, nonetheless this pathogen can be found throughout the environment in soil, animal wastes, vegetation, food, and in numerous animal species and humans, evidencing its survival skills [34]. Since its inability to form spores, the high stress resistance of *L. monocytogenes* is frequently related to the formation of biofilms, increasing survival, and eventually promoting dissemination over a vast range of adverse environmental conditions [35].

Phenotypically, *L. monocytogenes* can be differentiated from other *Listeria* species by biochemical tests. It shows beta-hemolytic activity, a disability to reduce nitrate to nitrite, a positive catalase reaction, and a positive Vogues-Proskauer test [11]. Furthermore, *L. monocytogenes* cells have phosphatidylinositol-specific phospholipase C (PI-PLC) activity, with the capacity of fermenting α-methyl D-glucoside, D-arabitol, L-rhamnose, lactose, maltose, and sucrose [11, 36-39].

At the genomic level, the *Listeria* genome is conserved and very stable. Accordingly, the genome of *L. monocytogenes* and other *Listeria* species are usually similar, reflecting the strong phylogenetic closeness between listeriae. They consist of circular chromosomes, with low G+C content (average of 38%), sizes ranging from 2.8 to 3.0 Mbp, and encoding approximately 2900 open reading frames. A significant number of putative protein-encoding genes have also been found, both in *L. monocytogenes* (Figure 1, represented in red) and *L. innocuum* (Figure 1, represented in green), in particular encoding surface and secreted proteins, transcription regulators, and transporters [14].

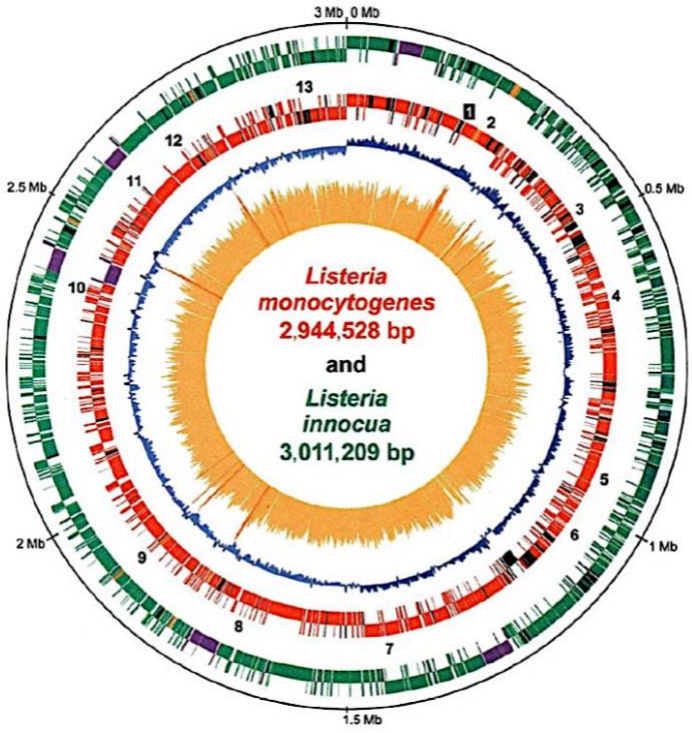

Figure 1 - Circular genome maps of *L. monocytogenes* EGD-e and *L. innocua* CLIP 11262. From the outside: Circles 1 and 2: *L. innocua* and *L. monocytogenes* genes on the plus and minus strands, respectively. Color code: green - *L. innocua* genes; red - *L. monocytogenes* genes; black - specific genes of *L. monocytogenes* or *L. innocua*; orange - rRNA operons; purple - prophages. Numbers presented on the second circle designate the position of known virulence genes. Circle 3: G/C bias (G+C/G-C) of *L. monocytogenes*. Circle 4: G+C content of *L. monocytogenes*. The scale in megabases (Mb) is shown on the exterior of the genome circles, with the origin of replication at position 0 (adapted from [14]).

Listeria genomes show a very strong level of conservation in terms of genetic content and structure, since inversions and rearrangements of large DNA fragments tend to be uncommon. Nonetheless, there are some underlying genetic variations between *Listeria* genomes, intimately correlated to the capacity of *L. monocytogenes* to cause diseases. The major virulence functions of *L. monocytogenes* are encoded on a cluster of seven genes (*plcA*, *plcB*, *hly*, *prfA*, *actA*, *orfX* and *mlp*) called the pathogenicity island 1 (LIPI-1). This 9 kb cluster has some of the most critical virulence factors needed for *L. monocytogenes* cell infection cycle, being almost exclusively present and functional in pathogenic strains of *L. monocytogenes* and *L. ivanovii* [10, 40, 41]. As a matter of fact, non-pathogenic species lack the most relevant virulence genes from the homologous regions [42, 43].

1.2.3. Listeriosis

Pathophysiology and treatment

L. monocytogenes is the causative agent of a rare, but potentially life-threatening, invasive illness called listeriosis, which has become a major foodborne disease. Human contamination with this bacterium occurs predominantly after consumption of contaminated food products as *Listeria* has the strength of surviving extreme gastric conditions, reaching the intestinal lumen. The transgression of the intestinal barrier by this bacterium is host-specific and essentially mediated by Internalin A, which interacts with the E-cadherin (Ecad) expressed by villus epithelial folds [44]. Once is internalized, it crosses the intestinal epithelial barrier and is released in the lamina propria [45]. In the intestine, if the immune system does not control the infection, *L. monocytogenes* travels through mesenteric lymph nodes and bloodstream, ending up both in the liver and spleen, the main target organs for microbial colonization [44, 46, 47]. Moreover, in immunocompromised patients, this pathogen can traverse the blood-brain barrier or the fetoplacental barrier and cause meningitis, sepsis, abortion or stillbirth (Figure 2) [44, 48, 49]. Host survival is therefore dependent on the development of an efficient adaptive immune response.

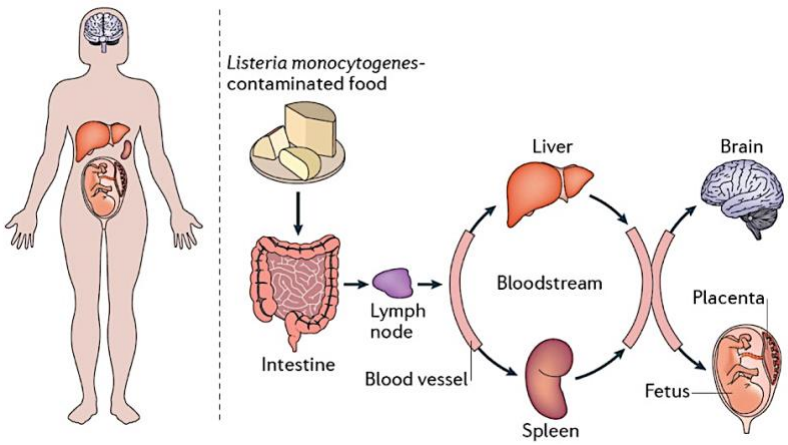

Figure 2 - *L. monocytogenes* infection of a human host (adapted from [49]).

The ability of the microorganism to cause illness depends on the bacterial load, on its own bacterial pathogenic potential and, most importantly, on the functional status of the host immune system [10].

There are two forms of this illness, a non-invasive form and an invasive one. The non-invasive form generally happens in healthy immunocompetent hosts, where listeriosis can be asymptomatic or appear as a milder and self-limiting gastroenteritis. Nevertheless, individuals who suffer from specific health conditions, such as pregnant women, neonates, elderly, and patients carrying diabetes or HIV, with impact on their immune system are more prone to develop the invasive form [10, 50, 51]. In this case, listeriosis becomes a more dangerous and deadly disease, characterized by bacteremia, that could progress to septicemia or local organ infections, particularly in the central nervous or in the fetoplacental systems [48]. The most prevalent form of invasive listeriosis in non-pregnant humans (55-70% case reports) affects the CNS due to the *L. monocytogenes* tropism in the brain tissues [10, 51], with meningitis and meningoencephalitis as the main symptoms [52]. In pregnant adults, listeriosis can be devastating to the fetus, as one-third of the materno-fetal cases end up in stillbirth or abortions when the maternal immune response is debilitated. The late-onset neonatal listeriosis is less recurrent and the infection happens possibly after contact with mother fluids throughout birth [10, 48].

Antibiotics administration is currently the standard treatment for listeriosis, as there is no vaccine commercially available to prevent listeriosis. Consequently, early diagnosis is crucial to antibiotic therapy effectiveness, particularly in high-risk patients. Treatment of human listeriosis with antibiotics requires the use of β-lactam (penicillin and ampicillin) alone or in combination with aminoglycoside (gentamicin) as the treatment of choice. In humans allergic to β-lactams are administrated alternative antimicrobial compounds, such as erythromycin, fluoroquinolones, trimethoprim/sulfamethoxazole, and vancomycin [48, 53]. Gentamicin might cause teratogenic consequences on the fetus, hence pregnant women should not be treated with this drug [48].

In fact, the majority of *Listeria* species are susceptible to antibiotic treatment frequently used against Gram+ bacteria [54]. However, during the last few decades, the systematic misuse of antibiotics in humans and animals significantly contributed to the rise of antibiotic resistance, including *L. monocytogenes* [53, 55]. The major mechanism responsible for this antibiotic resistance in *L. monocytogenes* was achieved through the acquisition of movable genetic elements, as conjugative transposons, mobilizable plasmids, and self-transferable plasmids [53, 56].

Epidemiology

Our current understanding of the epidemiology of human listeriosis suggests, as mentioned before, that the organism is a common contaminant of food products, including unpasteurized milk, dairy products, refrigerated smoked seafood, soft cheese, and cooked ready-to-eat sausage. The fact that *L. monocytogenes* is able to survive and replicate in a variety of raw and processed foods, resisting to the most common food-preserving methods, coupled with the global movement of foods and ingredients, facilitates the spread of contaminated foodstuffs across borders, resulting in foodborne outbreaks. Moreover, this pathogen has the ability to produce a biofilm as a survival strategy in harsh environments, highlighting the importance to develop new anti-biofilm formation strategies [57]. The pattern of *Listeria* epidemiology is typically characterized by occasional cases or large invasive outbreaks [58]. Consequently, *L. monocytogenes* is not only a public health concern, but can also result in major economic losses.

In addition, it is known that domestic animals and mammals, like sheep, dogs, and cattle, are reservoirs of this pathogen [59]. Humans, particularly laboratory and slaughterhouse staff, can be asymptomatic fecal carriers of this bacterium [60].

Despite the environmental prevalence of *L. monocytogenes*, listeriosis is a rare illness with an incidence of 1-10 cases per million people reported every year [61-63]. Over the last few years, the number of annual cases has been increasing, predominantly in developed nations [61, 62]. Yet, regardless of its low occurrence, the average rate of clinical case deaths ranges from 20 to 30%, with elevated hospitalization rates associated as well, making it the deadliest foodborne disease [64].

Listeriosis has been notified in Portugal only since 2014, though there is no active surveillance program [65] and, according to the Surveillance Atlas of Infectious Diseases, 42 cases of listeriosis were identified in Portugal in 2017, with a 17% fatality rate [66].

A deeper understanding of the pathogen properties, environmental effects and the interaction of virulence factors with host vulnerability is required to establish better control measures to diminish the occurrence of listeriosis. Additionally, this underlines the need for adequate epidemiological and microbiological monitoring systems that should be efficient at preventing large-scale outbreaks, as food safety is becoming one of the main concerns in food processing industries and society.

1.2.4. Cellular infection cycle

The *L. monocytogenes* cell infection cycle (Figure 2) consists of several sequential steps that rely on the expression of numerous bacterial virulence factors. The potential that this bacterium has to cause and establish infection in several tissues is related to its exceptional capacity to cross physiological barriers since it can invade non-phagocytic cells

(epithelial and endothelial cells, enterocytes, fibroblasts and hepatocytes) and survive into professional phagocytes (macrophages, neutrophils and dendritic cells) [67, 68].

L. monocytogenes starts its cellular infection cycle with bacterial adhesion to the host cell membrane by expressing surface proteins (adhesins). Almost concurrently, it triggers its own internalization into non-phagocytic cells mainly through the interaction of the bacterial surface proteins, Internalin A (InlA) and B (InlB), with their corresponding eukaryotic membrane receptors, E-cadherin and c-Met, causing a localized restructuring of the host cell cytoskeleton around the bacterium-cell interaction site [49, 69, 70]. This invasion is mediated by a zipper-like process, where bacteria are involved by the host cell membrane, leading to the engulfment in a vacuole into the cytosol [71]. Shortly afterward, *L. monocytogenes* disrupts this vacuole through the expression of a pore-forming toxin, listeriolysin O (LLO), and two phospholipases (phosphatidyl-inositolphospholipase (PlcA) and phosphatidyl-choline-phospholipase C (PlcB)), being released in the cytosol. Reaching the host cell cytoplasm, *L. monocytogenes* starts to exploit cytoplasmic nutrients in order to replicate intracellularly. Moreover, *L. monocytogenes* employs an actin-based process of motility, by expressing an actin assembly-inducing protein (ActA) that hijack the host's own polymerization machinery to nucleate actin, leading to the formation of a structure denominated actin or comet tail [72]. This structure generates a propulsive force that allows the pathogen to eventually reach the cell periphery, inducing the formation of a protrusion and a secondary vacuole in the adjacent cells. The bacteria, enwrapped in double-membrane vacuoles, are then internalized into adjacent cells, disseminating to neighboring cells without being re-exposed to the extracellular environment. Briefly after, the secondary vacuole is promptly lysed, initiating a new cycle of infection (Figure 3) [70, 71].

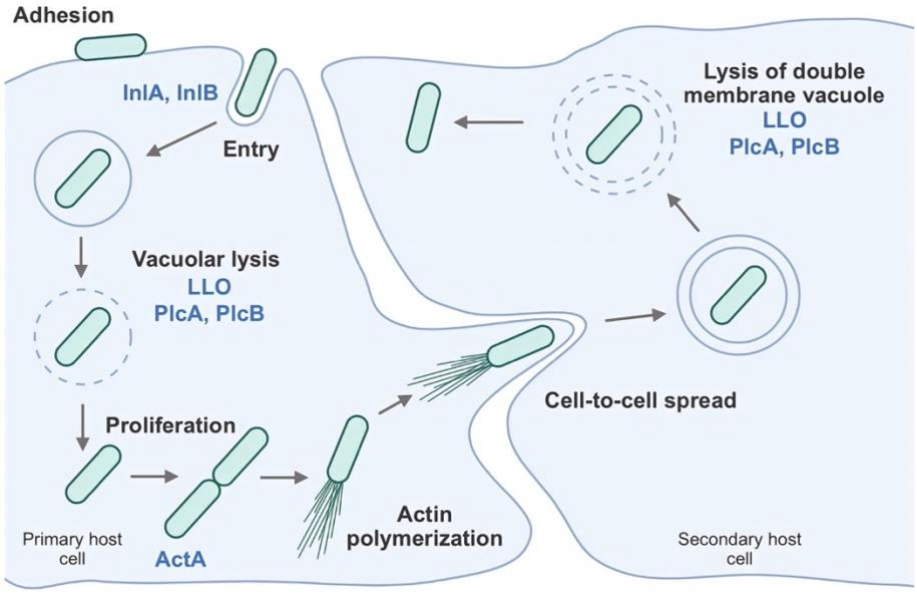

Figure 3 - Schematic illustration of the successive steps of *L. monocytogenes* cellular infection cycle and the major virulence factors involved.

1.2.5. Major virulence factors

The successful accomplishment of each step of *L. monocytogenes* intracellular life cycle is supported by the highly diverse supply of virulence proteins. The positive regulatory factor A (PrfA) plays a central role in the regulation of the correct expression of key virulence determinants of *L. monocytogenes*, since most of the PrfA controlled genes encode virulence factors involved in the major steps of the cellular infection cycle. Besides, it has been recognized approximately 160 *L. monocytogenes* EGD-e genes whose expression is somehow determined by PrfA [73].

The most representative virulence factors involved in the various stages of the intracellular infection cycle are briefly described in this section.

Adhesion

The initial step of the *L. monocytogenes* cell infection cycle is its adhesion to the eukaryotic host cell surface. This first bacterial contact is a crucial step for *L. monocytogenes* cellular infection, as the bacterium interacts with specific cell receptors and triggers the activation of signaling pathways that enable cell invasion [74].

The *Listeria* adhesion protein (LAP), formerly known as surface protein p104, is a 104 kDa alcohol acetaldehyde dehydrogenase that interacts with Hsp60, a heat shock protein, promoting bacterial adhesion into intestinal cells [75, 76]. It is also known that LAP can induce intestinal epithelial barrier dysfunction to promote bacterial translocation [77]. LapB is a sortase-anchored LPXTG surface adhesin that via a unique N-terminal domain appears to participate in adhesion, invasion, and virulence [78]. Ami is a protein with amidase activity essential for efficient bacterial adhesion and virulence. This 99 kDa autolytic protein contains an N-terminal catalytic domain and a C-terminal cell wall-anchoring (CWA) domain with eight glycine-tryptophan (GW) repeats. The C-terminal domain is accountable for the Ami association to the bacterial surface, probably through interaction with lipoteichoic acids (LTAs) [79, 80]. Furthermore, the GW modules of Ami are highly conserved and were shown to be involved in the Wall Teicoic Acids (WTA) L-rhamnosylation-dependent association of Ami to the *L. monocytogenes* surface [81].

FbpA is an adhesin needed for spleen and liver colonization in infected mice. In addition to its function as a fibronectin-binding enzyme, it also demonstrates activity as a chaperone, guaranteeing proper secretion of InlB and LLO [82, 83]. ActA is necessary for actin-based motility, however has shown to be involved in cell attachment and entry by recognition of heparan sulfate [84].

To date, several other proteins have been identified as contributors to bacterial adhesion, including InlF, DltA, RecA, and CtaP [73].

Invasion

The entry of *Listeria* into macrophage cells is predominantly driven by the macrophage itself, yet entry into non-professional phagocytes is assisted by many *Listeria* factors.

InlA and InlB were the first proteins identified as mediators directly implicated in *L. monocytogenes* internalization into non-phagocytic cell types [85, 86]. Both proteins are encoded by the *inlAB* gene locus and are members of the so-called internalin family. All members of this family have an N-terminal domain containing a signal peptide sequence, followed by a tandemly arranged leucine-rich repeats region (LRR) that are involved in protein-protein interactions, a conserved inter-repeat (IR) domain, and a variable C-terminal motif [87, 88].

InlA is an 80 kDa acidic protein with 800 amino acids, composed by 15 LRRs, covalently anchored to the peptidoglycan (PGN) through its C-terminal LPXTG motif [85, 89]. The LPXTG domain provides a covalent and stable anchoring to the cell wall, facilitated by sortase A (SrtA), a membrane-bound transpeptidase [85, 90]. The InlA LRR domain interacts with Ecad, a transmembrane glycoprotein and a major constituent of adherens junctions [91, 92]. *L. monocytogenes* was shown to use InlA to invade the tips of the intestinal villi, where cell extrusion induces a temporary defect in epithelial polarity, exposing the Ecad on the cell surface [93]. Recently, a live imaging study with intestinal organoids revealed that *L. monocytogenes* hijacks E-cad recycling in a Rab11a-dependent manner to translocate across the intestinal epithelium [94]. The engagement of Ecad by InlA disturbs the normal Ecad function, triggering complex signaling pathways and promoting cortical actin polymerization and rearrangement of the plasma membrane, ultimately leading to the bacteria internalization [95]. The association of InlA with Ecad is species-specific and, in *Homo sapiens*, relies on the presence of a proline residue at position 16 of the Ecad molecule. In fact, the extracellular domain of Ecad is enough to bind InlA and the intracellular domain binds to catenins [71, 96]. This association results in the phosphorylation of the Ecad receptor and subsequently its ubiquitination, supporting the successful bacterial uptake [96]. There is a high degree of homology between human and mouse Ecad, nonetheless the mouse Ecad is not recognized by InlA due to the replacement of the proline residue by glutamic acid at the same position [96].

InlB consists of a 67 kDa protein with 630 amino acids, composed by 8 LRRs and a C-terminal domain with three conserved GW repeated modules [85, 86, 97]. The GW modules mediate the attaching of InlB to the bacterial surface through non-covalent interactions with LTAs and PGN-bound wall teichoic acids [81, 98]. In addition, as for Ami, the L-Rhamnosylation of WTAs seems to promote the efficient surface association of InlB to the *L. monocytogenes* surface through interaction with a specific GW module domain [81]. InlB has a variety of host receptors, as the globular part of the complement component C1q (gC1qR),

hepatocyte growth factor (HGF) and glycosaminoglycans (GAGs) [99-101]. However, the receptor tyrosine kinase, c-Met, known as the physiological receptor for the HGF, is considered as the InlB signaling receptor [101]. InlB induces c-Met autophosphorylation and the recruitment of adaptor proteins such as Shc, Cbl, and Gab1 [102-104], subsequently activating PI3-kinase and GTPase Rac1 [105-107]. This signaling cascade stimulates c-Met ubiquitination, actin cytoskeleton rearrangements, and bacterial internalization via a clathrin-mediated endocytosis mechanism [102-104]. InlB-mediated entry is strongly dependent on the actin rearrangements that take place downstream the activation of c-Met. The actin polymerization is primarily regulated by Arp2/3 complex and through a signalling cascade involving, depending on the cell host type, GTPases Rac1 and Cdc42, Wave, N-WASP, and Abi1 [101, 106, 108-110]. For the completion of the bacterial internalization process is necessary actin depolymerization, achieved through LIM-Kinase and cofilin protein [71]. InlB operates in enterocytes as a facilitator of the InlA-dependent invasion pathway, thereby accelerating intestinal invasion [111, 112].

It has been shown that InlB plays a crucial role in the crossing of the placental barrier as well and the cooperation between InlA and InlB seems to be critical for the successful placental invasion [113].

In Figure 4 is schematically represented the internalization of *L. monocytogenes* into non-phagocytic cells via these two internalins.

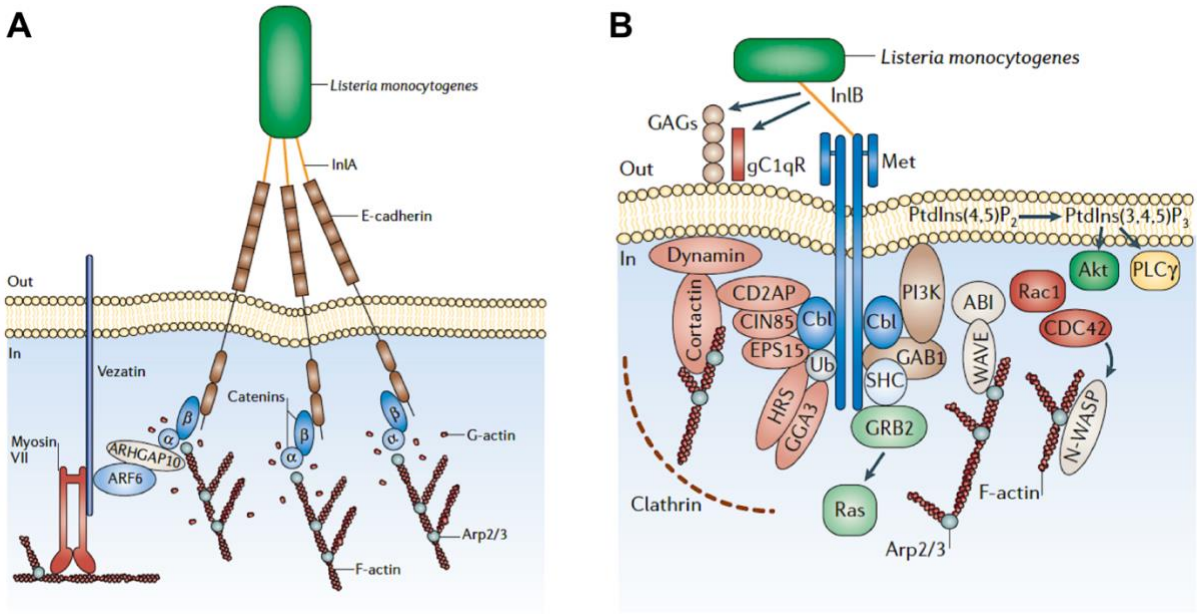

Figure 4 - Internalization of *L. monocytogenes* into non-phagocytic cells via (**A**) InlA and (**B**) InlB (adapted from [107]).

However, InlA and InlB do not play a part in direct brain infection *in vivo*, indicating that Ecad and the c-Met receptor do not contribute to blood-brain barrier crossing. Instead, it is necessary Internalin F (InlF) to mediate *L. monocytogenes* efficient colonization of the brain,

since it interacts with host cell vimentin and leads to the adhesion of mammalian brain endothelial cells [114]. Regarding the liver invasion, it is known that *L. monocytogenes* uses listeriolysin O to invade murine liver parenchymal cells [115].

Vip is a LPXTG protein anchored to the PGN by SrtA, absent from non-pathogenic *Listeria* species. Vip is required for effective *Listeria* entry into various epithelial cell lines [116]. Gp96 is a chaperone that acts as the host cell receptor for Vip, and the association of Vip/Gp96 appears to be very important for the invasion of eukaryotic cells by *Listeria* [116].

The surface-associated autolysin Auto (~62 kDa) is also implicated in bacterial internalization. This autolytic protein is encoded by the *aut* gene and has four C-terminal GW modules responsible for the protein association to the bacterial cell wall [117].

Vacuole lysis

Upon internalized by host cells, *L. monocytogenes* is temporarily engulfed within a phagocytic vacuole. In order to escape from this vacuole and reach the host cell cytoplasm, the bacteria secrete listeriolysin O (LLO) and phospholipases (PlcA and PlcB) [118, 119].

LLO consists of a pore-forming toxin, which is part of cholesterol-dependent pore-forming cytolysins (CDCs) family, secreted through the general secretion system (Sec). LLO is encoded by the *hly* gene, which was the first virulence gene identified in *Listeria* and is part of the pathogenicity island LIPI-1. This toxin oligomerizes in the vacuole membrane, forming arcs and pores that disrupt membrane integrity [120, 121]. The cytolytic LLO activity is optimum at the phagocytic vacuole's acidic pH (5.5) and diminishes at the cytoplasm's neutral pH [122]. The pH-dependent regulation protects the host cell against further membrane disruption, avoiding unwanted damage and establishing an intracellular niche for survival and spreading of *L. monocytogenes* [123, 124]. Efflux of potassium and calcium were found to be crucial for LLO-dependent internalization through the plasma membrane [125, 126]. Beyond this, LLO displays other functions, inducing several events in host cells, as NFκB activation, apoptosis, upregulation of adhesion molecules, and cytokines [127]. Furthermore, LLO affects the levels of intracellular calcium, transiently alters mitochondrial dynamics during infection, and represses the host immune response through diminishing protein SUMOylation [128-130].

Other important virulence factors were also shown to cooperate with the intravacuolar activity of LLO, mediating the disruption of the vacuoles. In particular, this intravacuolar activity is reinforced by the secretion of the phosphatidylinositol-specific phospholipase C, PI-PLC (*plcA*), and the broad range-phospholipase C, PC-PLC (*plcB*), which facilitates LLO-mediated escape from primary and secondary vacuoles, respectively [119].

In addition, there are other virulence factors that contribute to vacuole lysis, specifically PrsA2, SipZ, SvpA, Lsp, and ActA [73].

Intracellular survival, replication and cell-to-cell spread

During the intracellular replication stage, *L. monocytogenes* uses another major virulence factor, the hexose phosphate transporter (Hpt), who is responsible for facilitating the uptake of hexose phosphates. Hpt allows bacteria to use phosphorylated sugars, for instance glucose-1-phosphate, as a carbon energy source for intracellular growth and replication within the host cell cytosol [131]. In macrophages, the virulence factor OrfX contributes to the intracellular survival of bacteria. OrfX is a small secreted protein, positively regulated by PrfA, whose expression reduces the oxidative response of infected macrophages, through modulating the level of the nuclear host regulatory protein (RybP) [41].

For the infection to progress, *L. monocytogenes* needs to move in the host cytoplasm and spread to the surrounding cells. This cellular infection step is achieved by the expression of ActA. The polarized bacterial surface protein ActA is considered one of the most important virulence factors of *L. monocytogenes*, regulating the speed and directionality of the bacterial movement [132]. Surface expression of ActA induces the actin filaments polymerization since the N-terminal region of ActA mimics the activity of the WASP family proteins, the host cell actin nucleating factors [133], recruiting and activating the Arp2/3 complex, another host actin nucleator, at one pole of the bacteria [134, 135]. The polymerization results in a structure resembling a comet tail that allows bacterial propulsion, movement, and invasion of nearby cells. The central domain of ActA, a proline-rich repeat region, is not necessary for motility, but is crucial for the recruitment of proteins of the Ena/VASP protein family, responsible for modulating bacterial speed and directionality [136, 137]. *L. monocytogenes* ActA mutants have been shown to be avirulent and non-motile in the mouse model, proving ActA importance in motility and cell-to-cell spread [72, 138]. As previously mentioned, ActA is also implicated in other cellular infection events, as attachment and internalization into different cells [139].

The bacterial movement within the host cytoplasm cell is random and when *L. monocytogenes* reaches the cell plasma membrane during its intracellular movement, induces the formation of cell protrusions and internalization into the adjacent cell, without re-exposure to the extracellular environment.

1.3. Gram-positive cell envelope

The bacterial cell envelope is a complex multi-layer structure that provides structural stability and plays a fundamental role in protection from the external environment while enabling the exchange of nutrients and waste products. The cell envelopes of most of the bacteria fit into one of two main structures, Gram- and Gram+. Earlier, this differentiation was based on the result of Gram staining and later it was discovered that these differences were caused by diverse cell wall composition. In Gram- organisms, cell envelope is composed of an

inner membrane, a PGN cell wall, and an outer membrane. Gram+ bacteria do not have an outer membrane, yet are surrounded by much thicker layers of PGN, which constitutes approximately 40% of the overall mass of the cell wall, conferring resistance to turgor pressure and protecting from outside hostilities [140, 141].

The PGN is a highly polymerized macromolecule, constituted of linear and parallel glycan strands linked perpendicularly by short peptide bridges. These glycan strands are made of alternating N-acetylglucosamine (Glc*N*Ac) and N-acetylmuramic acid (Mur*N*Ac) residues linked by β(1-4) bonds [142].

In *L. monocytogenes*, like in others Gram+, several surface proteins are linked to the cell envelope by non-covalent interactions generally promoted by protein domains containing tandem repeat sequences [87]. These domains allow protein binding to either PGN [143] or to secondary cell wall polymers, such as teichoic acids (TA) [117], which includes lipoteichoic acids (LTAs) and wall teichoic acids (WTAs) (Figure 5) [144, 145].

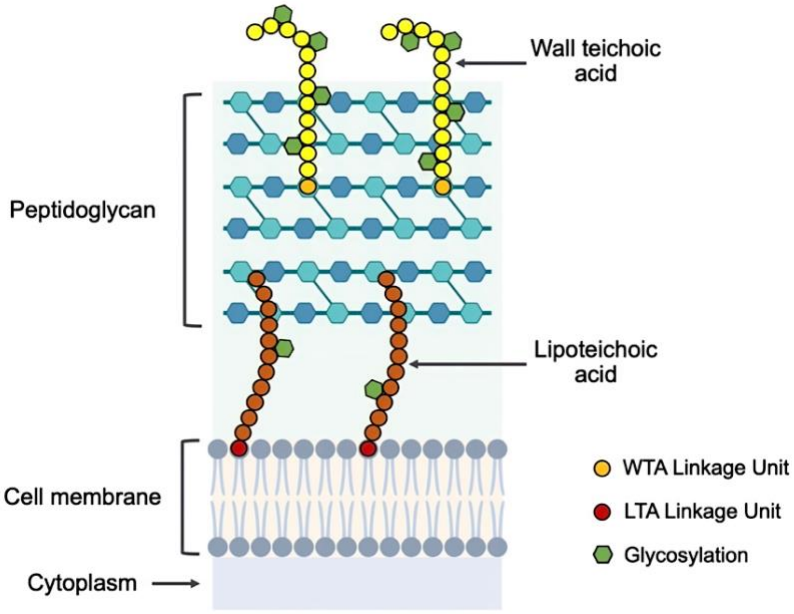

Figure 5 - Schematic representation of cell wall structure of Gram+ bacteria.

1.3.1. Teichoic acids

The Gram+ PGN is abundantly decorated with several families of secondary glycopolymers, including teichuronic acids, teichoic acids, and S-layer protein-associated glycans [144]. Teichoic acids (TAs) are the only ones of these produced in *Listeria*, where they can make up 60% of the dry cell wall mass [146].

Discovered in 1805 [147], TAs are a family of cell surface glycopolymers comprising phosphodiester-linked polyol repeat units [148]. TAs perform critical functions in the cell envelope, regulating the porosity and rigidity of the cell wall, and affecting the bacterium's morphology [144, 145, 149, 150]. Moreover, TAs have a high abundance of phosphate groups,

who confers them strong anionic properties and contributes to the bacterial surface net negative charge. This is related to several cell-envelope processes, such as cationic homeostasis and the trafficking of proteins, nutrients, and antibiotics [149]. It is also known that TAs play a role in the targeting and anchoring of surface proteins [144]. TAs include both LTAs, which are retained on the cytoplasmic membrane surface by a lipid anchor, and WTAs, which are covalently attached to PGN via a phosphodiester linkage.

1.3.1.1. Wall teichoic acids

Wall teichoic acids comprehend a class of anionic glycopolymers covalently attached to the PGN walls of Gram+ bacteria [145]. The WTA polymer is divided into two essential constituents, a disaccharide linkage unit and a main chain polymer constituted of phosphodiester-linked polyol repeat units [149]. The disaccharide linkage unit consists of a conserved GroP-N-acetylmannosamine (ManNAc)-β(1,4)-Glc*N*Ac triad linked by a phosphodiester bond to the C6 hydroxyl group of MurNAc residues (Figure 6A) [149].

WTAs comprises polymeric complexes that are highly diverse at a biochemical and structural level, with differences mainly seen in the kind of backbone monomers and glycosyl substituent groups [151]. The best described and most usual WTA backbone (type I) comprehend repeat units of either 1,3-L-α-glycerol-phosphate (GroP) or 1,5-D-ribitol-phosphate (RboP) (Figure 6B) [145].

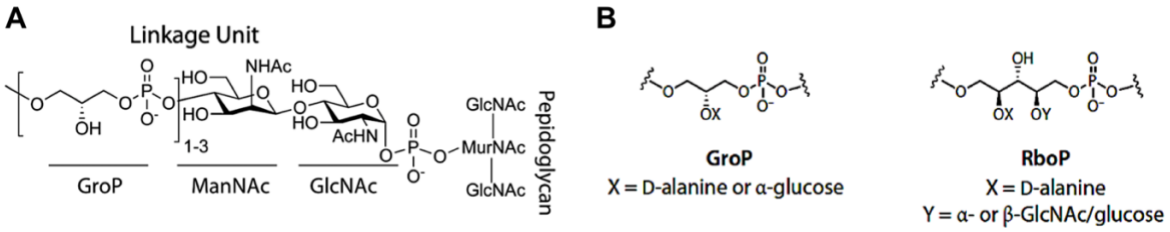

Figure 6 - Structural components of the WTA glycopolymers. (**A**) disaccharide linkage unit constituted by GroP-ManNAc-P, covalently attached to PGN; (**B**) most usual WTA repeat units structures. Abbreviations: GroP, 1,3-L-α-glycerol-phosphate; ManNAc, N-acetylmannosamine; GlcNAc, N-acetylglucosamine; MurNAc, acid N-acetylmuramic; RboP, 1,5-D-ribitol-phosphate (adapted from [145]).

Unlike LTAs, where polymer structure and chemical identity of the substituent groups are conserved across listeriae [152, 153], WTAs display high variability, even within the same species [144]. In *L. monocytogenes*, WTAs are constituted of repeated ribitol-phosphate (RboP) subunits, of which hydroxyl groups can be replaced by diverse monosaccharides [144, 154]. Specific WTA substitution patterns are distinctive of specific *L. monocytogenes* serotypes. N-acetylglucosamine is prevalent in serogroups 1/2 and 3, and in serotype 4b, yet serogroup 1/2 also includes L-rhamnose and serotype 4b contains D-galactose and D-glucose (Figure 7) [155].

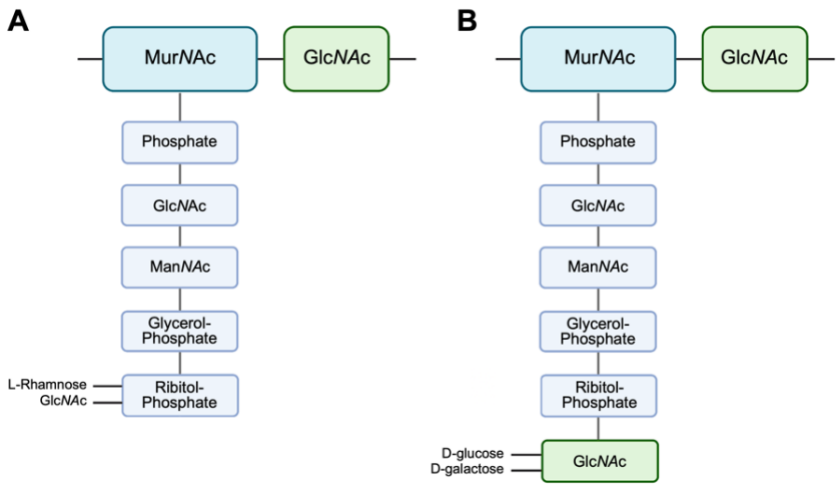

Figure 7 - Schematic representation of the WTA structure of *L. monocytogenes* serotypes 1/2a (**A**) and 4b (**B**).

1.3.1.2. WTA L-rhamnosylation in *L. monocytogenes*

WTAs polymers play numerous roles in the cell wall, such as in the regulation of cell morphology, division machinery, ion homeostasis, and autolytic activity [145]. In addition, WTAs have a key role in Gram+ pathogens survival, regulating necessary mechanisms for host infection, colonization, protection against antimicrobial peptides (AMPs) and drugs [81, 145, 156]. WTA glycosylation mechanisms have been proven to be very important in Gram+ pathogens, namely *L. monocytogenes* strain EGD-e (Sv1/2) WTA decorated with L-rhamnose is known to confer resistance to the action of AMPs, promote efficient surface association of virulence factors, and decrease susceptibility to some antibiotics [81, 157, 158]. This decoration of *L. monocytogenes* WTAs with L-rhamnose involves the expression of the *rmlACBD* locus and the glycosyltransferase RmlT [158].

During *in vivo* mouse infection, it was observed high expression levels of *rmlACBD* genes. The RmlACBD proteins induce the transformation of glucose-1-phosphate into thymidine-diphosphate (dTDP)-linked form of L-rhamnose [159]. The functional *rmlACBD* locus is therefore mandatory for the association of L-rhamnose with WTAs, since it delivers the necessary molecular system for L-rhamnose synthesis [158]. WTA glycosylation is mediated by a class of enzymes known as glycosyltransferases, which are responsible for identifying and transferring nucleotide-sugar substrates to a WTA subunit [160].

The decoration of WTAs with L-rhamnose prerequisites the expression of the *rmlT* gene, which encodes the rhamnosyltransferase RmlT, making the WTA rhamnosylation of *L. monocytogenes* strictly dependent from RmlT [158]. L-rhamnose can be synthesized in the absence of RmlT, as this glycosyltransferase does not affect the *rmlACBD* locus transcription. Nonetheless, it was shown that the lack of *rmlT* gene causes a depletion of L-rhamnose in WTAs, proving that L-rhamnosyltransferase activity performed by RmlT is indeed essential for WTA glycosylation [158].

As stated previously, there has been revealed a critical involvement of L-rhamnosylated WTAs in *L. monocytogenes* resistance against AMPs, highlighting the importance of WTA glycosylation in the mechanisms of bacterial immune evasion [158]. AMPs are part of a large family of small cationic peptides (<10 kDa) synthesized by a wide variety of organisms across all domains of life, forming the primary defense against invading pathogens [161]. These peptides have a broad antimicrobial spectrum activity against microorganisms, covering Gram+ and Gram- bacteria, fungi and viruses, since they combine with membrane and/or cytoplasmic components, modifying cellular functions [162]. The action of WTA L-rhamnosylation in facilitating *L. monocytogenes* resistance to AMPs is likely due to obstructing the crossing of its cell wall by these molecules. It modifies the permeability of the cell wall in order to promote the entrapment of AMPs and postponing their harmful interaction with the plasma membrane, thereby enhancing survival. Contrary to D-alanylation [163], WTA L-rhamnosylation does not affect *L. monocytogenes* cell surface charge, which is consistent with the electrostatically neutral nature of L-rhamnose [158].

WTA L-rhamnosylation is also involved in the efficient surface association of *L. monocytogenes* virulence factors, namely Ami and InlB. Both Ami and InlB are members of a protein family where bacterial surface association is facilitated by Glycine-Tryptophan (GW) modules and WTA L-rhamnosylation promotes their efficient surface association through interaction with these GW domains. More specifically, it contributes to the functional levels of autolysis in *L. monocytogenes* and for the efficient bacterial adhesion in eukaryotic cells, providing the appropriate association of the autolysin Ami to the bacterial cell surface [80, 81]. Furthermore, it interferes with the retaining and displaying of InlB, a major *L. monocytogenes* virulence factor implicated in the bacterial uptake into non-phagocytic cells. Consequently, this makes WTA L-rhamnosylation a bacterial surface modification mechanism with consequences in *L. monocytogenes* physiology and pathogenesis, since it regulates the association and stabilization of non-covalently surface-bound virulence proteins that share a common cell surface-binding motif [81].

WTA modifications have also been implicated in the sensitivity to some antibiotics. In fact, the deficiency of WTA L-rhamnosylation in *L. monocytogenes* Sv1/2a strain slightly enhances the bacterial sensitivity to gentamicin and mutants lacking the genes coding the glycosyltransferases responsible for WTA decoration with rhamnose and N-acetylglucosamine displayed an improved sensitivity to gentamicin, ampicillin, and benzylpenicillin [157].

Taking this into consideration, WTA glycosylation appears to be a mechanism employed by *L. monocytogenes* to attach virulence factors at its bacterial surface and to surpass the action of both host AMPs and antibiotics (Figure 8).

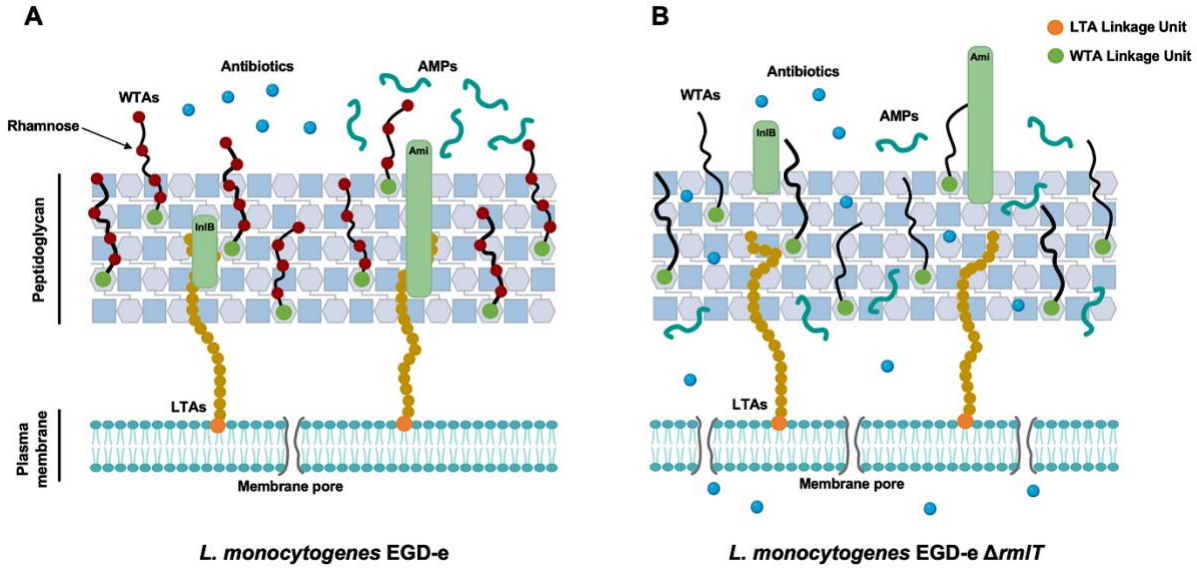

Figure 8 - Schematic representation of *L. monocytogenes* with WTA L-rhamnosylation (**A**) and without WTA L-rhamnosylation (**B**).

1.4. High-Throughput Screening in drug discovery

Drug Discovery consists of the procedure through which new drugs are identified and/or designed. A variety of scientific disciplines, as biology, chemistry, and pharmacology, are involved in the Drug Discovery process.

High-Throughput Screening (HTS) involves a highly complex and multidisciplinary approach to drug discovery that has achieved global popularity in the last decades and has become a standard technique for drug discovery in the pharmaceutical industry. It is essentially a method of screening and assaying a large number of chemical compounds against selected and specific targets, in order to obtain a vast amount of experimental data in a relatively short time. The primary goal of HTS is to find hits that have the intended effect on the target. HTS can be divided into several steps of target identification and validation, screening assay development and optimization, and hits identification [164, 165].

Target identification and validation

HTS begins with the recognition of a target or a pathway by basic academic or clinical research, by studying the underlying molecular mechanisms of the illness that are important to its emergence and progression. Proteins, mutations, and polymorphisms in the coding and non-coding regions of the genome, as well as transcriptional and post-translational regulatory processes, can all be used as targets [164].

Target identification can be sustained by the incorporation of pertinent information from the different datasets nowadays available [166]. The recent advances in the “omics” datasets, as genomics, proteomics, metabolomics, transcriptomics, and epigenomics are critical in target and drug discovery, since it helps supporting strong gene/protein variant correlations and therefore contributes to the discovery of new biomarkers.

Identification of the target is followed by target validation, the characterization of the molecular mechanisms exploited by the target. A suitable target should fulfil clinical and commercial requirements, while being safe and efficient. A target is considered druggable when its functional significance in the disease or pathogenesis is capable of modulation through genetic and/or chemical experimentation. Genetic manipulation of cells/animal model organisms can be achieved, for example, by clustered regularly interspaced short palindromic repeats (CRISPR-Cas9) or transcription activator-like effector nucleases (TALENs), while chemical validation can be accomplished through identified compounds or antibodies [164, 167].

Screening assay development and optimization

Drug discovery involves the development of a primary screening assay that investigates the target or pathway under study. Furthermore, it requires secondary assays, which evaluate the biological relevance of the hits previously found on the primary screens [168]. These assays can be performed by cell-based or biochemical assays.

Cell-based assays refer to different experiments based on cell culture methods, using living cells. They are the most frequently used for HTS and allow the testing of thousands of compounds efficiently and rapidly prior to animal testing, measuring cell proliferation, toxicity, motility, and morphology. Cell-based reporter gene experiments are developed up on target sequences fused to reporters, such as luciferase, in which the readout is a luminescent protein controlled by a specific gene promoter [164, 169].

The biochemical assays use purified or partly purified target proteins to find candidates for drug development. The most popular assay readouts employed in HTS biochemical assay methods are optical, namely fluorescence, luminescence, and absorbance. Fluorescence-based systems are one of the most effective detection techniques used for HTS [170]. Biochemical assays systems perform better statistically than cell-based assays, however their applications are limited considering that not all targets can be purified [171].

Phenotypic assays are another option that evaluates the phenotypic or biochemical changes caused by abnormal signaling pathways in cell lines or model organisms, as *Danio rerio* and *Caenorhabditis elegans* [172-174].

As prior mentioned, drug discovery workflows besides the primary assays also include the development of secondary assays. Primary screening permits direct high throughput

binding measurements of small compounds and mistakes about the binding of target-compound are common during this step. In this context, the secondary assays are performed to verify hits efficacy by a series of functional cellular assays, re-confirming compounds' actions and defining selectivity and specificity. Therefore, secondary screening assays are essential to guarantee that hits produced from high throughput screening are accurately converted into leads. Usually, if a cell-based assay is chosen for the primary assay, a biochemical screen will be chosen as a secondary screen [164, 175].

The biology and feasibility define the type of test chosen for HTS. Normally, the assays used are homogeneous, robust and highly reproducible. Positive and negative controls must be carefully chosen and a statistical factor Z' should be calculated to determine the performance and quality of the assay. Z'-factor is based on means and standard deviations of controls ($Z' = 1 - (3SD_{high\ control} + 3SD_{low\ control}) / |Mean_{high\ control} - Mean_{low\ control}|$) and helps determine how sensitive the assay will be finding hits. An adequate value of Z' factor varies from 0.5-1 and the closer the Z'-factor is to 1, the more robust is the screen [173, 176-178].

Hits identification

Hit identification is the most important step to identify compounds that interfere with the target. An efficacious hit identification process relies on the use of high-quality library compounds, available commercially through sellers or synthesized by academic researchers. These libraries are composed of fragments (<300 Da), small organic molecules, and larger structures of high molecular sizes, including purified natural products, natural product extracts, and purified metabolites [164, 179].

The main purpose of the hit identification process is to successfully identify hits with the highest chance to be developed into drug-like compounds.

1.4.1. High-Throughput Screening performed in *L. monocytogenes*

Several HTS studies against *L. monocytogenes* have been performed, resulting in the discovery of new antibacterial molecules and targets.

A library of WP1130-derivative molecules was screened for anti-infective efficacy in macrophages, discovering a molecule capable to decrease intracellular growth of *L. monocytogenes* without significant cellular toxicity effects [180].

Another HTS performed against *Listeria* screened a small molecule library enriched for compounds that impact neurological functions, revealing 26 novel inhibitors of intracellular infection. The compounds were able to reduce the ability of the pathogen to escape the vacuole to start its intracellular replication. The findings from this study implied that clinically authorized neurological medicines could be developed as alternative therapeutics [181].

Furthermore, a HTS approach, using a library of molecules with known biological activities, was developed to gain insight into host-pathogen interactions. The screen produced 21 compounds that changed *L. monocytogenes* infection. The results obtained suggested a reproducible screening method for the detection of drugs with an impact on molecular pathways needed for intracellular invasion [182].

In a more recent study, a library of around 9 000 compounds was screened, indicating a potential target that could be used for the development of new drugs against *L. monocytogenes*, the GTP cyclohydrolase I [183].

1.4.2. High-Throughput Screening against glycosylations and WTAs

Protein glycosylation is a common post-translational modification, that forms glycoproteins and modulates several critical biological processes. Bacterial glycosylation is implicated in host-pathogen interaction, affecting pathogen virulence and host resistance [184, 185]. Hence, pathogenic bacteria have evolved chemically varied glycosylation systems, which has become attractive targets for the development of new antimicrobial drugs.

A HTS approach to identify selective inhibitors for the *Escherichia coli* glycosyltransferase MurG was developed. MurG is involved in peptidoglycan biosynthesis, thus making it an appealing target, since it is needed for the survival of bacterial cells. It was screened about 64 000 molecules from a variety of different compound libraries, discovering several compounds with MurG inhibition properties [186].

Another HTS experiment was carried out for the identification of bacterial glycosyltransferase inhibitors. NleB from *Escherichia coli* and SseK from *Salmonella enterica* consist of type III secretion system effectors which act as glycosyltransferase enzymes. They can disrupt the normal functioning of the host innate immune system and therefore were considered antimicrobial targets. The molecules with inhibiting NleB/SseK activity here discovered yielded a possible alternative therapeutic approach to antibiotics [187].

The cell wall polymers WTAs are potential targets for future therapies to fight resistant bacterial infections due to their involvement in pathogenesis [188]. WTAs in *Staphylococcus aureus* (*S. aureus*) are known to have great importance in virulence and resistance to β-lactam antibiotics. A HTS process was developed to identify possible WTA inhibitors, assaying 55 000 compounds. A small molecule, named 1835F03, was found to inhibit the biosynthesis of the *S. aureus* WTAs [189].

Moreover, employing a phenotypic screening approach, it was acknowledged several inhibiting molecules of the *S. aureus* WTAs synthesis, predicted to be chemically synergistic with β-lactams [190]. By screening a library of around 20 000 compounds, researchers were able to find a series of inhibitors of TarG, a wall teichoic acid transport protein [191].

2. Objectives

Rising rates of antibiotic resistance are mainly due to their overuse and misuse, as well as a lack of new drug development by the pharmaceutical industry [192]. The development of new antibiotics remains thus vital to keep ahead of resistance. However, conventional antibiotics induce a high selection pressure for antibiotic resistance mechanisms. An alternative strategy is to disarm pathogens by directly targeting virulence factors without killing bacteria or halting their growth.

Wall teichoic acids (WTAs) consist of a class of anionic glycopolymers present at Gram+ cell wall. In *L. monocytogenes* the absence of rhamnose in the WTAs decreases surface anchoring of virulence factors and resistance to antimicrobial peptides and antibiotics [81, 157, 158]. The cell wall rhamnosylation appears therefore as a promising target for innovative antivirulence strategies against *L. monocytogenes*, preventing drug resistance development and preserving the gut microbiota.

The aim of this work was to screen for 1- new antimicrobial compounds against *L. monocytogenes*, and 2- new drugs decreasing WTA rhamnosylation as a complementary strategy to fight *L. monocytogenes* infections. For this purpose, a High-Throughput Screening was performed to find potentials candidate hits, confirm by dose-response experiments the more promising candidates, and validate the use of these candidate drugs by performing *in vitro* (cultured cell lines) studies.

3. Materials and Methods

3.1. Bacterial strains, cell lines and growth conditions

The bacterial strains used in this study are listed in Table 2. *L. monocytogenes* EGD-e and EGD-e Δ*rmlT* were cultured in Brain Heart Infusion (BHI) medium (BD) at 37 ºC with agitation under aerobic conditions. *E. coli* XL1-Blue MRF' and *E. coli* BL21(DE3) were cultured in Lysogeny Broth (LB) medium, both also aerobically at 37 ºC with agitation.

For bacterial invasion assays were used Human cervical adenocarcinoma HeLa cells (ATCC CCL-2) cultured in Dulbecco's modified Eagle medium (DMEM) supplemented with 10% fetal bovine serum (FBS). The HeLa cells were grown at 37 ºC in a 5% CO_2 humidified atmosphere, without antibiotics.

Table 2 - Bacterial strains and plasmid used in this study.

Bacterial strains and plasmid	Genotype or Description	Source
Listeria monocytogenes		
EGD-e	Wild-type; serotype 1/2a	[14]
EGD-e Δ*rmlT*	EGD-e *rmlT* (*lmo1080*) deletion mutant	[158]
Escherichia coli		
XL1-Blue MRF'	Δ(*mcrA*)*183* Δ(*mcrCB-hsdSMR-mrr*)*173 endA1 supE44 thi-1 recA1 gyrA96 relA1 lac* [F´ *proAB lacI*^{q}ZΔ*M15* Tn*10* (Tet^{r})]	Stratagene, La Jolla, USA
BL21(DE3)	F^{-} *ompT hsdS*$_B$ ($r_B^- m_B^-$) *gal dcm* (DE3)	Invitrogen
Plasmid		
pDUVET	Encodes GFP-gp17; Amp^{R}	From M. Loessner

3.2. Plasmid purification and bacterial transformation

pDUVET plasmid (Figure 9), kindly provided by Martin J. Loessner [193], encodes GFP-gp17 fusion protein. The GFP-gp17 protein consists of rhamnose binding protein (gp17) fused with GFP. pDUVET plasmid was purified from the *E. coli* XL1-Blue MRF' (maintenance strain) through NZYMiniprep® kit following the manufacturer's instructions. This procedure relies on the alkaline lysis of bacterial cells followed by adsorption of DNA onto silica in the

presence of high salt. Afterwards, 100 ng of the plasmid DNA was incubated with chemical competent cells of *E. coli* BL21(DE3) (protein expression strain) for 30 minutes, subjected to a heat shock at 42 ºC for 45 seconds followed by a second incubation on ice for 15 minutes. Five times of the mix volume was added of LB-medium to induce cell recovery and the cells were shaken at 200 rpm at 37 ºC during 1 hour. Cells were, then, plated on LB-agar plates supplemented with ampicillin (Amp) and incubated at 37º overnight. Positive clones were confirmed by colony PCR.

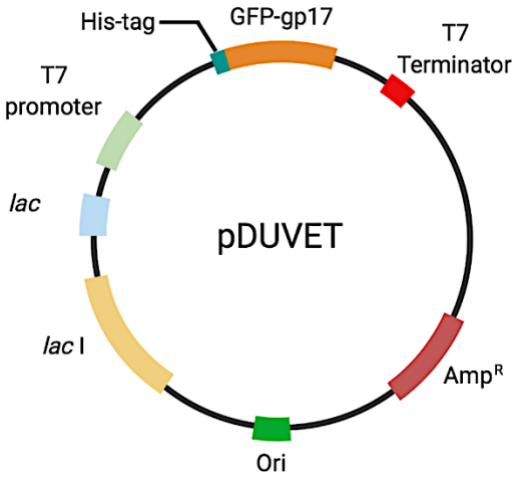

Figure 9 - Schematic representation of pDUVET plasmid.

3.3. Optimization of bacterial recombinant protein expression

To evaluate the optimal induction conditions for protein expression, several temperatures and induction times were tested. For this purpose, one colony of *E. coli* BL21(DE3) strain harboring pDUVET encoding GPF-gp17 was inoculated in LB medium with Amp and incubated overnight at 37 ºC and 200 rpm (pre-culture). A 1:100 volume of this overnight culture was used to inoculate LB + Amp and was incubated at 37 ºC and 200 rpm until the optical density at 600 nm (OD_{600nm}) reached approximately 0.4-0.5.

The culture was then divided into two halves, inducing one of the halves with 0.5 mM Isopropyl β-D-1-thiogalactopyranoside (IPTG) and leaving the other uninduced. Then, each condition was again divided to test different induction temperatures: 25 ºC, 30 ºC, and 37 ºC. From each condition, samples at 2h, 4h, 6h, and overnight were recovered. Accordingly, 1 mL of each condition were pelleted down at 16 000 xg for 2 minutes at room temperature, discarding the supernatant, and stored at -20 ºC.

Frozen pellets were resuspended in Lysis buffer (50 mM NaH_2PO_4, 300 mM NaCl, 10 mM imidazole, pH 8.0) and cells were sonicated (Branson 250; Branson, Danbury, CT) with 3 cycles of 30 seconds (50 W output and 70% duty cycle). Following, the samples were centrifuged at 14 000 xg for 30 minutes at 4 °C to remove cellular debris and the supernatants,

corresponding to the protein soluble fraction, were collected. Soluble fractions were separated by sodium dodecyl sulfate-polyacrylamide gel electrophoresis (SDS-PAGE) and stained with Coomassie Blue.

3.4. GFP-gp17 purification

The protein expression and purification followed the protocol of Bielmann, *et al.* [193] with some modifications.

A single colony of *E. coli* BL21(DE3) strain harboring pDUVET encoding GPF-gp17 was inoculated in LB medium supplemented with Amp and incubated overnight at 37 ºC in a shaker at 200 rpm (pre-culture). Then, 4 L of LB with Amp were prepared from pre-culture (1:100 dilution) and incubated at 37 ºC and 200 rpm until the OD_{600nm} reached around 0.4-0.5. The culture was cooled down for 30 minutes at room temperature and protein expression was induced by adding IPTG to a final concentration of 0.5 mM at 25 °C overnight in LB + Amp medium. The cells were harvested by centrifugation (4 000 xg, 30 minutes, 4 ºC) and frozen at -80 ºC to potentiate cell lysis. Pellets were then resuspended in Lysis buffer (50 mM NaH_2PO_4, 300 mM NaCl, 10 mM imidazole, pH 8.0), and sonicated (Branson 250; Branson, Danbury, CT) with 3 cycles of 30 seconds each (50 W output and 70% duty cycle). Cell lysates were centrifugated (14 000 xg, 30 minutes, 4 °C) to remove cellular debris and the supernatant corresponding to the soluble fraction was recovered.

The protein purification was carried out through Immobilized Metal Affinity Chromatography (IMAC). Ni-NTA resin (Qiagen**;** 6BCL-QHNI-100 ABT) was equilibrated with 10 column volumes (CV) of purified water and 10 CV of Lysis Buffer. Ni-NTA resin was, then, added to the soluble fraction and incubated at 4 °C for 1 hour under constant agitation, using a roller rotator. Following, Ni-NTA column was washed with 20 CV of Wash buffer (50 mM NaH_2PO_4, 300 mM NaCl, 30 mM imidazole, pH 8.0) to remove any non-specific protein binders. GPF-gp17 was eluted by 1 CV of increasing concentration of imidazole buffer: Elution buffer 100 (50 mM NaH_2PO_4, 300 mM NaCl, 100 mM imidazole, pH 8.0), Elution buffer 200 (50 mM NaH_2PO_4, 300 mM NaCl, 200 mM imidazole, pH 8.0) and Elution buffer 300 (50 mM NaH_2PO_4, 300 mM NaCl, 300 mM imidazole, pH 8.0).

Purified fractions were separated by SDS-PAGE and stained with Coomassie Blue. Fractions with only a single band corresponding to GPF-gp17 molecular weight were pooled. In order to dilute the imidazole, buffer exchange to Storage buffer (50 mM Na_2HPO_4, 100 mM NaCl, 1% Glycerol, pH 8.0) was done using an Amicon concentrator with a 30 kDa membrane.

Purified GPF-gp17 was quantified using NanoDrop 1000 spectrophotometer (Thermo Fisher Scientific, Waltham, MA, USA) and concentration adjusted to 2.14 mg/mL.

3.5. High-Throughput Screening process

A high-throughput screening (HTS) of around 10 000 synthetic small molecules (Chembridge DIVERSet library) was implemented in 96-well plates following an in-house protocol. Compounds in the library are stored in dimethyl sulfoxide (DMSO) at 1 mM in 384-well plates at -20 ºC.

The major characteristics of the Chembridge DIVERSet library molecules are structure heterogeneity, novelty and desirable pharmacological properties as they satisfy the Lipinski's rule of five. Lipinski's rule of five indicates the high drug-likeness potential of new molecules [194].

To proceed with the HTS, 96-well plates (Nunclon 96 round bottom; Orange Scientific, Braine-l'Alleud, Belgium) were loaded with 50 µL of BHI medium using an automated bulk dispenser (Multidrop Combi; Thermo Fisher Scientific, Waltham, MA, USA). Library chemical compounds were added to columns 1-11 at a final concentration of 1 µM by an automated liquid handler (JANUS Automated Workstation; PerkinElmer, Waltham, MA) equipped with a pin tool (V&P Scientific, San Diego, CA, United States).

From overnight pre-cultures, *L. monocytogenes* EGD-e and *L. monocytogenes* EGD-e Δ*rmlT* were diluted in BHI to 0.2 OD_{600nm}. Then, to start cultures at 0.1 OD_{600nm}, 50 µL of *L. monocytogenes* EGD-e were added to wells of columns 1-11, containing BHI and test compounds. Wells in column 12 were compound-free and, for each assay, 50 µL of *L. monocytogenes* EGD-e as a negative control and of *L. monocytogenes* EGD-e Δ*rmlT* as positive control were added. Figure 10 illustrates the HTS plates template.

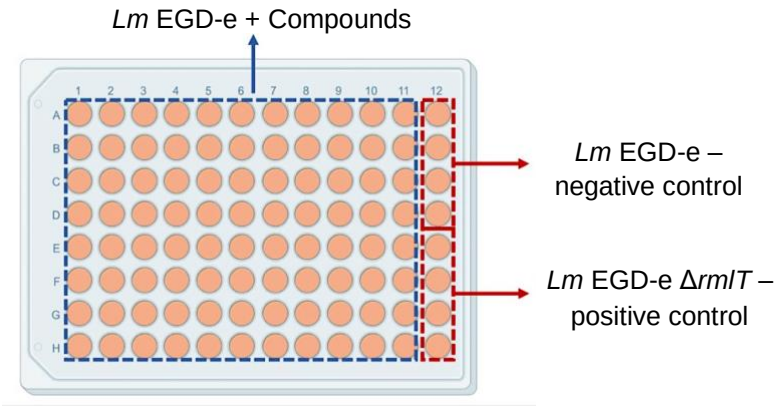

Figure 10 - Organization of the 96-well plate for the screening campaign. *L. monocytogenes* (*Lm*) EGD-e with compounds (columns 1-11). *L. monocytogenes* EGD-e as a negative control (column 12, wells 12A-12D) and *L. monocytogenes* EGD-e Δ*rmlT* as a positive control (column 12, wells 12E-12H).

Plates were then sealed with a Breathe-Easy sealing membrane (Sigma-Aldrich) and incubated at 37 ºC with 200 rpm for 16 hours. Bacterial growth was measured by OD_{600nm} read in a microplate reader, Synergy 2 (BioTek Synergy HT, Winooski, VT).

Then, cells were pelleted by centrifugation at 4 000 xg for 10 minutes at room temperature. Bacterial cells were washed in phosphate-buffered saline (PBS) to remove culture medium. Then, bacteria were incubated in PBS with GFP-gp17 at 17 µg/mL for 20 minutes at room temperature. Once the incubation period was over, cells were washed three times with PBS under the same conditions and finally resuspended in 20 mM Tris with 4% SDS. Relative GFP fluorescence was measured using a microplate reader at 485/528 nm with 120 units of sensitivity at Synergy 2 (BioTek Synergy HT, Winooski, VT).

3.6. Dose-response experiments for hit confirmation

Positive hits obtained in the primary screening were further confirmed via dose-response assays, following the experimental protocol in section E of Material and Methods. The library compounds were assayed in serial two-fold dilutions at concentrations ranging from 0.5 µM to 4 µM, with adequate positive (*L. monocytogenes* EGD-e Δ*rmlT*) and negative (*L. monocytogenes* EGD-e and *L. monocytogenes* EGD-e + DMSO) controls. The hits obtained in the initial dose-response experiments were re-tested, this time with concentrations ranging from 1 µM to 16 µM.

The chemical compounds that also demonstrate antibacterial properties were also tested, using 3 concentrations: 1, 2 and 4 µM.

3.7. Compounds minimum inhibitory concentration (MIC)

Chemical compounds with antimicrobial activity found during the screening were ordered from MolPort (https://www.molport.com). The compounds were dissolved in DMSO, and the minimum inhibitory concentration (MIC) was determined using a range of concentrations from 0.01 µM to 2 µM. Cultures of *L. monocytogenes* EGD-e were prepared from overnight pre-cultures by diluting to 1:100 and inoculated in 96-well plates (Nunclon 96 round bottom; Orange Scientific, Braine-l'Alleud, Belgium) with the respective compound concentration. Bacterial growth was monitored overnight by measuring the OD_{600nm} every 15 minutes using a microplate reader Synergy 2 equipment (BioTek Synergy HT, Winooski, VT).

To confirm the concentration range in which compounds were having an effect, the protocol was scaled-up to 20 mL cultures. The cultures were started at 0.02 OD_{600nm} and bacterial growth curves were obtained by measuring the OD_{600nm} every 30 minutes for 9 hours. The MIC was established as the lowest concentration in which the compound inhibited bacterial growth after the 9 hours of incubation.

To address the action of the compounds during bacterial exponential growth phase, compounds were added in the mid-exponential phase. DC001 was tested from 0.01 µM to 2 µM and DC002 from 0.01 µM to 10 µM.

3.8. HeLa toxicity assays

To evaluate the potential cytotoxic effects of compounds, HeLa cells were seeded in 24-well culture plates (Nuncleon Delta Surface; Thermo Fisher Scientific, Waltham, MA, USA) in DMEM medium supplemented with 10% FBS (Lonza). After 24 hours incubation, culture medium from the plates was replaced by culture medium containing the compounds DC001 and DC002 at six increasing concentrations,1, 2, 4, 8, 16, and 32 µM, and cells were incubated at 37 ºC with 5% CO_2 during 16 hours. Moreover, it was added only DMEM medium supplemented with 10% FBS as a control.

After incubation, phase-contrast images from HeLa cells were visualized and acquired using a 20x 0.4 NA objective lens from Olympus CKX41 microscope (Olympus Inc., Tokyo, Japan) equipped with a digital camera (SC30 Olympus; Olympus Inc., Tokyo, Japan) and using an Olympus cellSens® Microscope Imaging Software (version 1.17; Olympus Inc., Tokyo, Japan).

Furthermore, following incubation, cells supernatant containing death cells was recovered and attached live cells were washed two times with PBS 1X. Cells were harvest with trypsin and resuspended in DMEM with 10% FBS. Cellular suspension was mixed with the dead cells suspension and centrifuged at 450 xg for 5 minutes. Pellets containing both live and dead cells were resuspended in FACS buffer (PBS 1X with 2% FBS). Cellular suspensions were then filtrated to be further analyzed by flow cytometry.

Analysis of cellular viability was performed by flow cytometry using propidium iodide (PI), a fluorescence impermeable dye that binds to DNA. At least 10 000 cells for each sample were collected in Accuri C6 flow cytometer (BD Bioscience, San Diego, CA, USA). Initially, live cells were gated to exclude possible cell debris by creating a gate on the FSC versus SSC plots. Then, live cells were gated to remove doublets with FSC-A versus FSC-H plots, with singlets clustered diagonally. Following, single cells were analyzed using a FL3-A gate, sensitive to light between 610 and 625 nm, suitable for detecting emissions of PI when bound to DNA. Autofluorescence from the samples was measured by analyzing cells without PI staining. Also, untreated HeLa cells were stained with PI and used as a negative control. Data were analyzed using FlowJo (version 10; Tree Star, Ashland, OR, USA). Three independent assays were performed.

3.9. Bacteria invasion assays

HeLa (ATCC CCL-2) cell lines were propagated at 37 ºC with 5% CO_2 in DMEM medium supplemented with 10% FBS (Lonza) in a 24-well plate (Nuncleon Delta Surface; Thermo Fisher Scientific, Waltham, MA, USA). Overnight pre-culture of *L. monocytogenes* EGD-e was diluted in fresh medium (1:10) and agitated at 37 ºC until reaching an OD_{600nm} of

0.6-0.7. Bacterial cultures were then pelleted down (7 500 xg, 2 minutes) and bacteria washed and finally resuspend in DMEM without FBS.

Before infection, HeLa cells were washed two times with medium without FBS. Confluent cell monolayers (~5.0 x 10^5 cells/well) in the 24-well plates (Nuncleon Delta Surface; Thermo Fisher Scientific, Waltham, MA, USA) were infected for 1 hour at 37 ºC with 5% CO_2 with ~2.5 x 10^7 bacteria at a multiplicity of infection (MOI) of 50. After infection, inoculum medium was removed from each well. The cells were incubated with 20 µg/mL gentamicin solution (Lonza), in order to eliminate the remaining extracellular bacteria, and with the respective compounds (DC001 and DC002) at a final concentration of 1, 2, and 4 µM during 90 minutes. A control (*L. monocytogenes* EGD-e incubated with only gentamicin) was used in parallel. Cells were then washed with calcium and magnesium-containing PBS and lysed with 0.2% Triton X-100. Lysates were recovered and serial diluted in PBS. Serial dilutions were plated in BHI-agar plates and intracellular viable bacteria were quantified by counting the resulting colony forming units (CFUs). Three independent assays were performed.

3.10. Statistical Analysis

The software GraphPad Prism (GraphPad Software, San Diego, CA, USA) was used for all statistical calculations and for generating the graphical output. The differences between samples were considered to be non-significant (ns) for $\rho>0.05$ and and statistically significant for: * $\rho<0.05$, ** $\rho<0.01$, *** $\rho<0.001$ and **** $\rho<0.0001$.

The HTS was validated using two factors:

Z'-factor, applied to ensure assays quality, and calculated using the following equation:

$$Z' = 1 - \frac{3\,(SD_{high\ control} + SD_{low\ control})}{(Mean_{high\ control} - Mean_{low\ control})}$$

B-score, a statistical scoring technique, was calculated by normalizing the mean values across all wells in the plates.

HTS looked at positive hits that do not affect bacterial growth, measured by Optical density (OD_{600nm}), but that significantly decrease the level of rhamnose at the bacterial cell surface, measured by GFP-fluorescence (RFUs).

For each 96-well plate the threshold for significant positive hits was calculated through the following equation:

$$Threshold = Mean_{\ RFUs/OD600nm\ of\ compounds\ tested} - 3 \times SD_{\ RFUs/OD600nm\ of\ compounds\ tested}$$

For dose-response experiments, the values obtained by measuring the OD_{600nm} and the RFUs were normalized with the values of the negative control (*L. monocytogenes* EGD-e + DMSO), in order to discard the potential effect of DMSO on bacteria. ANOVA test was employed to compare the means of the groups.

In the toxicity assays, a One-way ANOVA was used with Dunnett's post-hoc test for comparison of means relative to the mean of the control group.

For the invasion assays, the average of replicate values from the treated samples (*L. monocytogenes* EGD-e + hit molecules) were normalized to the non-treated samples (*L. monocytogenes* EGD-e). These values were expressed as the percentage of bacteria that survived when compared to the control group, which was established as 100%. ANOVA was used with Dunnett's post-hoc test for comparison of means relative to the mean of the control group.

4. Results

4.1. Expression and purification of GFP-gp17

The fusion 6xHis-tagged protein GFP-gp17 was needed for the screening process. pDUVET plasmid, provided by Martin J. Loessner [193], encodes the GFP-gp17 protein. This protein consists of rhamnose binding protein (gp17) fused with GFP. It was needed to express and purify GFP-gp17 since it binds to rhamnose and allows to perceive the levels of rhamnose present at the bacterial surface.

To determine the optimal conditions for GFP-gp17 expression, the effect of different incubation temperatures and post-induction incubation times was evaluated. Supernatants of cell lysates, corresponding to the soluble fraction were separated by SDS-PAGE and stained with Coomassie Blue. Results reveal that the optimal conditions for GFP-gp17 (75 kDa) expression in *E. coli* BL21(DE3) were at 25 °C overnight and 30 ºC for 6 hours (Figure 11).

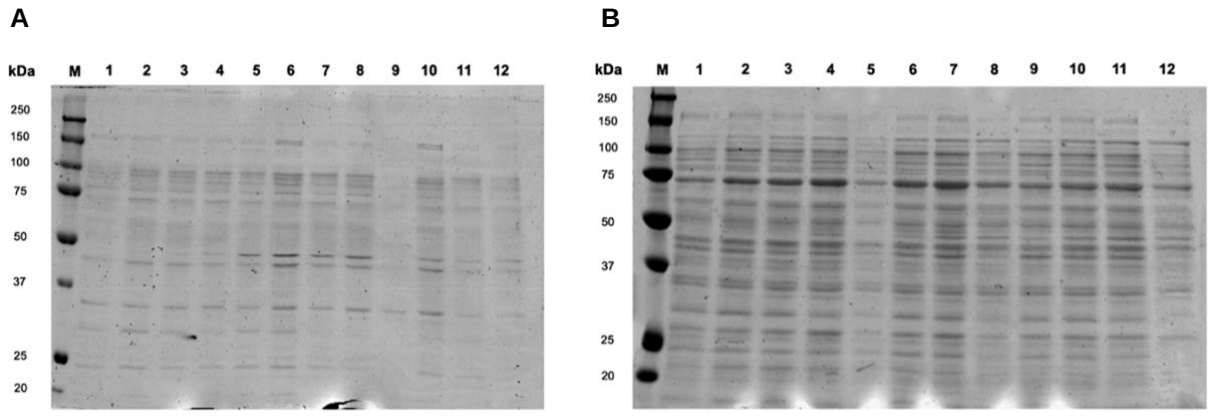

Figure 11 - SDS-PAGE gels stained with Coomassie Blue of the optimization of bacterial recombinant GFP-gp17 protein expression. (**A**) Not induced; (**B**) Induced with 0.5 mM IPTG; M: protein marker; lane 1: 2h of incubation at 25 ºC; lane 2: 4h of incubation at 25 ºC; lane 3: 6h of incubation at 25 ºC; lane 4: overnight incubation at 25 ºC; lane 5: 2h of incubation at 30 ºC; lane 6: 4h of incubation at 30 ºC; lane 7: 6h of incubation at 30 ºC; lane 8: overnight incubation at 30 ºC; lane 9: 2h of incubation at 37 ºC; lane 10: 4h of incubation at 37 ºC; lane 11: 6h of incubation at 37 ºC; lane 12: overnight incubation at 37 ºC.

Accordingly, GFP-gp17 was expressed in *E. coli* BL21(DE3) at 25 °C overnight and purified by IMAC using Ni-NTA resin. The fractions were separated by SDS-PAGE followed by Coomassie Blue staining. Figure 12A shows the resulting Coomassie stained SDS-gels with the total lysate, soluble fraction, flow through, wash with 10 column volumes (CV) and 20 CV and Figure 12B shows the respective eluted fractions containing (His)6-GFP-gp17.

The gel profile in Figure 12B shows very intense bands corresponding to the molecular weight of GFP-gp17 (75 kDa), thus proving its purity. After pooling the fractions, the final concentration was adjusted to 2.14 mg/mL. The amount of purified protein was enough to do around 25% of the screen.

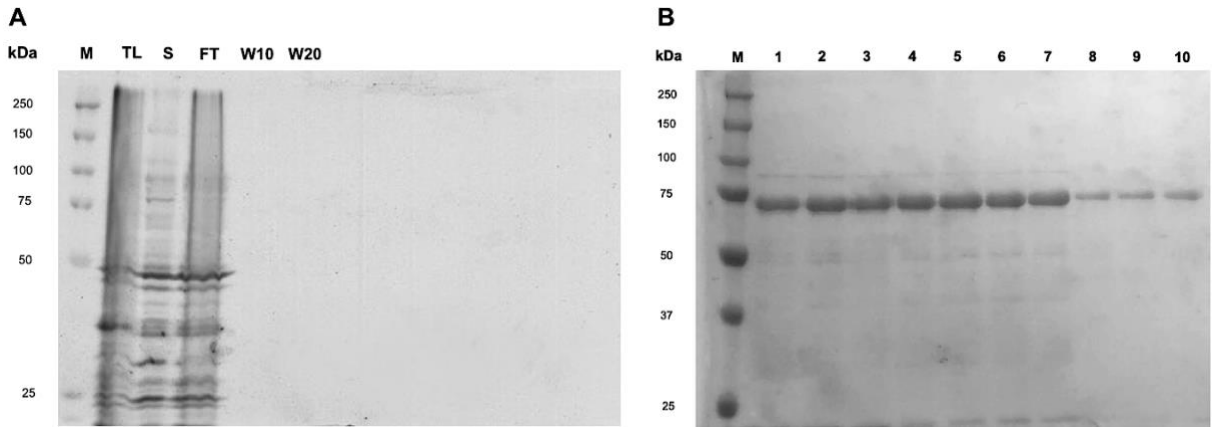

Figure 12 - Purification of GFP-gp17 from *E. coli* BL21(DE3). (**A**) Coomassie stained SDS gels showing the protein marker (M), total lysate (TL), soluble (S), flow through (FT), Wash 10 (W10) and Wash 20 (W20); (**B**) SDS-PAGE analysis of the protein elution with imidazole. M: protein marker; lanes 1-4: elution with 100 mM imidazole; lanes 5-7: elution with 200 mM imidazole; lanes 8-10: elution with 300 mM imidazole.

4.2. Initial screening of chemical compounds and dose-response assays

To identify potential drug candidates impairing the levels of rhamnose at the bacterial cell surface and/or molecules with antibacterial activity, a library of ~10 000 compounds (Chembridge DIVERSet library) was screened (Figure 13). In 96-well plates, bacteria were incubated for 16 hours with the library chemical compounds. Positive (*L. monocytogenes* EGD-e Δ*rmlT*) and negative controls (*L. monocytogenes* EGD-e) were also added to each plate. Culture growth was monitored by OD_{600nm}. Following, bacteria were incubated with the GFP-gp17 protein and the levels of rhamnose were measured by Relative GFP fluorescence (RFUs).

Background noise was excluded from all raw OD_{600nm} values and each OD_{600nm} value was normalized to the average of the values of the entire plate, except the controls. For the GFP fluorescence analysis, the average value of the fluorescence of bacteria lacking rhamnose (*L. monocytogenes* EGD-e Δ*rmlT* mutant) was removed from all GFP raw values. Each value of GFP fluorescence was also normalized to the average of the values of the entire plate, except the controls. Consequently, two values ranging between -1 and 1 were achieved for each compound tested. Dividing the two values, a ratio $RFUs/OD_{600nm}$ was obtained.

For each plate assay tested in the initial screen, a statistically significant threshold was calculated, using the equation: $\text{Mean}_{\text{RFUs/OD600nm of compounds tested}} - 3 \times \text{SD}_{\text{RFUs/OD600nm of compounds tested}}$. Compounds with a ratio $RFUs/OD_{600nm}$ below the threshold were defined as hits, possibly interfering with the presence of rhamnose at the surface of the bacteria without affecting bacterial growth.

Additionally, compounds were also defined as hits if they significantly inhibit the bacterial growth.

Z'-factor, a statistical data assay quality indicator that shows how successfully the controls are separated, was calculated and was found to be 0.76, indicating excellent quality screens.

From the initial screening, 123 hits (~1.23%) were identified as potential inhibitors of the rhamnose levels at the bacterial surface and 2 hits (~0.02%) were identified with high capacity of antimicrobial activity.

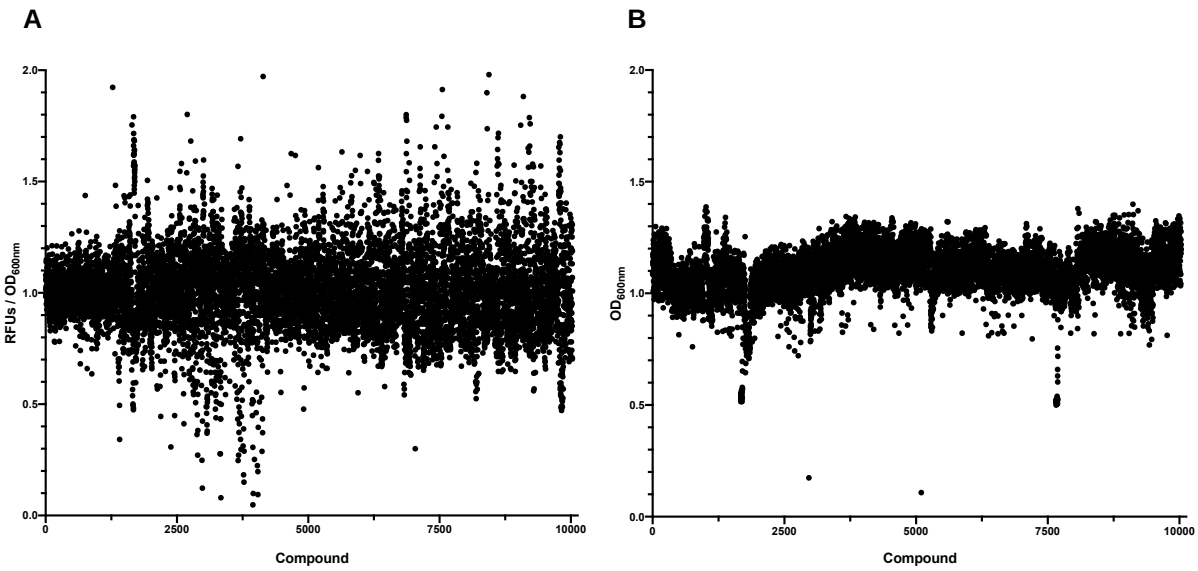

Figure 13 - Graphical representation of the high-throughput screening results. A library of ~10 000 compounds was screened at 1 µM in a 96-well plate format. Each plate contained 4 wells each of a positive (*L. monocytogenes* EGD-e Δ*rmlT*) and negative control (*L. monocytogenes* EGD-e). For each plate was calculated a significant threshold (Mean $_{RFUs/OD600nm\ of\ compounds\ tested}$ − 3 x SD $_{RFUs/OD600nm}$) and compounds with a ratio RFUs/OD_{600nm} below this value were considered hits, possibly inhibiting rhamnose at the surface of the bacteria. Additionally, compounds that inhibited bacterial growth were considered as hits as well. (**A**) Scatter plot of results of the potentials candidate hits for inhibitors of the rhamnose at the bacterial surface; (**B**) Scatter plot of results of the potentials molecules with bacterial growth inhibition activity.

Each compound was only tested once in this initial screen, subsequently false positives/negatives were expected. Verifying the legitimacy of the active compounds is critical in any HTS experiment since mistakes are statistically likely to arise when working with a huge number of compounds. Accordingly, the compounds identified in the primary screen were retested via dose-response assays. The experimental protocol followed for the dose-response experiments was the same as described before for the initial screening.

Compounds were assayed in serial two-fold dilutions in order to confirm their activity. None of the 123 compounds shown a dose-response profile at the range of tested concentrations (Figure S1 and S2, supplementary material). However, the 2 compounds that have shown antimicrobial properties in the initial screen, still presented the inhibitory potential

in the range of concentrations tested in the assay (Table 3). From now on, these compounds will be referred to as DC001 and DC002 (Figure 14).

The HTS developed was robust enough with a Z'-factor value indicating excellent quality screens. The primary screening was able to identify an acceptable number of hits molecules that led to the discovery of 2 highly promising compounds with antimicrobial properties.

Table 3 - Summary of the screening results.

Target	Plates screened	Compounds screened	Primary hits	Dose-response confirmed hits
Rhamnose	114	~10 000	123	0
Bacterial growth			2	2

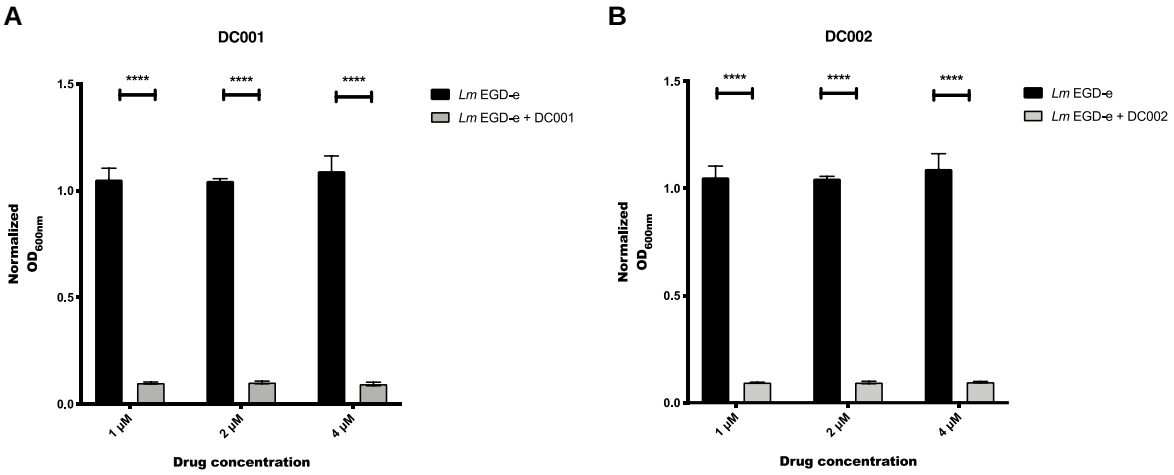

Figure 14 - Dose-response of *L. monocytogenes* (*Lm*) treated with DC001 and DC002. (**A**) *L. monocytogenes* incubated with DC001 at 1, 2 and 4 µM. (**B**) *L. monocytogenes* incubated with DC002 at 1, 2 and 4 µM. OD_{600nm} was normalized to the negative control (*L. monocytogenes* EGD-e + DMSO). Error bars represent the standard deviation. Statistically significant differences are represented as: **** $\rho<0.0001$.

4.3. Minimum inhibitory concentration (MIC)

MIC assays were performed to determine the spectrum of bacterial inhibitory potential of DC001 and DC002, and thus to discover the lowest concentration of the drugs required to inhibit the visible growth of the microorganism. In 96-well plates, it was diluted an overnight pre-culture of *L. monocytogenes* EGD-e to 1:100 in medium and inoculated with several concentrations of DC001 and DC002. The growth was monitored overnight by measuring the OD_{600nm} every 15 minutes using a microplate reader.

DC001 started affecting the bacterial growth of *L. monocytogenes* at 0.25 μM and was able to completely inhibited the growth at 0.75 μM, therefore having an intermediary activity range of 0.1-0.75 μM (Figure 15A). DC002 did not show any antimicrobial activity up to 1 μM, thus having an intermediary activity range of 0.75-1 μM (Figure 15B).

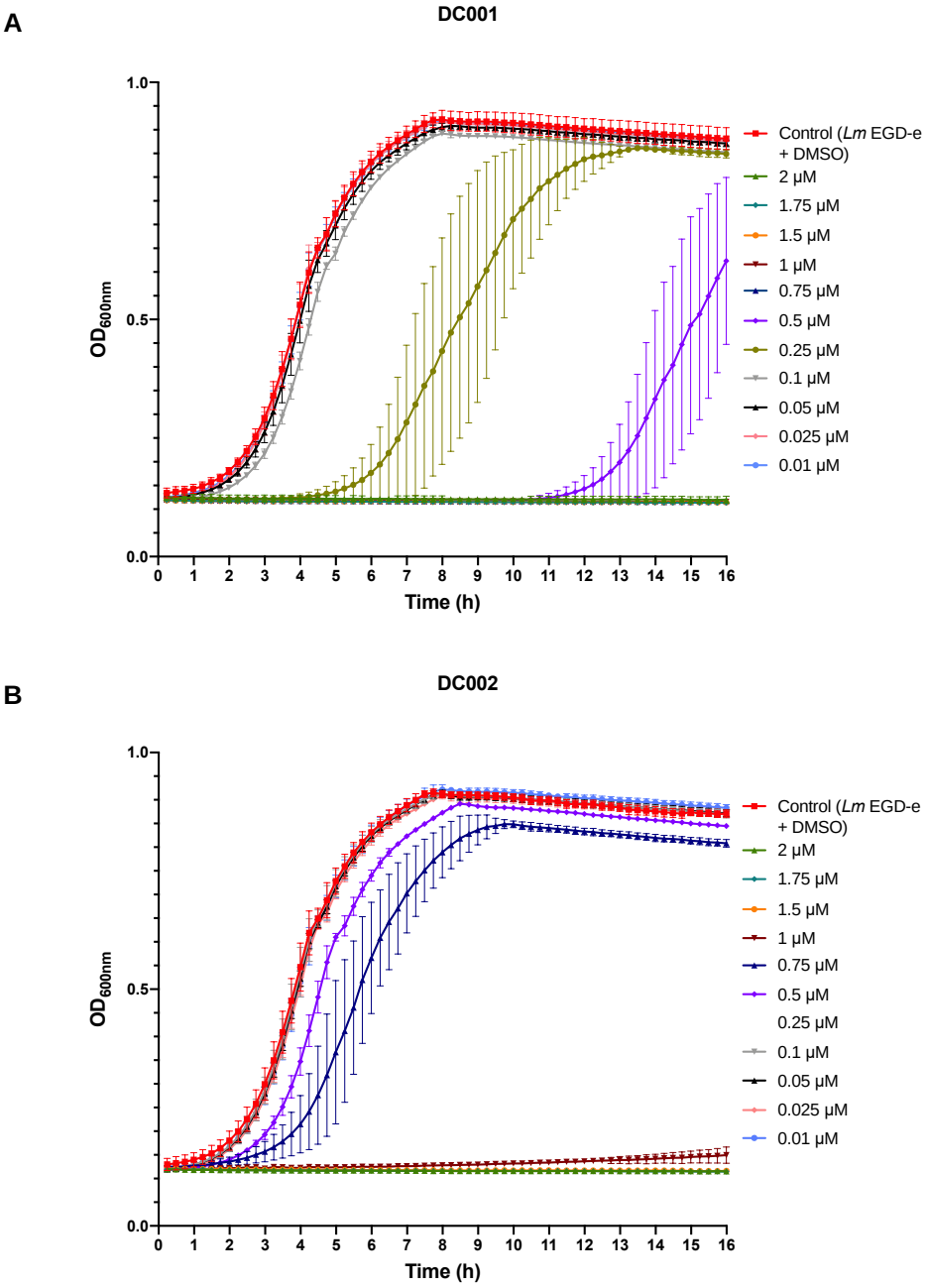

Figure 15 - Determination of minimum inhibitory concentration based on growth curve assay performed in 96-well plates. Growth curves were obtained by measuring the OD_{600nm} every 15 minutes for 16 hours. (**A**) Growth curves of *L. monocytogenes* incubated with the several concentrations of DC001; (**B**) Growth curves of *L. monocytogenes* incubated with the several concentrations of DC002. Values are the mean ± SD (n=3), error bars represent the standard deviation.

Following this, the protocol was scaled up to a larger culture volume (20 mL), since the action of antimicrobial compounds can be slightly different in a larger bacterial culture. In this situation, MIC value of DC001 was established at 0.25 μM (Figure 16A) and the MIC value of DC002 at 0.75 μM (Figure 16B).

The scale-up experiment confirmed the hypothesis that the action of the compounds changes slightly in a larger bacterial culture. Comparing to the previous results, MIC of DC001 decreased, from 0.75 μM to 0.25 μM, whereas MIC of DC002 reduced from 1 μM to 0.75 μM.

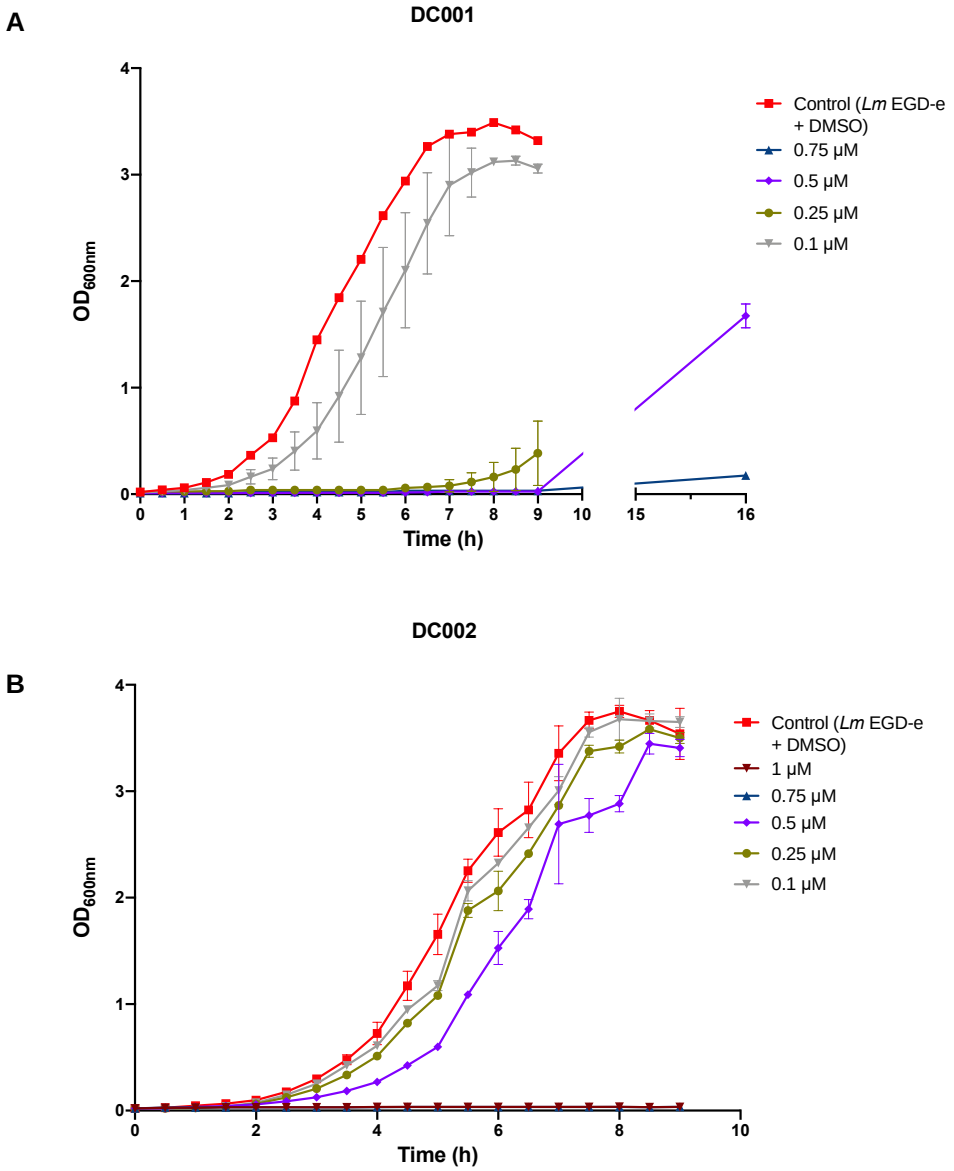

Figure 16 - Determination of minimum inhibitory concentration based on growth curve assay performed in a 20 mL culture. Growth curves were obtained by measuring the OD_{600nm} every 30 minutes for 9 hours. (**A**) Growth curves of *L. monocytogenes* incubated with several concentrations of DC001; (**B**) Growth curves of *L. monocytogenes* incubated with several concentrations of DC002. Values are the mean ± SD (n=3), error bars represent the standard deviation.

4.4. Effect of DC001 and DC002 on exponential phase bacteria

Different concentrations of DC001 and DC002 were tested to address their effects on *L. monocytogenes* EGD-e in exponential growth phase, to simulate a real *in vivo* infection. The experimental protocol was the same as for the MICs, yet compounds were added in the mid-exponential phase. DC001 demonstrated having an effect on exponential phase bacteria from 0.5 µM (Figure 17A), whereas DC002 exhibited a clear effect from 4 µM and a slight inhibition from 2 µM (Figure 17B).

Bacteria in exponential phase demonstrated to be more resistant to DC001 and DC002 comparing to the results of the MICs assays.

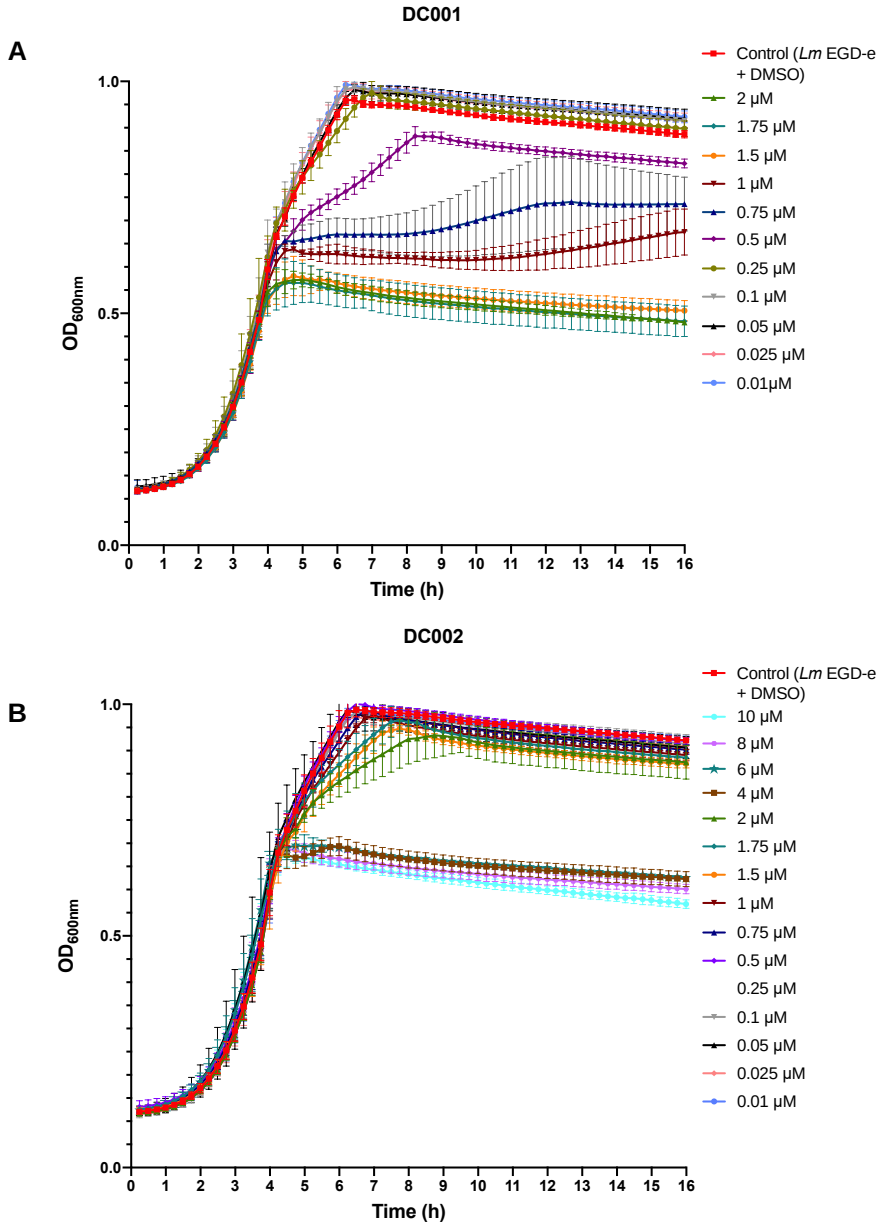

Figure 17 - Determination of DC001 and DC002 effects on exponential bacteria. Growth curves were obtained by measuring the OD_{600nm} every 15 minutes for 16 hours. (**A**) Growth curves of *L. monocytogenes* incubated with increasing concentrations of DC001; (**B**) Growth curves of *L. monocytogenes* incubated with increasing concentrations of DC002. Values are the mean ± SD (n=3), error bars represent the standard deviation.

4.5. Cytotoxic effects of the compounds in HeLa cells

To discern the cytotoxic effect of DC001 and DC002 in human cells, these compounds were screened against HeLa cells at several concentrations. Cytotoxicity studies are fundamental in determining the potential toxicity of the compounds. Knowing which concentrations are non-toxic to cells is critical to choose concentrations that do not harm the eukaryotic cells.

HeLa cells were seeded in 24-well culture plates in DMEM with FBS. After 24 hours of incubation, the culture medium of the wells was replaced by culture medium containing DC001 and DC002 at increasing concentrations and plates were incubated for 16 hours. A control, only DMEM medium supplemented with FBS was also made.

Following incubation, phase-contrast images from HeLa cells were acquired using a 20x 0.4 NA objective lens from Olympus CKX41 microscope equipped with a digital camera. From the images, it is possible to see that both compounds start to have some slight cytotoxic effects on HeLa cells from a concentration of 4 µM, with this cytotoxic effect being clearly visible at 8 µM (Figure 18).

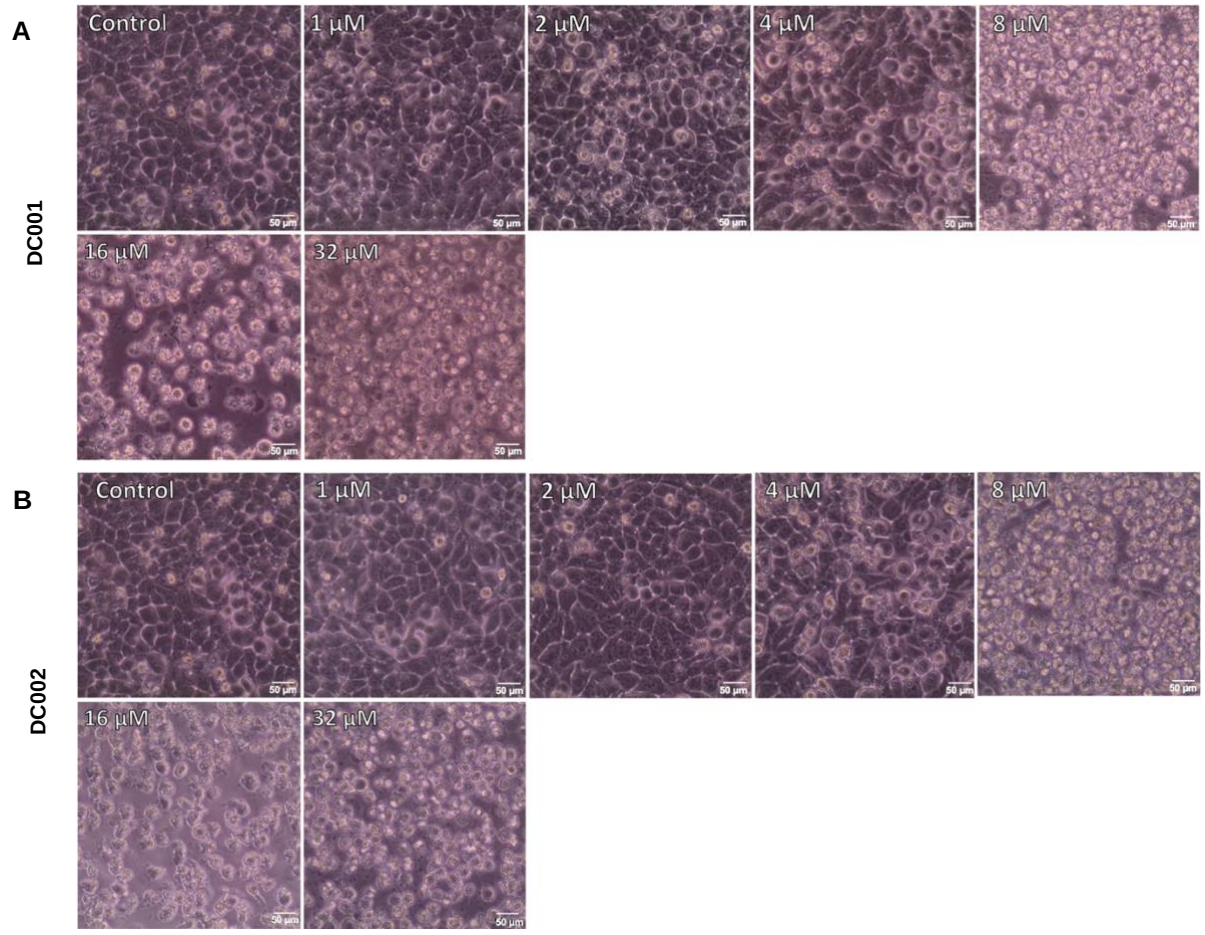

Figure 18 - Phase-contrast microscopy images of HeLa cells incubated with several concentrations of DC001 (**A**) and DC002 (**B**) for 16 hours. HeLa cells images were acquired using an Olympus CKX41 microscope equipped with a digital camera and Olympus cellSens® Microscope Imaging Software. A control (HeLa cells incubated with DMEM with 10% FBS) was also made. Scale bars, 50 µm.

To corroborate previous observations in the microscope, cellular viability was assessed by flow cytometry following PI staining. Live cells were gated to remove the cell debris and gated again to remove doublets. Following, cells were analyzed for PI fluorescence (Figure S3, supplementary material). Results from three independent experiments demonstrated that both DC001 and DC002 compounds are non-toxic to HeLa cells up at a concentration of 4 μM (Figure 19).

Hence, up to 4 μM, both molecules do not damage HeLa cells in terms of cellular integrity. Accordingly, concentrations up to 4 μM of DC001 and DC002 can be tested on *Listeria*-infected HeLa cells.

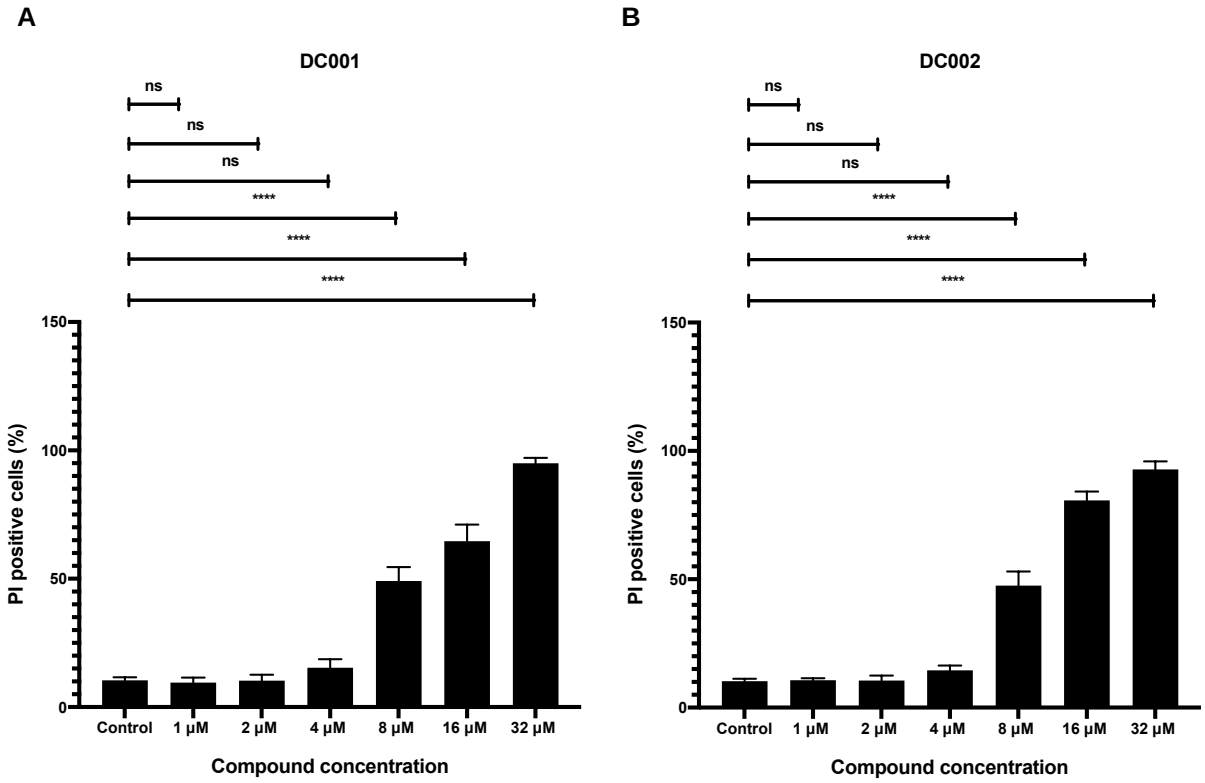

Figure 19 - Flow cytometry analysis of the percentage of PI positive HeLa cells following treatment with DC001 (**A**) and DC002 (**B**). Values are the mean ± SD (n=3), error bars represent the standard deviation. At least 10 000 cells for each sample were collected in Accuri C6 flow cytometer. Untreated HeLa cells were stained with PI and used as a negative control. Data were analyzed using FlowJo. Statistically significant differences are represented as: **** $\rho<0.0001$. Non-statistically significant differences are represented as: ns.

4.6. Bacterial invasion assays in epithelial cells

DC001 and DC002 were tested *in vitro* to ascertain their ability to inhibit *L. monocytogenes* growth/propagation in HeLa cells. The pathogenic *L. monocytogenes* can infect non-phagocytic cells, including epithelial cells, like HeLa cells. Therefore, HeLa cells are frequently used in *L. monocytogenes* studies [195-197].

HeLa cells were infected with *L. monocytogenes* EGD-e and then incubated with gentamicin in order to kill extracellular bacteria. At the same time, DC001 and DC002 were added at a final concentration of 1, 2, and 4 µM. Infected cells were then lysed and intracellular bacteria were plated in serial dilutions for CFUs counting.

DC001 did not show any activity reducing the levels of intracellular *L. monocytogenes* at the tested concentrations (Figure 20A). DC002, despite showing a slight increase in intracellular bacteria, has no bactericidal activity on intracellular bacteria at the concentrations tested as well (Figure 20B).

Although the compounds had an antibacterial effect when directly incubated in bacterial cultures, they did not present any action against *Listeria*-infected HeLa cells under the conditions tested.

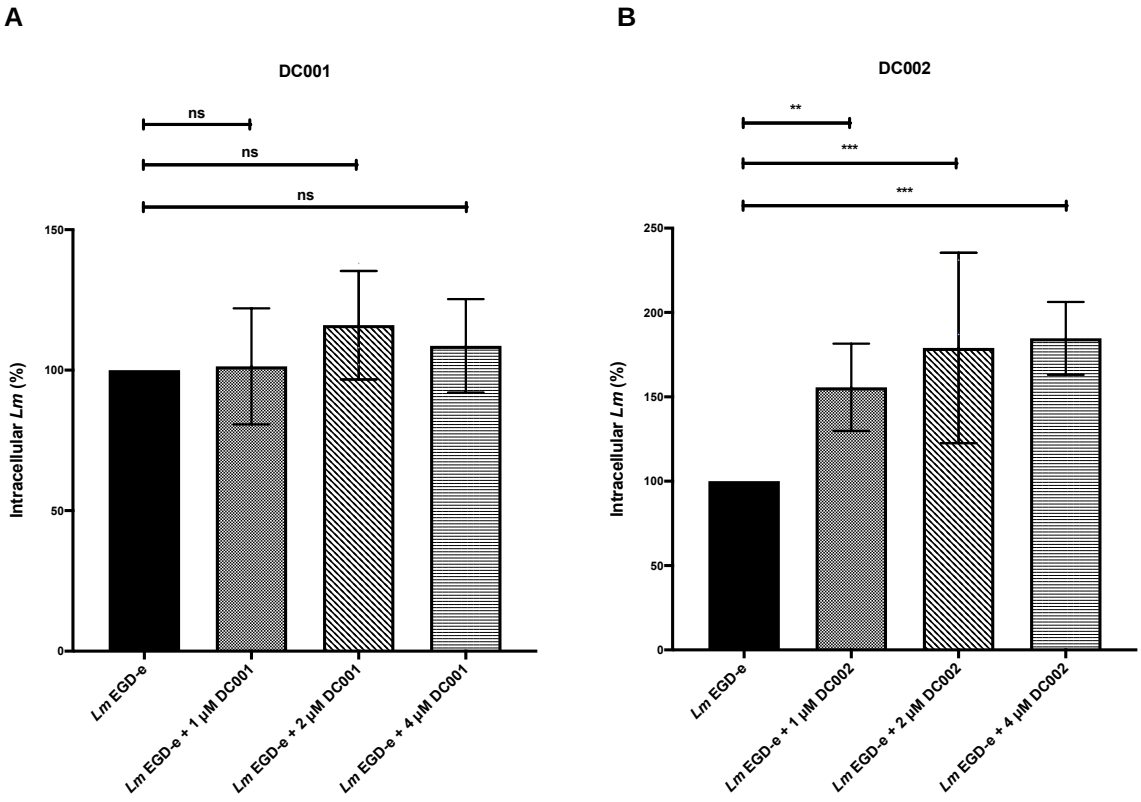

Figure 20 - Quantification of viable intracellular bacteria after HeLa cells infection with *L. monocytogenes* in exponential-phase and treatment with DC001 (**A**) and DC002 (**B**), at 1, 2 and 4 µM. The averaged replicate values from the treated samples were normalized to the non-treated samples (control). These values were expressed as the percentage of bacteria that survived in comparison to control, established at 100%. Values are the mean ± SD (n=3), error bars represent the standard deviation. Each treatment was performed in triplicate. Statistically significant differences are represented as: ** $\rho<0.01$, and *** $\rho<0.001$. Non-statistically significant differences are represented as: ns.

5. Discussion

L. monocytogenes is one of the most invasive foodborne pathogens with significant public health and economic consequences, as it has been linked to several lethal listeriosis outbreaks [58]. Antibiotic resistance in *L. monocytogenes* is not currently a huge concern, however strains of *L. monocytogenes* isolated from food products have already begun to show antibiotic resistance [53], meaning that future outbreaks will be more challenging to control. Antibiotic resistance, particularly multidrug resistance, has arisen and developed among foodborne bacteria, such as in *L. monocytogenes*, over the last few decades. In this bacteria, resistance to antibiotics is thought to be accomplished mainly through the acquisition of movable genetic elements [56]. Resistance to antibiotics is on the rise at a dangerous rate and, as a result, there is an urgent need for the continuous discovery of novel antimicrobials compounds to compete with the constantly evolving bacteria.

In this study, we described the development of a small-molecule HTS assay that can be exploited for the discovery of novel molecules targeting cell wall glycosylations. Over 10 000 synthetic small molecules from Chembridge DIVERSet library (Chembridge, San Diego, CA, United States) were tested. The main characteristics of the compounds in this library are structure diversity, novelty and desirable pharmacological properties, since they fulfil the Lipinski's rule of five. The Lipinski's rule of five was developed to indicate the high drug-likeness potential of new molecules. In the drug discovery setting this guideline prioritized chemical compounds that molecular weight is less than 500 daltons, that has no more than 5 hydrogen bond donors and no more than 10 hydrogens bond acceptors, and which has an octanol-water partition coefficient log P of less than 5 [194]. HTS of small-molecule libraries has proven to be a powerful technique, contributing to the discovery and development of several new drugs [198, 199].

The Chembridge DIVERSet library (Chembridge, San Diego, CA, United States) was tested to discover compounds that decrease the levels of rhamnose at bacterial cell surface without affecting bacterial growth and also to identify potential new antibiotic molecules against *L. monocytogenes*. The decoration of WTAs with L-rhamnose is strictly dependent on the RmlT glycosyltransferase [158]. As a result, inhibiting RmlT protein would prevent the presence of rhamnose at the bacterial surface. The absence of rhamnose would render *Listeria* less virulent by reducing its surface-exposed virulence factors [81] and more susceptible to AMPs and antibiotics [157], without inducing selection pressure for resistance mechanisms due to the fact the WTA rhamnosylation (WTA-rha) is not essential for the bacterial growth. Additionally, with the rise in antibiotic resistance, discovering novel antibiotics against *L. monocytogenes* is critical since drug-resistant infections pose a serious danger to human, animal, and environmental health. Other HTS studies on *L. monocytogenes* have been performed, resulting in the discovery of new antibacterial molecules and targets [180, 181, 183, 200], emphasizing the usefulness of these types of assays against pathogenic bacteria.

The high-throughput screening here implemented offers a method to test a large number of diverse chemical compounds that would impair the level of rhamnose at the bacterial cell surface. This type of screen is called “Targeted Screen” and have advantages and disadvantages compared with other types of screens such as Diversity Screens and RNAi Screens. Targeted Screens have the advantage of looking for a drug that selectively binds to/inhibit a specific target with a mechanism of action usually known [201]. Furthermore, the high amount of microbial genomes sequenced turns possible to identify conserved target proteins across bacterial families, resulting in the discovery of drugs with a wide spectrum action [202]. In contrast, the significant disadvantage of a targeted screening is the existence of only a single target that leads to a reduction in the number of possible hits compared to other screening procedures. Also, considering it depends exclusively on the mechanism of action of one target, in the absence of complete knowledge, makes targeted screening more challenging [201].

In the HTS process, the Z’-factor was calculated. Z’-factor is a routinely statistic measure that reflects how effectively the positive and negative controls are separated, indicating the quality of the assays. A value of Z’-factor between 0.5-1.0 represents a robust assay with a statistically reliable separation of positive and negative controls [177, 178]. A Z’-factor value of 0.76 was obtained in this HTS, confirming a satisfactory assay. Analyzing the literature, the Z’-factors in other antimicrobial discovery HTS studies appear to vary between 0.68-0.80 [203-206], indicating that the Z’-score value here obtained was the expected for this type of assay.

In the HTS here implemented, bacteria were incubated with the respective compounds and then culture growth was monitored by OD_{600nm}. Following, bacteria were incubated with the GFP-gp17 protein and the quantity of rhamnose was measured by Relative GFP fluorescence, obtaining a ratio $RFUs/OD_{600nm}$.

The background noise was removed from all the raw values of OD_{600nm}. Next, each OD_{600nm} value was normalized to the average of the values of the entire plate (excluding the controls). For GFP fluorescence, the average value of the fluorescence of bacteria lacking rhamnose (*L. monocytogenes* EGD-e Δ*rmlT* mutant) was removed from all GFP raw values. Following, each value of GFP fluorescence was also normalized to the average of the values of the entire plate (excluding the controls). Therefore, two values between -1 and 1 were obtained for each compound tested. Dividing the two values, a ratio $RFUs/OD_{600nm}$ was achieved. For each 96-well plate tested, a significant threshold was calculated ($\text{Mean}_{\text{RFUs/OD600nm of compounds tested}} - 3 \times \text{SD}_{\text{RFUs/OD600nm of compounds tested}}$). Molecules with a ratio $RFUs/OD_{600nm}$ below the threshold were defined as hits, theoretically capable to reduce rhamnose levels at the bacterial cell surface without affecting the bacterial growth.

In the equation used to calculate the threshold, it was chosen 3 x SD since 99.7% of data observed following a normal distribution lies within 3 standard deviations of the mean, ensuring that the error is below 5%. If it was chosen 1 x SD or 2 x SD, it would be lost many values outside (68.2% and 95.4%, respectively).

A low value of RFUs and a high value of OD_{600nm} (low ratio RFUs/OD_{600nm}) means that the compound is possibly affecting the rhamnose at the bacterial surface without disturbing the growth of the bacteria, therefore disarming the pathogen without inducing a selective pressure for resistance. On the other hand, a ratio value of 1 means that the molecule does not have any effect on the bacteria. For example, compounds with a RFUs/OD_{600nm} ratio of 0.8 and 1.2, in a plate with a threshold of 1.1, are a hit and a non-hit, respectively.

Considering that the bacterial growth is measured by optical density at 600 nm, it enables the discovery of molecules with antibacterial growth action, that could be used as novel antimicrobials.

The primary HTS identified 123 molecules (~1.23%) that met the initial selection criteria for rhamnose reduction at the bacterial cell surface and 2 compounds (~0.02%) with antibacterial activity. The identified hits were then re-tested in dose-response assays to eliminate the false positive hits. The dose-response assays revealed that none of the 123 compounds showed activity decreasing rhamnose at the bacterial cell surface for the range of concentrations tested (Figure S1 and S2, supplementary material). Reversely, the 2 antibacterial molecules were confirmed for the antimicrobial activity (DC001 and DC002). A hit rate of 0.02% resulting from the screening of 10 000 small molecules encounters the expectation for the developed methodology, as usual hit rates from experimental HTS can vary between 0.01-0.14% [207]. Increasing the number of compounds tested as much as possible could help increase the success rate [208]. Likewise, selecting a specific chemical space [209], which contains molecules previously known to have a certain desired action on the target, would boost the hit rate [210].

The high false-positive rate present in the HTS could be due to the edge effect that generates noise and variability. The edge effect consists of the cells growing or behaving differently in edge wells compared to inner wells and is a common and well-recognized problem in this type of screening. As a result of this effect, wells near the plate's edges frequently exhibit different readouts than those at the plate's center. It is thought that this issue is due to a temperature gradient across the plate that is generated when the plate is in the incubator. Since the edge wells reach 37 °C faster than the inner wells, the outer wells tend to respond differently than the inner wells in the screening [211]. Furthermore, variable evaporation across the plate wells has also been reported to be implicated in the edge effect [212, 213]. To try to reduce the variability caused by this effect, we applied a statistical criterion, the B-score. The B-score normalizes the value of a well with the average of the values of the wells around,

accounting for data variability, as it removes unwanted column and row positional biases [214, 215]. Even applying this criterion, the results remained with a lot of variability. Both false negative and false positive hits are unavoidable when working with a large number of compounds and verifying the authenticity of the compounds is essential in any HTS experiment. As a matter of fact, the edge effect led to several false positive hits in the primary screening, inducing reproducibility issues, as the dose-response assays revealed. An effort to minimize these variations in the screening could have been done, for example excluding perimeter wells (columns 1 and 12; rows A and H) and instead filling those wells with only culture medium [216]. Having this in mind, in the dose-response experiments, it was only used the inner wells of the plates, exposing the screen reproducibility issues. At the compound concentration used for the screen, no molecule showed impact in the rhamnose levels at the bacterial cell surface. It is important to highlight that only a single concentration, 1 μM, was tested in the primary screening. While it might be tempting to increase the compound concentration in the screening to try to comprise weaker hits, this may only produce a higher false-positive hit rate [217]. Besides, in the initial screens campaigns, is usual to only test a single concentration of the compounds. Further testings with increasing concentrations of the hit molecules are commonly performed after the initial identification [203, 205, 206].

The two molecules with antibacterial activity discovered in the screening were purchased from another supplier and assays were performed to find out the respective MICs. Obtaining the molecules from a different supplier is essential to confirm the action of the compounds, avoiding single-sourcing risks [218].

MICs are defined as the lowest concentration of an antibiotic that is able to suppress the observable growth of a microorganism after overnight incubation. Accordingly, MICs assays were achieved by diluting an overnight pre-culture to 1:100 in medium and inoculating with the respective compound concentration. When starting a culture by placing a few microorganisms into the culture medium, bacteria have to adapt to the new environmental growth conditions (lag phase). In contrast, exponential phase bacteria already have an established bacterial community and are at the peak of their growth [219-221]. Consequently, different growth phases have different bacterial fitness, a physiological feature that determines population dynamics and is characterized as the capacity to modify metabolism, adapting to environmental conditions [222, 223].

When addressing the action of the compounds against exponential phase bacteria, *Listeria* exhibited a more resistant phenotype to the hit drugs compared to the results of the MICs assays. MIC value of DC001 was found to be 0.25 μM, whereas against exponential phase bacteria demonstrated having effect only from 0.5 μM. DC002 was found to have a MIC value of 0.75 μM and exhibited a clear effect against exponential phase bacteria only from 4 μM. This is expected considering the experiments were carried out in different fitness phases.

The concentrations tested were identical in both experiments, so in the MICs assays, the same number of compound molecules was added for a smaller number of bacteria. As stated before, MICs experiments were accomplished by addressing the effects of the compounds since the beginning of a bacterial culture (lag phase), as this is the standard and definition itself of this type of experiment. DC001 and DC002 action was also verified against exponential phase bacteria with the purpose of simulating a real *in vivo* infection. In the case of an *in vivo* infection, the antibiotic when administered would be in a patient with a proliferating infection, which is more similar to the exponential phase of culture [224, 225].

Listeriosis, the infectious disease caused by *L. monocytogenes*, is frequently treated with β-lactam antibiotics, penicillin and ampicillin, alone or in combination with gentamicin [48]. Antimicrobial susceptibility of *L. monocytogenes* isolates from patients were evaluated by broth microdilution method, according to the European Committee on Antimicrobial Susceptibility Testing international guidelines. In this study, $MICs_{90}$ (MIC value at which ≥ 90% of the isolates are inhibited) were found to be 1.43 μM for ampicillin, 0.7 μM for penicillin, and 1.04 μM for gentamicin [226]. Hence, it is possible to notice that the MICs of DC001 and DC002 are within the MIC ranges described in the literature of the currently antimicrobials used in the treatment of listeriosis, indicating the DC001 and DC002 are, at least, as potent as clinical antibiotics.

Once the MICs were established, several drug concentrations were screened against HeLa cells and the potential cytotoxic effects were addressed by a flow cytometry analysis. Results from flow cytometry-based assay revealed the concentration values in which compounds did not exhibit cytotoxic effects against HeLa cells. Based on these results, 1, 2 and 4 μM of each compound were tested against intracellular *Listeria*, since these concentrations were observed to not affect the viability of the eukaryotic cells.

L. monocytogenes has the ability to infect non-phagocytic cells, including epithelial cells. HeLa are epithelial cells and one of the most researched and used cell lines, it offers practicability and reproducibility, while being easy to maintain. Furthermore, the value of this cell line as a suitable tissue culture model for studying *L. monocytogenes* infection has been distinctly proved [195]. To provide consistent invasion of confluent HeLa cell monolayers, the MOI and the bacterial invasion time employed were crucial. It was used a MOI of 50 with a 1 hour invasion period, as it is frequently shown in the literature as the standard for good invasion phenotypes [196, 197]. The capacity of this facultative intracellular pathogen to induce its internalization into non-phagocytic cells is the key to its success. Taking this into consideration, an invasion assay was chosen over other assays, since it is the most appropriate protocol to address the behaviour of intracellular bacteria [227, 228].

The concentrations of the compounds tested in the Hela cells infected with bacteria were higher than the respective MICs to increase the probability of the molecules entering into the cells. DC001 and DC002 were added to the HeLa cells along with gentamicin solution.

Since gentamicin, at the concentration used, can not penetrate eukaryotic cells, it will only kill extracellular bacteria and not damage the intracellular *Listeria*, allowing to perceive only the effect of DC001 and DC002.

Neither DC001 and DC002 were able to kill intracellular *L. monocytogenes* in HeLa cells. This inability is most likely due to the compounds not being capable of penetrating the eukaryotic cells at the tested concentrations (1, 2 and 4 μM). If higher concentrations were tested, it would increase the probability of the molecules entering the cells and acting against the bacteria. However, toxicology studies revealed that concentrations of DC001 and DC002 greater than 4 μM had cytotoxic effects on HeLa cells. Moreover, the number of bacteria that infect the cells may not be enough to observe differences between the control and the treated samples. DC002 presented a slight increase in intracellular bacteria, probably due to the limitations of the technique.

If an assay was carried out with a longer incubation time with the compounds, enabling the intracellular bacteria to multiply, it would perhaps make it possible to observe differences. Following the addition of gentamicin, various incubation periods can be employed for a better understanding of the entrance efficiency and the ability of *Listeria* to replicate within infected cells [229, 230].

It is important to bear in mind that the molecules were only tested in HeLa cells and testing the compounds in other cells lines would be the next stage in the project. Perhaps if the compounds were tested in other cell lines, the outcomes would be different and the action of the drugs on intracellular *Listeria* would be perceptible. For example, previous studies reported that Caco-2 and human epithelial HEp-2 are appropriate for the evaluation of adherence, invasion, and virulence of *L. monocytogenes* [125, 231]. Additionally, since *Listeria* can also infect phagocytic host cells, especially macrophages [68], testing also in these cells would possibly give other results.

It is also noteworthy that DC001 and DC002 found in the screening, were directly used and have not yet been optimized in any way. Drug optimization consists of the process where a candidate drug is designed to optimized its therapeutic activity. Biochemical enhancement of the molecules could improve drug efficacy, helping the drugs entrance into the eukaryotic cells and improving their action. Likewise, drug delivery to a desired site is a difficult challenge in the treatment of many illnesses. Using drug carriers can considerably improve the effectiveness and lessen the adverse effects of medications administered [232]. Several drug carriers have already been studied to improve the action of antibiotics against intracellular bacteria. In particular, there are various reports of loading antibiotics into liposomes, microspheres, and nanoplexes, that seemed to improved delivery to infected cells [233]. Moreover, recently have been reported an improvement of drug efficacy by combination with

ionic liquids [234]. Additionally, fullerenols $C_{60}(OH)_n$ are acknowledged to increase HeLa cells permeability with minimal cytotoxicity effects [235].

The encapsulation of ampicillin and gentamicin, the most common treatment choice to fight listeriosis, in liposomes, was studied and results revealed a decrease in the survival of *L. monocytogenes* [236] and an increase of bactericidal activity [237], respectively.

Therefore, implementing a combination of enhancers or drug carriers with the DC001 and DC002, would possibly improve the action and entrance of the molecules.

According to the chemical similarity principle, two compounds with identical structures are likely to exert similar biological activities, making chemical similarity a fundamental concept in drug discovery [238]. The action mechanisms of the antibiotics found are not known, consequently to infer the possible action mechanisms, compounds analogues of DC001 and DC002 were search with 80% and 90% similarity, respectively, using the hit2lead website (www.hit2lead.com). DC001 has 28 analogues, with 5 of them with known functions: interfering in transcription, inhibiting the human tyrosyl-DNA phosphodiesterase 1, inhibiting JMJD2A-Tudor Domain and vitamin D receptor, inhibiting nucleotide binding oligomerization domain containing 1 (human) and inhibiting tumor necrosis factor (human), and antiviral activity against Hepatitis B virus infected in human HepG2(2.2.15) cells. DC002 has 15 analogues, with 8 of them with known functions: inhibiting the p38, inhibiting the *Mycobacterium tuberculosis* H37Rv growth, binding affinity to human P2Y1 receptor, bactericidal action against *S. aureus* biofilms, antiprion activity, cytotoxicity activity against human BJ, HEK293, HepG2 and Raji cells, and action in treating Kcnq related disorders.

The intense rise of bacterial pathogens resistant to antibacterial agents underlines the urgent need for the development of new antimicrobial drugs. HTS has become an important approach in finding novel compounds that may develop into clinical therapeutic drugs. The new in-house HTS protocol here described, despite not discovering molecules with anti-rhamnose activity, was able to successfully identify two compounds with antimicrobial activity. Although compounds presented an antibacterial action when directly incubated in bacterial cultures, they are not capable of acting against *Listeria*-infected HeLa cells under the conditions tested. Further testing with different cell lines and longer incubation periods could reveal the antimicrobial action of the molecules. Discovering the action mechanisms of DC001 and DC002 would assist understand how these drugs work against *L. monocytogenes* and consequently to decide the best protocol to implement. Testing the compounds against other Gram+ and Gram- pathogenic bacteria would allow discerning if the DC001 and DC002 have a broad-spectrum activity.

6. Conclusion

Antibiotic resistance is a dire problem that is facing the global community, consequently the development of new drugs is imperative. HTS is an empowering method used as a starting point for drug discovery, and the findings in this dissertation highlight the importance of HTS campaigns. The HTS process here implemented did not identify compounds with action against WTA rhamnosylation. Nonetheless, our method successfully identified 2 compounds with antimicrobial activity, DC001 and DC002. Further investigation is now necessary to demonstrate the antimicrobial activity of these compounds against intracellular *Listeria in vitro* and *in vivo*, as well as their capacity to act against other bacterial pathogens.

7. References

1. O'Byrne, C. and M. Utratna, *Listeria monocytogenes: at the coalface of host-pathogen research.* Bioeng Bugs, 2010. **1**(6): p. 371-377.
2. Murray, E., Webb, RA., Swann, MBR. , *A disease of rabbits characterised by a large mononuclear leucocytosis, caused by a hitherto undescribed bacillos bacterium monocytogenes (n.sp.).* J Pathol Bacteriol., 1926. **29**: p. 407-439.
3. Pirie, J., *A new disease of veld rodents, "Tiger River disease.".* Publ South African Inst Med Res., 1927. **3**: p. 163-186.
4. Harvey, J., *The Genus Listerella Pirie.* Science, 1940. **9**: p. 383.
5. Doganay, M., *Listeriosis: clinical presentation.* FEMS Immunol Med Microbiol, 2003. **35**(3): p. 173-175.
6. Low, J.C. and W. Donachie, *A review of Listeria monocytogenes and listeriosis.* Vet J, 1997. **153**(1): p. 9-29.
7. Burn, C.G., *Clinical and Pathological Features of an Infection Caused by a New Pathogen of the Genus Listerella.* Am J Pathol, 1936. **12**(3): p. 341-348 1.
8. Schlech, W., *Overview of listeriosis.* Food Control, 1996. **7**: p. 183-186.
9. Hain, T., et al., *Pathogenomics of Listeria spp.* Int J Med Microbiol, 2007. **297**(7-8): p. 541-557.
10. Vazquez-Boland, J.A., et al., *Listeria pathogenesis and molecular virulence determinants.* Clin Microbiol Rev, 2001. **14**(3): p. 584-640.
11. Orsi, R.H. and M. Wiedmann, *Characteristics and distribution of Listeria spp., including Listeria species newly described since 2009.* Appl Microbiol Biotechnol, 2016. **100**(12): p. 5273-5287.
12. Leclercq, A., et al., *Listeria thailandensis sp. nov.* Int J Syst Evol Microbiol, 2019. **69**(1): p. 74-81.
13. Liao, J., M. Wiedmann, and J. Kovac, *Genetic Stability and Evolution of the sigB Allele, Used for Listeria Sensu Stricto Subtyping and Phylogenetic Inference.* Appl Environ Microbiol, 2017. **83**(12).
14. Glaser, P., et al., *Comparative genomics of Listeria species.* Science, 2001. **294**(5543): p. 849-852.
15. Seeliger, H.P.R. and K. Höhne, *Chapter II Serotyping of Listeria monocytogenes and Related Species*, in *Methods in Microbiology*, T. Bergan and J.R. Norris, Editors. 1979, Academic Press. p. 31-49.
16. Borucki, M.K. and D.R. Call, *Listeria monocytogenes serotype identification by PCR.* J Clin Microbiol, 2003. **41**(12): p. 5537-5540.
17. Nightingale, K., et al., *Combined sigB allelic typing and multiplex PCR provide improved discriminatory power and reliability for Listeria monocytogenes molecular serotyping.* J Microbiol Methods, 2007. **68**(1): p. 52-59.

18. Kerouanton, A., et al., *Evaluation of a multiplex PCR assay as an alternative method for Listeria monocytogenes serotyping.* J Microbiol Methods, 2010. **80**(2): p. 134-137.
19. Orsi, R.H., H.C. den Bakker, and M. Wiedmann, *Listeria monocytogenes lineages: Genomics, evolution, ecology, and phenotypic characteristics.* Int J Med Microbiol, 2011. **301**(2): p. 79-96.
20. Rothrock, M.J., et al., *Listeria Occurrence and Potential Control Strategies in Alternative and Conventional Poultry Processing and Retail.* Frontiers in Sustainable Food Systems, 2019. **3**(33).
21. Shi, W., et al., *Prevalence, antibiotic resistance and genetic diversity of Listeria monocytogenes isolated from retail ready-to-eat foods in China.* Food Control, 2015. **47**: p. 340-347.
22. Matloob, M. and M. Griffiths, *Ribotyping and automated ribotyping of Listeria monocytogenes.* Methods Mol Biol, 2014. **1157**: p. 85-93.
23. Fox, E.M., et al., *PFGE analysis of Listeria monocytogenes isolates of clinical, animal, food and environmental origin from Ireland.* J Med Microbiol, 2012. **61**(Pt 4): p. 540-547.
24. Haase, J.K., et al., *The ubiquitous nature of Listeria monocytogenes clones: a large-scale Multilocus Sequence Typing study.* Environ Microbiol, 2014. **16**(2): p. 405-416.
25. Maury, M.M., et al., *Uncovering Listeria monocytogenes hypervirulence by harnessing its biodiversity.* Nat Genet, 2016. **48**(3): p. 308-313.
26. Koopmans, M.M., et al., *Listeria monocytogenes meningitis in the Netherlands, 1985-2014: A nationwide surveillance study.* J Infect, 2017. **75**(1): p. 12-19.
27. Grundling, A., et al., *Listeria monocytogenes regulates flagellar motility gene expression through MogR, a transcriptional repressor required for virulence.* Proc Natl Acad Sci U S A, 2004. **101**(33): p. 12318-12323.
28. Peel, M., W. Donachie, and A. Shaw, *Temperature-dependent expression of flagella of Listeria monocytogenes studied by electron microscopy, SDS-PAGE and western blotting.* J Gen Microbiol, 1988. **134**(8): p. 2171-2178.
29. Rocourt, J. and C. Buchrieser, *The genus Listeria and Listeria monocytogenes: phylogenetic position, taxonomy and identification.* Listeria, Listeriosis, and Food Safety, 2007: p. 1-20.
30. Junttila, J.R., S.I. Niemela, and J. Hirn, *Minimum growth temperatures of Listeria monocytogenes and non-haemolytic Listeria.* J Appl Bacteriol, 1988. **65**(4): p. 321-327.
31. Shahamat, M., A. Seaman, and M. Woodbine, *Survival of Listeria monocytogenes in high salt concentrations.* Zentralbl Bakteriol A, 1980. **246**(4): p. 506-511.

32. Ibarra-Sánchez, L.A., M.L. Van Tassell, and M.J. Miller, *Invited review: Hispanic-style cheeses and their association with Listeria monocytogenes.* Journal of Dairy Science, 2017. **100**(4): p. 2421-2432.
33. de Noordhout, C.M., et al., *The global burden of listeriosis: a systematic review and meta-analysis.* Lancet Infect Dis, 2014. **14**(11): p. 1073-1082.
34. Orndorff, P.E., et al., *Host and bacterial factors in listeriosis pathogenesis.* Vet Microbiol, 2006. **114**(1-2): p. 1-15.
35. Colagiorgi, A., et al., *Listeria monocytogenes Biofilms in the Wonderland of Food Industry.* Pathogens, 2017. **6**(3).
36. Johnson, J., et al., *Natural atypical Listeria innocua strains with Listeria monocytogenes pathogenicity island 1 genes.* Appl Environ Microbiol, 2004. **70**(7): p. 4256-4266.
37. Mengaud, J., C. Braun-Breton, and P. Cossart, *Identification of phosphatidylinositol-specific phospholipase C activity in Listeria monocytogenes: a novel type of virulence factor?* Mol Microbiol, 1991. **5**(2): p. 367-372.
38. Farber, J.M. and P.I. Peterkin, *Listeria monocytogenes, a food-borne pathogen.* Microbiol Rev, 1991. **55**(3): p. 476-511.
39. Bille, J., et al., *API Listeria, a new and promising one-day system to identify Listeria isolates.* Appl Environ Microbiol, 1992. **58**(6): p. 1857-1860.
40. Kreft, J., et al., *Pathogenicity islands and other virulence elements in Listeria.* Curr Top Microbiol Immunol, 2002. **264**(2): p. 109-125.
41. Prokop, A., et al., *OrfX, a Nucleomodulin Required for Listeria monocytogenes Virulence.* mBio, 2017. **8**(5).
42. Buchrieser, C., *Biodiversity of the species Listeria monocytogenes and the genus Listeria.* Microbes Infect, 2007. **9**(10): p. 1147-1155.
43. Schmid, M.W., et al., *Evolutionary history of the genus Listeria and its virulence genes.* Syst Appl Microbiol, 2005. **28**(1): p. 1-18.
44. Dussurget, O., *New insights into determinants of Listeria monocytogenes virulence.* Int Rev Cell Mol Biol, 2008. **270**: p. 1-38.
45. Nikitas, G., et al., *Transcytosis of Listeria monocytogenes across the intestinal barrier upon specific targeting of goblet cell accessible E-cadherin.* J Exp Med, 2011. **208**(11): p. 2263-2277.
46. Cossart, P., *Illuminating the landscape of host-pathogen interactions with the bacterium Listeria monocytogenes.* Proc Natl Acad Sci U S A, 2011. **108**(49): p. 19484-19491.
47. Cossart, P. and A. Lebreton, *A trip in the "New Microbiology" with the bacterial pathogen Listeria monocytogenes.* FEBS Lett, 2014. **588**(15): p. 2437-2445.
48. Allerberger, F. and M. Wagner, *Listeriosis: a resurgent foodborne infection.* Clin Microbiol Infect, 2010. **16**(1): p. 16-23.

49. Radoshevich, L. and P. Cossart, *Listeria monocytogenes: towards a complete picture of its physiology and pathogenesis.* Nat Rev Microbiol, 2018. **16**(1): p. 32-46.
50. Swaminathan, B. and P. Gerner-Smidt, *The epidemiology of human listeriosis.* Microbes Infect, 2007. **9**(10): p. 1236-1243.
51. Hernandez-Milian, A. and A. Payeras-Cifre, *What is new in listeriosis?* BioMed research international, 2014. **2014**: p. 358051-358051.
52. Disson, O. and M. Lecuit, *Targeting of the central nervous system by Listeria monocytogenes.* Virulence, 2012. **3**(2): p. 213-221.
53. Olaimat, A.N., et al., *Emergence of Antibiotic Resistance in Listeria monocytogenes Isolated from Food Products: A Comprehensive Review.* Comprehensive Reviews in Food Science and Food Safety, 2018. **17**(5): p. 1277-1292.
54. Dortet, L.V.-C., E.; Cossart, P. , *Listeria monocytogenes. In M. Schaechter (Ed.).* Encyclopedia of Microbiology. 2009, Paris, France: Institute Pasteur.
55. Wilson, A., et al., *Phenotypic and Genotypic Analysis of Antimicrobial Resistance among Listeria monocytogenes Isolated from Australian Food Production Chains.* Genes (Basel), 2018. **9**(2).
56. Charpentier, E. and P. Courvalin, *Antibiotic resistance in Listeria spp.* Antimicrob Agents Chemother, 1999. **43**(9): p. 2103-2108.
57. Lee, B.H., et al., *Biofilm Formation of Listeria monocytogenes Strains Under Food Processing Environments and Pan-Genome-Wide Association Study.* Front Microbiol, 2019. **10**: p. 2698.
58. Reimer, A., et al., *Shared genome analyses of notable listeriosis outbreaks, highlighting the critical importance of epidemiological evidence, input datasets and interpretation criteria.* Microb Genom, 2019. **5**(1).
59. Abay, S., et al., *Pathogenicity, genotyping and antibacterial susceptibility of the Listeria spp. recovered from stray dogs.* Microb Pathog, 2019. **126**: p. 123-133.
60. Heymann, D.L., *Control of communicable diseases manual*. 18th ed. 2004, Washington DC: American Public Health Association. 700.
61. Denny, J. and J. McLauchlin, *Human Listeria monocytogenes infections in Europe--an opportunity for improved European surveillance.* Euro Surveill, 2008. **13**(13).
62. Goulet, V., et al., *Increasing incidence of listeriosis in France and other European countries.* Emerg Infect Dis, 2008. **14**(5): p. 734-740.
63. Lomonaco, S., D. Nucera, and V. Filipello, *The evolution and epidemiology of Listeria monocytogenes in Europe and the United States.* Infect Genet Evol, 2015. **35**: p. 172-183.
64. Gould, L.H., et al., *Surveillance for foodborne disease outbreaks - United States, 1998-2008.* MMWR Surveill Summ, 2013. **62**(2): p. 1-34.

65. Magalhaes, R., et al., *Cheese-related listeriosis outbreak, Portugal, March 2009 to February 2012.* Euro Surveill, 2015. **20**(17).
66. *Europe Centre for Disease Prevention and Control. Surveillance Atlas of Infectious Diseases. 2018.*
67. Cossart, P. and A. Toledo-Arana, *Listeria monocytogenes, a unique model in infection biology: an overview.* Microbes Infect, 2008. **10**(9): p. 1041-1050.
68. Pamer, E.G., *Immune responses to Listeria monocytogenes.* Nat Rev Immunol, 2004. **4**(10): p. 812-823.
69. Rolhion, N. and P. Cossart, *How the study of Listeria monocytogenes has led to new concepts in biology.* Future Microbiol, 2017. **12**: p. 621-638.
70. Bonazzi, M., M. Lecuit, and P. Cossart, *Listeria monocytogenes internalin and E-cadherin: from bench to bedside.* Cold Spring Harb Perspect Biol, 2009. **1**(4): p. a003087.
71. Pizarro-Cerda, J., A. Kuhbacher, and P. Cossart, *Entry of Listeria monocytogenes in mammalian epithelial cells: an updated view.* Cold Spring Harb Perspect Med, 2012. **2**(11).
72. Kocks, C., et al., *L. monocytogenes-induced actin assembly requires the actA gene product, a surface protein.* Cell, 1992. **68**(3): p. 521-531.
73. Camejo, A., et al., *The arsenal of virulence factors deployed by Listeria monocytogenes to promote its cell infection cycle.* Virulence, 2011. **2**(5): p. 379-394.
74. Suarez, M., et al., *A role for ActA in epithelial cell invasion by Listeria monocytogenes.* Cell Microbiol, 2001. **3**(12): p. 853-864.
75. Jagadeesan, B., et al., *LAP, an alcohol acetaldehyde dehydrogenase enzyme in Listeria, promotes bacterial adhesion to enterocyte-like Caco-2 cells only in pathogenic species.* Microbiology (Reading), 2010. **156**(Pt 9): p. 2782-2795.
76. Burkholder, K.M. and A.K. Bhunia, *Listeria monocytogenes uses Listeria adhesion protein (LAP) to promote bacterial transepithelial translocation and induces expression of LAP receptor Hsp60.* Infect Immun, 2010. **78**(12): p. 5062-5073.
77. Drolia, R., et al., *Listeria Adhesion Protein Induces Intestinal Epithelial Barrier Dysfunction for Bacterial Translocation.* Cell Host Microbe, 2018. **23**(4): p. 470-484 e7.
78. Reis, O., et al., *LapB, a novel Listeria monocytogenes LPXTG surface adhesin, required for entry into eukaryotic cells and virulence.* J Infect Dis, 2010. **202**(4): p. 551-562.
79. Asano, K., et al., *Autolysin amidase of Listeria monocytogenes promotes efficient colonization of mouse hepatocytes and enhances host immune response.* Int J Med Microbiol, 2011. **301**(6): p. 480-487.

80. Milohanic, E., et al., *The autolysin Ami contributes to the adhesion of Listeria monocytogenes to eukaryotic cells via its cell wall anchor.* Mol Microbiol, 2001. **39**(5): p. 1212-1224.
81. Carvalho, F., S. Sousa, and D. Cabanes, *l-Rhamnosylation of wall teichoic acids promotes efficient surface association of Listeria monocytogenes virulence factors InlB and Ami through interaction with GW domains.* Environ Microbiol, 2018. **20**(11): p. 3941-3951.
82. Dramsi, S., et al., *FbpA, a novel multifunctional Listeria monocytogenes virulence factor.* Mol Microbiol, 2004. **53**(2): p. 639-649.
83. Osanai, A., et al., *Fibronectin-binding protein, FbpA, is the adhesin responsible for pathogenesis of Listeria monocytogenes infection.* Microbiol Immunol, 2013. **57**(4): p. 253-562.
84. Alvarez-Domínguez, C., et al., *Host cell heparan sulfate proteoglycans mediate attachment and entry of Listeria monocytogenes, and the listerial surface protein ActA is involved in heparan sulfate receptor recognition.* Infection and immunity, 1997. **65**(1): p. 78-88.
85. Gaillard, J.L., et al., *Entry of L. monocytogenes into cells is mediated by internalin, a repeat protein reminiscent of surface antigens from gram-positive cocci.* Cell, 1991. **65**(7): p. 1127-1141.
86. Dramsi, S., et al., *Entry of Listeria monocytogenes into hepatocytes requires expression of inlB, a surface protein of the internalin multigene family.* Mol Microbiol, 1995. **16**(2): p. 251-261.
87. Cabanes, D., et al., *Surface proteins and the pathogenic potential of Listeria monocytogenes.* Trends Microbiol, 2002. **10**(5): p. 238-245.
88. Dussurget, O., J. Pizarro-Cerda, and P. Cossart, *Molecular determinants of Listeria monocytogenes virulence.* Annu Rev Microbiol, 2004. **58**: p. 587-610.
89. Dhar, G., K.F. Faull, and O. Schneewind, *Anchor structure of cell wall surface proteins in Listeria monocytogenes.* Biochemistry, 2000. **39**(13): p. 3725-3733.
90. Bierne, H., et al., *Inactivation of the srtA gene in Listeria monocytogenes inhibits anchoring of surface proteins and affects virulence.* Mol Microbiol, 2002. **43**(4): p. 869-881.
91. Mengaud, J., et al., *E-Cadherin Is the Receptor for Internalin, a Surface Protein Required for Entry of L. monocytogenes into Epithelial Cells.* Cell, 1996. **84**(6): p. 923-932.
92. Lecuit, M., et al., *Internalin of Listeria monocytogenes with an intact leucine-rich repeat region is sufficient to promote internalization.* Infection and immunity, 1997. **65**(12): p. 5309-5319.

93. Pentecost, M., et al., *Listeria monocytogenes invades the epithelial junctions at sites of cell extrusion.* PLoS Pathog, 2006. **2**(1): p. e3.
94. Kim, M., et al., *Live Imaging Reveals Listeria Hijacking of E-Cadherin Recycling as It Crosses the Intestinal Barrier.* Curr Biol, 2021. **31**(5): p. 1037-1047 e4.
95. Bonazzi, M., et al., *Successive post-translational modifications of E-cadherin are required for InlA-mediated internalization of Listeria monocytogenes.* Cell Microbiol, 2008. **10**(11): p. 2208-2222.
96. Lecuit, M., et al., *A single amino acid in E-cadherin responsible for host specificity towards the human pathogen Listeria monocytogenes.* EMBO J, 1999. **18**(14): p. 3956-3963.
97. Braun, L., et al., *InlB: an invasion protein of Listeria monocytogenes with a novel type of surface association.* Mol Microbiol, 1997. **25**(2): p. 285-294.
98. Jonquières, R., et al., *Interaction between the protein InlB of Listeria monocytogenes and lipoteichoic acid: a novel mechanism of protein association at the surface of gram-positive bacteria.* Mol Microbiol, 1999. **34**(5): p. 902-914.
99. Braun, L., B. Ghebrehiwet, and P. Cossart, *gC1q-R/p32, a C1q-binding protein, is a receptor for the InlB invasion protein of Listeria monocytogenes.* EMBO J, 2000. **19**(7): p. 1458-1466.
100. Jonquieres, R., J. Pizarro-Cerda, and P. Cossart, *Synergy between the N- and C-terminal domains of InlB for efficient invasion of non-phagocytic cells by Listeria monocytogenes.* Mol Microbiol, 2001. **42**(4): p. 955-965.
101. Shen, Y., et al., *InlB-Dependent Internalization of Listeria Is Mediated by the Met Receptor Tyrosine Kinase.* Cell, 2000. **103**(3): p. 501-510.
102. Ireton, K., B. Payrastre, and P. Cossart, *The Listeria monocytogenes protein InlB is an agonist of mammalian phosphoinositide 3-kinase.* J Biol Chem, 1999. **274**(24): p. 17025-17032.
103. Sun, H., et al., *Host adaptor proteins Gab1 and CrkII promote InlB-dependent entry of Listeria monocytogenes.* Cell Microbiol, 2005. **7**(3): p. 443-457.
104. Basar, T., Y. Shen, and K. Ireton, *Redundant roles for Met docking site tyrosines and the Gab1 pleckstrin homology domain in InlB-mediated entry of Listeria monocytogenes.* Infect Immun, 2005. **73**(4): p. 2061-2074.
105. Bierne, H., et al., *A role for cofilin and LIM kinase in Listeria-induced phagocytosis.* J Cell Biol, 2001. **155**(1): p. 101-112.
106. Ireton, K., et al., *A role for phosphoinositide 3-kinase in bacterial invasion.* Science, 1996. **274**(5288): p. 780-782.
107. Hamon, M., H. Bierne, and P. Cossart, *Listeria monocytogenes: a multifaceted model.* Nat Rev Microbiol, 2006. **4**(6): p. 423-434.

108. Ireton, K. and P. Cossart, *Interaction of invasive bacteria with host signaling pathways.* Curr Opin Cell Biol, 1998. **10**(2): p. 276-283.
109. Bierne, H. and P. Cossart, *Listeria monocytogenes surface proteins: from genome predictions to function.* Microbiol Mol Biol Rev, 2007. **71**(2): p. 377-397.
110. Bierne, H., et al., *WASP-related proteins, Abi1 and Ena/VASP are required for Listeria invasion induced by the Met receptor.* J Cell Sci, 2005. **118**(Pt 7): p. 1537-1547.
111. Pentecost, M., et al., *Listeria monocytogenes internalin B activates junctional endocytosis to accelerate intestinal invasion.* PLoS Pathog, 2010. **6**(5): p. e1000900.
112. Bergmann, B., et al., *InlA- but not InlB-mediated internalization of Listeria monocytogenes by non-phagocytic mammalian cells needs the support of other internalins.* Mol Microbiol, 2002. **43**(3): p. 557-570.
113. Disson, O., et al., *Conjugated action of two species-specific invasion proteins for fetoplacental listeriosis.* Nature, 2008. **455**(7216): p. 1114-1118.
114. Ghosh, P., et al., *Invasion of the Brain by Listeria monocytogenes Is Mediated by InlF and Host Cell Vimentin.* mBio, 2018. **9**(1).
115. Kanayama, Y.J., et al., *Listeriolysin O, but not Murine E-cadherin, is Involved in Invasion of Listeria monocytogenes into Murine Liver Parenchymal Cells.* Open Microbiol J, 2015. **9**: p. 81-83.
116. Cabanes, D., et al., *Gp96 is a receptor for a novel Listeria monocytogenes virulence factor, Vip, a surface protein.* EMBO J, 2005. **24**(15): p. 2827-2838.
117. Cabanes, D., et al., *Auto, a surface associated autolysin of Listeria monocytogenes required for entry into eukaryotic cells and virulence.* Mol Microbiol, 2004. **51**(6): p. 1601-1614.
118. Birmingham, C.L., et al., *Listeriolysin O allows Listeria monocytogenes replication in macrophage vacuoles.* Nature, 2008. **451**(7176): p. 350-354.
119. Smith, G.A., et al., *The two distinct phospholipases C of Listeria monocytogenes have overlapping roles in escape from a vacuole and cell-to-cell spread.* Infect Immun, 1995. **63**(11): p. 4231-4237.
120. Ruan, Y., et al., *Listeriolysin O Membrane Damaging Activity Involves Arc Formation and Lineaction -- Implication for Listeria monocytogenes Escape from Phagocytic Vacuole.* PLoS Pathog, 2016. **12**(4): p. e1005597.
121. Gilbert, R.J., *Cholesterol-dependent cytolysins.* Adv Exp Med Biol, 2010. **677**: p. 56-66.
122. Geoffroy, C., et al., *Purification, characterization, and toxicity of the sulfhydryl-activated hemolysin listeriolysin O from Listeria monocytogenes.* Infect Immun, 1987. **55**(7): p. 1641-1646.

123. Glomski, I.J., A.L. Decatur, and D.A. Portnoy, *Listeria monocytogenes mutants that fail to compartmentalize listerolysin O activity are cytotoxic, avirulent, and unable to evade host extracellular defenses.* Infect Immun, 2003. **71**(12): p. 6754-6765.
124. Beauregard, K.E., et al., *pH-dependent perforation of macrophage phagosomes by listeriolysin O from Listeria monocytogenes.* J Exp Med, 1997. **186**(7): p. 1159-1163.
125. Dramsi, S. and P. Cossart, *Listeriolysin O-mediated calcium influx potentiates entry of Listeria monocytogenes into the human Hep-2 epithelial cell line.* Infect Immun, 2003. **71**(6): p. 3614-3618.
126. Vadia, S. and S. Seveau, *Fluxes of Ca2+ and K+ are required for the listeriolysin O-dependent internalization pathway of Listeria monocytogenes.* Infect Immun, 2014. **82**(3): p. 1084-1091.
127. Kayal, S., et al., *Listeriolysin O-dependent activation of endothelial cells during infection with Listeria monocytogenes: activation of NF-kappa B and upregulation of adhesion molecules and chemokines.* Mol Microbiol, 1999. **31**(6): p. 1709-1722.
128. Repp, H., et al., *Listeriolysin of Listeria monocytogenes forms Ca2+-permeable pores leading to intracellular Ca2+ oscillations.* Cell Microbiol, 2002. **4**(8): p. 483-491.
129. Stavru, F., et al., *Listeria monocytogenes transiently alters mitochondrial dynamics during infection.* Proc Natl Acad Sci U S A, 2011. **108**(9): p. 3612-3617.
130. Ribet, D., et al., *Listeria monocytogenes impairs SUMOylation for efficient infection.* Nature, 2010. **464**(7292): p. 1192-1195.
131. Chico-Calero, I., et al., *Hpt, a bacterial homolog of the microsomal glucose- 6-phosphate translocase, mediates rapid intracellular proliferation in Listeria.* Proc Natl Acad Sci U S A, 2002. **99**(1): p. 431-436.
132. Pillich, H., M. Puri, and T. Chakraborty, *ActA of Listeria monocytogenes and Its Manifold Activities as an Important Listerial Virulence Factor.* Curr Top Microbiol Immunol, 2017. **399**: p. 113-132.
133. Campellone, K.G. and M.D. Welch, *A nucleator arms race: cellular control of actin assembly.* Nat Rev Mol Cell Biol, 2010. **11**(4): p. 237-251.
134. Welch, M.D., A. Iwamatsu, and T.J. Mitchison, *Actin polymerization is induced by Arp 2/3 protein complex at the surface of Listeria monocytogenes.* Nature, 1997. **385**(6613): p. 265-269.
135. Welch, M.D., et al., *Interaction of human Arp2/3 complex and the Listeria monocytogenes ActA protein in actin filament nucleation.* Science, 1998. **281**(5373): p. 105-108.
136. Lasa, I., et al., *The amino-terminal part of ActA is critical for the actin-based motility of Listeria monocytogenes; the central proline-rich region acts as a stimulator.* Mol Microbiol, 1995. **18**(3): p. 425-436.

137. Auerbuch, V., et al., *Ena/VASP proteins contribute to Listeria monocytogenes pathogenesis by controlling temporal and spatial persistence of bacterial actin-based motility.* Mol Microbiol, 2003. **49**(5): p. 1361-1375.
138. Domann, E., et al., *A novel bacterial virulence gene in Listeria monocytogenes required for host cell microfilament interaction with homology to the proline-rich region of vinculin.* EMBO J, 1992. **11**(5): p. 1981-1990.
139. Alvarez-Dominguez, C., R. Roberts, and P.D. Stahl, *Internalized Listeria monocytogenes modulates intracellular trafficking and delays maturation of the phagosome.* J Cell Sci, 1997. **110 (Pt 6)**: p. 731-743.
140. Silhavy, T.J., D. Kahne, and S. Walker, *The bacterial cell envelope.* Cold Spring Harb Perspect Biol, 2010. **2**(5): p. a000414.
141. Shockman, G.D. and J.F. Barrett, *Structure, function, and assembly of cell walls of gram-positive bacteria.* Annu Rev Microbiol, 1983. **37**: p. 501-527.
142. Vollmer, W., *Structural variation in the glycan strands of bacterial peptidoglycan.* FEMS Microbiol Rev, 2008. **32**(2): p. 287-306.
143. Buist, G., et al., *LysM, a widely distributed protein motif for binding to (peptido)glycans.* Mol Microbiol, 2008. **68**(4): p. 838-847.
144. Weidenmaier, C. and A. Peschel, *Teichoic acids and related cell-wall glycopolymers in Gram-positive physiology and host interactions.* Nat Rev Microbiol, 2008. **6**(4): p. 276-287.
145. Brown, S., J.P. Santa Maria, Jr., and S. Walker, *Wall teichoic acids of gram-positive bacteria.* Annu Rev Microbiol, 2013. **67**: p. 313-336.
146. Fiedler, F., et al., *The biochemistry of murein and cell wall teichoic acids in the genus Listeria.* Systematic and Applied Microbiology, 1984. **5**(3): p. 360-376.
147. Armstrong, J.J., et al., *882. Isolation and structure of ribitol phosphate derivatives (teichoic acids) from bacterial cell walls.* Journal of the Chemical Society (Resumed), 1958(0): p. 4344-4354.
148. Ward, J.B., *Teichoic and teichuronic acids: biosynthesis, assembly, and location.* Microbiol Rev, 1981. **45**(2): p. 211-243.
149. Neuhaus, F.C. and J. Baddiley, *A continuum of anionic charge: structures and functions of D-alanyl-teichoic acids in gram-positive bacteria.* Microbiol Mol Biol Rev, 2003. **67**(4): p. 686-723.
150. Percy, M.G. and A. Grundling, *Lipoteichoic acid synthesis and function in gram-positive bacteria.* Annu Rev Microbiol, 2014. **68**: p. 81-100.
151. Naumova, I.B., et al., *Cell wall teichoic acids: structural diversity, species specificity in the genus Nocardiopsis, and chemotaxonomic perspective.* FEMS Microbiol Rev, 2001. **25**(3): p. 269-284.

152. Uchikawa, K., I. Sekikawa, and I. Azuma, *Structural studies on lipoteichoic acids from four Listeria strains.* J Bacteriol, 1986. **168**(1): p. 115-222.
153. Ruhland, G.J. and F. Fiedler, *Occurrence and biochemistry of lipoteichoic acids in the genus Listeria.* Systematic and Applied Microbiology, 1987. **9**(1): p. 40-46.
154. Fiedler, F., *Biochemistry of the cell surface of Listeria strains: a locating general view.* Infection, 1988. **16 Suppl 2**: p. S92-S97.
155. Uchikawa, K., I. Sekikawa, and I. Azuma, *Structural studies on teichoic acids in cell walls of several serotypes of Listeria monocytogenes.* J Biochem, 1986. **99**(2): p. 315-327.
156. Swoboda, J.G., et al., *Wall teichoic acid function, biosynthesis, and inhibition.* Chembiochem, 2010. **11**(1): p. 35-45.
157. Meireles, D., et al., *Listeria monocytogenes Wall Teichoic Acid Glycosylation Promotes Surface Anchoring of Virulence Factors, Resistance to Antimicrobial Peptides, and Decreased Susceptibility to Antibiotics.* Pathogens, 2020. **9**(4).
158. Carvalho, F., et al., *L-Rhamnosylation of Listeria monocytogenes Wall Teichoic Acids Promotes Resistance to Antimicrobial Peptides by Delaying Interaction with the Membrane.* PLoS Pathog, 2015. **11**(5): p. e1004919.
159. Giraud, M.F. and J.H. Naismith, *The rhamnose pathway.* Curr Opin Struct Biol, 2000. **10**(6): p. 687-696.
160. Lairson, L.L., et al., *Glycosyltransferases: structures, functions, and mechanisms.* Annu Rev Biochem, 2008. **77**: p. 521-555.
161. Cederlund, A., G.H. Gudmundsson, and B. Agerberth, *Antimicrobial peptides important in innate immunity.* FEBS J, 2011. **278**(20): p. 3942-3951.
162. Corrêa, J.A.F., et al., *Fundamentals on the molecular mechanism of action of antimicrobial peptides.* Materialia, 2019. **8**: p. 100494.
163. Vadyvaloo, V., et al., *Cell-surface alterations in class IIa bacteriocin-resistant Listeria monocytogenes strains.* Microbiology (Reading), 2004. **150**(Pt 9): p. 3025-3033.
164. Roy, A., *Early Probe and Drug Discovery in Academia: A Minireview.* High Throughput, 2018. **7**(1).
165. Carnero, A., *High throughput screening in drug discovery.* Clin Transl Oncol, 2006. **8**(7): p. 482-490.
166. Santos, R., et al., *A comprehensive map of molecular drug targets.* Nat Rev Drug Discov, 2017. **16**(1): p. 19-34.
167. Bunnage, M.E., et al., *Know your target, know your molecule.* Nat Chem Biol, 2015. **11**(6): p. 368-372.
168. Inglese, J., et al., *High-throughput screening assays for the identification of chemical probes.* Nat Chem Biol, 2007. **3**(8): p. 466-479.

169. Shukla, A., *High Throughput Screening of Small Molecule Library: Procedure, Challenges and Future.* Journal of Cancer Prevention & Current Research, 2016. **5**: p. 154.
170. Eggeling, C., et al., *Highly sensitive fluorescence detection technology currently available for HTS.* Drug Discov Today, 2003. **8**(14): p. 632-641.
171. Zang, R., et al., *Cell-Based Assays in High-Throughput Screening for Drug Discovery.* International Journal of Biotechnology for Wellness Industries, 2012. **1**.
172. Bulterijs, S. and B.P. Braeckman, *Phenotypic Screening in C. elegans as a Tool for the Discovery of New Geroprotective Drugs.* Pharmaceuticals (Basel), 2020. **13**(8).
173. Inglese, J., C.E. Shamu, and R.K. Guy, *Reporting data from high-throughput screening of small-molecule libraries.* Nat Chem Biol, 2007. **3**(8): p. 438-441.
174. Murphey, R.D. and L.I. Zon, *Small molecule screening in the zebrafish.* Methods, 2006. **39**(3): p. 255-261.
175. Macarron, R. and R.P. Hertzberg, *Design and implementation of high throughput screening assays.* Mol Biotechnol, 2011. **47**(3): p. 270-285.
176. Hughes, J.P., et al., *Principles of early drug discovery.* Br J Pharmacol, 2011. **162**(6): p. 1239-1249.
177. Zhang, J.-H. and K.R. Oldenburg, *Z-Factor*, in *Encyclopedia of Cancer*, M. Schwab, Editor. 2009, Springer Berlin Heidelberg: Berlin, Heidelberg. p. 3227-3228.
178. Zhang, J.H., T.D. Chung, and K.R. Oldenburg, *A Simple Statistical Parameter for Use in Evaluation and Validation of High Throughput Screening Assays.* J Biomol Screen, 1999. **4**(2): p. 67-73.
179. Dandapani, S., et al., *Selecting, Acquiring, and Using Small Molecule Libraries for High-Throughput Screening.* Curr Protoc Chem Biol, 2012. **4**: p. 177-191.
180. Charbonneau, M.E., et al., *Small molecule deubiquitinase inhibitors promote macrophage anti-infective capacity.* PLoS One, 2014. **9**(8): p. e104096.
181. Lieberman, L.A. and D.E. Higgins, *Inhibition of Listeria monocytogenes infection by neurological drugs.* Int J Antimicrob Agents, 2010. **35**(3): p. 292-296.
182. Lieberman, L.A. and D.E. Higgins, *A small-molecule screen identifies the antipsychotic drug pimozide as an inhibitor of Listeria monocytogenes infection.* Antimicrob Agents Chemother, 2009. **53**(2): p. 756-764.
183. Schussler, S., et al., *Structure of GTP cyclohydrolase I from Listeria monocytogenes, a potential anti-infective drug target.* Acta Crystallogr F Struct Biol Commun, 2019. **75**(Pt 9): p. 586-592.
184. Lin, B., et al., *Role of Protein Glycosylation in Host-Pathogen Interaction.* Cells, 2020. **9**(4).

185. Lu, Q., S. Li, and F. Shao, *Sweet Talk: Protein Glycosylation in Bacterial Interaction With the Host.* Trends Microbiol, 2015. **23**(10): p. 630-641.
186. Hu, Y., et al., *Identification of selective inhibitors for the glycosyltransferase MurG via high-throughput screening.* Chem Biol, 2004. **11**(5): p. 703-711.
187. Qaidi, S.E., et al., *High-Throughput Screening for Bacterial Glycosyltransferase Inhibitors.* Frontiers in Cellular and Infection Microbiology, 2018. **8**.
188. Pasquina, L.W., J.P. Santa Maria, and S. Walker, *Teichoic acid biosynthesis as an antibiotic target.* Curr Opin Microbiol, 2013. **16**(5): p. 531-537.
189. Swoboda, J.G., et al., *Discovery of a small molecule that blocks wall teichoic acid biosynthesis in Staphylococcus aureus.* ACS Chem Biol, 2009. **4**(10): p. 875-883.
190. Labroli, M.A., et al., *Discovery of potent wall teichoic acid early stage inhibitors.* Bioorg Med Chem Lett, 2016. **26**(16): p. 3999-4002.
191. Wang, H., et al., *Discovery of wall teichoic acid inhibitors as potential anti-MRSA beta-lactam combination agents.* Chem Biol, 2013. **20**(2): p. 272-284.
192. Aslam, B., et al., *Antibiotic resistance: a rundown of a global crisis.* Infect Drug Resist, 2018. **11**: p. 1645-1658.
193. Bielmann, R., et al., *Receptor binding proteins of Listeria monocytogenes bacteriophages A118 and P35 recognize serovar-specific teichoic acids.* Virology, 2015. **477**: p. 110-118.
194. Lipinski, C.A., et al., *Experimental and computational approaches to estimate solubility and permeability in drug discovery and development settings.* Adv Drug Deliv Rev, 2001. **46**(1-3): p. 3-26.
195. Francis, M.S. and C.J. Thomas, *Effect of multiplicity of infection on Listeria monocytogenes pathogenicity for HeLa and Caco-2 cell lines.* J Med Microbiol, 1996. **45**(5): p. 323-330.
196. Cruz, R., et al., *Epithelial Keratins Modulate cMet Expression and Signaling and Promote InlB-Mediated Listeria monocytogenes Infection of HeLa Cells.* Front Cell Infect Microbiol, 2018. **8**: p. 146.
197. Weiglein, I., et al., *Listeria monocytogenes infection of HeLa cells results in listeriolysin O-mediated transient activation of the Raf-MEK-MAP kinase pathway.* FEMS Microbiol Lett, 1997. **148**(2): p. 189-195.
198. Coussens, N.P., et al., *Small-Molecule Screens: A Gateway to Cancer Therapeutic Agents with Case Studies of Food and Drug Administration-Approved Drugs.* Pharmacol Rev, 2017. **69**(4): p. 479-496.
199. Markossian, S., et al., *Small-Molecule Screening for Genetic Diseases.* Annu Rev Genomics Hum Genet, 2018. **19**: p. 263-288.

200. Palmer, M.E., et al., *The Listeria monocytogenes sigmaB regulon and its virulence-associated functions are inhibited by a small molecule.* mBio, 2011. **2**(6).
201. Friedrich, B., C. Scully, and J. Brannan, *Assessment of High-Throughput Screening (HTS) Methods for High-Consequence Pathogens.* Journal of Bioterrorism & Biodefense, 2011. **2**.
202. Arigoni, F., et al., *A genome-based approach for the identification of essential bacterial genes.* Nat Biotechnol, 1998. **16**(9): p. 851-856.
203. Barker, S., et al., *Drug screening to identify compounds to act as co-therapies for the treatment of Burkholderia species.* PLOS ONE, 2021. **16**(3): p. e0248119.
204. Smith, K.P. and J.E. Kirby, *Validation of a High-Throughput Screening Assay for Identification of Adjunctive and Directly Acting Antimicrobials Targeting Carbapenem-Resistant Enterobacteriaceae.* Assay Drug Dev Technol, 2016. **14**(3): p. 194-206.
205. Jeong, J., et al., *Pathogen Box screening for hit identification against Mycobacterium abscessus.* PLoS One, 2018. **13**(4): p. e0195595.
206. Lyu, W., et al., *High Throughput Screening for Natural Host Defense Peptide-Inducing Compounds as Novel Alternatives to Antibiotics.* Front Cell Infect Microbiol, 2018. **8**: p. 191.
207. Zhu, T., et al., *Hit identification and optimization in virtual screening: practical recommendations based on a critical literature analysis.* J Med Chem, 2013. **56**(17): p. 6560-6572.
208. Volochnyuk, D.M., et al., *Evolution of commercially available compounds for HTS.* Drug Discov Today, 2019. **24**(2): p. 390-402.
209. Bruns, R.F. and I.A. Watson, *Rules for identifying potentially reactive or promiscuous compounds.* J Med Chem, 2012. **55**(22): p. 9763-9772.
210. Hansson, M., et al., *On the Relationship between Molecular Hit Rates in High-Throughput Screening and Molecular Descriptors.* J Biomol Screen, 2014. **19**(5): p. 727-737.
211. Maddox, C.B., L. Rasmussen, and E.L. White, *Adapting Cell-Based Assays to the High Throughput Screening Platform: Problems Encountered and Lessons Learned.* JALA Charlottesv Va, 2008. **13**(3): p. 168-173.
212. Das, V., et al., *Reproducibility of Uniform Spheroid Formation in 384-Well Plates: The Effect of Medium Evaporation.* J Biomol Screen, 2016. **21**(9): p. 923-930.
213. Mansoury, M., et al., *The edge effect: A global problem. The trouble with culturing cells in 96-well plates.* Biochem Biophys Rep, 2021. **26**: p. 100987.
214. Brideau, C., et al., *Improved statistical methods for hit selection in high-throughput screening.* J Biomol Screen, 2003. **8**(6): p. 634-647.

215. Caraus, I., et al., *Detecting and overcoming systematic bias in high-throughput screening technologies: a comprehensive review of practical issues and methodological solutions.* Brief Bioinform, 2015. **16**(6): p. 974-986.
216. Larsson, P., et al., *Optimization of cell viability assays to improve replicability and reproducibility of cancer drug sensitivity screens.* Sci Rep, 2020. **10**(1): p. 5798.
217. McDowell, L.L., et al., *Perspective on Antibacterial Lead Identification Challenges and the Role of Hypothesis-Driven Strategies.* SLAS Discov, 2019. **24**(4): p. 440-456.
218. Dahlin, J.L. and M.A. Walters, *The essential roles of chemistry in high-throughput screening triage.* Future Med Chem, 2014. **6**(11): p. 1265-1290.
219. Schaechter, M., O. Maaloe, and N.O. Kjeldgaard, *Dependency on medium and temperature of cell size and chemical composition during balanced grown of Salmonella typhimurium.* J Gen Microbiol, 1958. **19**(3): p. 592-606.
220. Monod, J., *The growth of bacterial cultures.* Annu Rev Microbiol, 1949. **3**(1): p. 371-394.
221. Buchanan, R.E., *Life Phases in a Bacterial Culture.* The Journal of Infectious Diseases, 1918. **23**(2): p. 109-125.
222. Laurent, F., et al., *Fitness and competitive growth advantage of new gentamicin-susceptible MRSA clones spreading in French hospitals.* J Antimicrob Chemother, 2001. **47**(3): p. 277-283.
223. Lenski, R.E., et al., *Evolution of competitive fitness in experimental populations of E. coli: what makes one genotype a better competitor than another?* Antonie Van Leeuwenhoek, 1998. **73**(1): p. 35-47.
224. Leekha, S., C.L. Terrell, and R.S. Edson, *General principles of antimicrobial therapy.* Mayo Clin Proc, 2011. **86**(2): p. 156-167.
225. Smith, H., *Pathogenicity and the microbe in vivo. The 1989 Fred Griffith Review Lecture.* J Gen Microbiol, 1990. **136**(3): p. 377-393.
226. Kuch, A., et al., *Molecular diversity and antimicrobial susceptibility of Listeria monocytogenes isolates from invasive infections in Poland (1997-2013).* Sci Rep, 2018. **8**(1): p. 14562.
227. Edwards, A.M. and R.C. Massey, *Invasion of human cells by a bacterial pathogen.* J Vis Exp, 2011(49).
228. Vaudaux, P. and F.A. Waldvogel, *Gentamicin antibacterial activity in the presence of human polymorphonuclear leukocytes.* Antimicrob Agents Chemother, 1979. **16**(6): p. 743-749.
229. Kuhbacher, A., P. Cossart, and J. Pizarro-Cerda, *Internalization assays for Listeria monocytogenes.* Methods Mol Biol, 2014. **1157**: p. 167-178.

230. Dhanda, A.S., et al., *Listeria monocytogenes Exploits Host Caveolin for Cell-to-Cell Spreading.* mBio, 2020. **11**(1).
231. Gaillard, J.L., et al., *In vitro model of penetration and intracellular growth of Listeria monocytogenes in the human enterocyte-like cell line Caco-2.* Infect Immun, 1987. **55**(11): p. 2822-2829.
232. Atbiaw, N., *Review on targeted drug delivery against intracellular pathogen.* Pharmacy & Pharmacology International Journal, 2018. **6**.
233. Chifiriuc, M., et al., *Antibiotic Drug Delivery Systems for the Intracellular Targeting of Bacterial Pathogens*. 2016.
234. Yang, D.D., et al., *Synergistic interactions of ionic liquids and antimicrobials improve drug efficacy.* iScience, 2021. **24**(1): p. 101853.
235. Liu, N., et al., *Concentrations dominated membrane permeability variation by fullerol nanoparticles on a single living HeLa cell.* J Mater Chem B, 2016. **4**(34): p. 5755-5760.
236. Bakker-Woudenberg, I.A., A.F. Lokerse, and F.H. Roerdink, *Effect of lipid composition on activity of liposome-entrapped ampicillin against intracellular Listeria monocytogenes.* Antimicrob Agents Chemother, 1988. **32**(10): p. 1560-1564.
237. Lutwyche, P., et al., *Intracellular delivery and antibacterial activity of gentamicin encapsulated in pH-sensitive liposomes.* Antimicrob Agents Chemother, 1998. **42**(10): p. 2511-2520.
238. Yan, X., et al., *Chemical Structure Similarity Search for Ligand-based Virtual Screening: Methods and Computational Resources.* Curr Drug Targets, 2016. **17**(14): p. 1580-1585.

8. Supplementary material

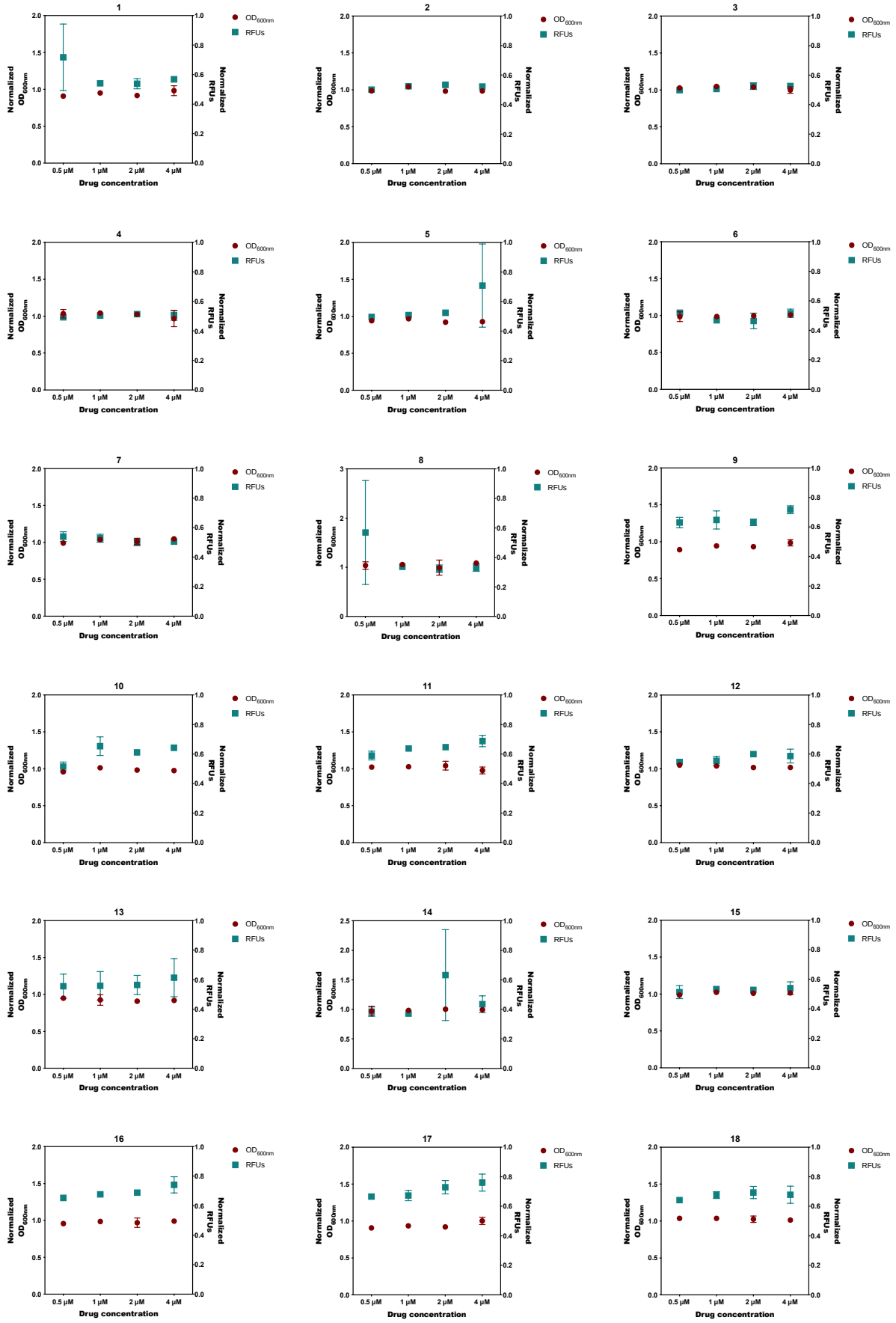
1
2
3
4
5
6
7
8
9
10
11
12
13
14
15
16
17
18
OD600nm
RFUs
Normalized OD600nm
Normalized RFUs
0.5 µM
1 µM
2 µM
4 µM
Drug concentration

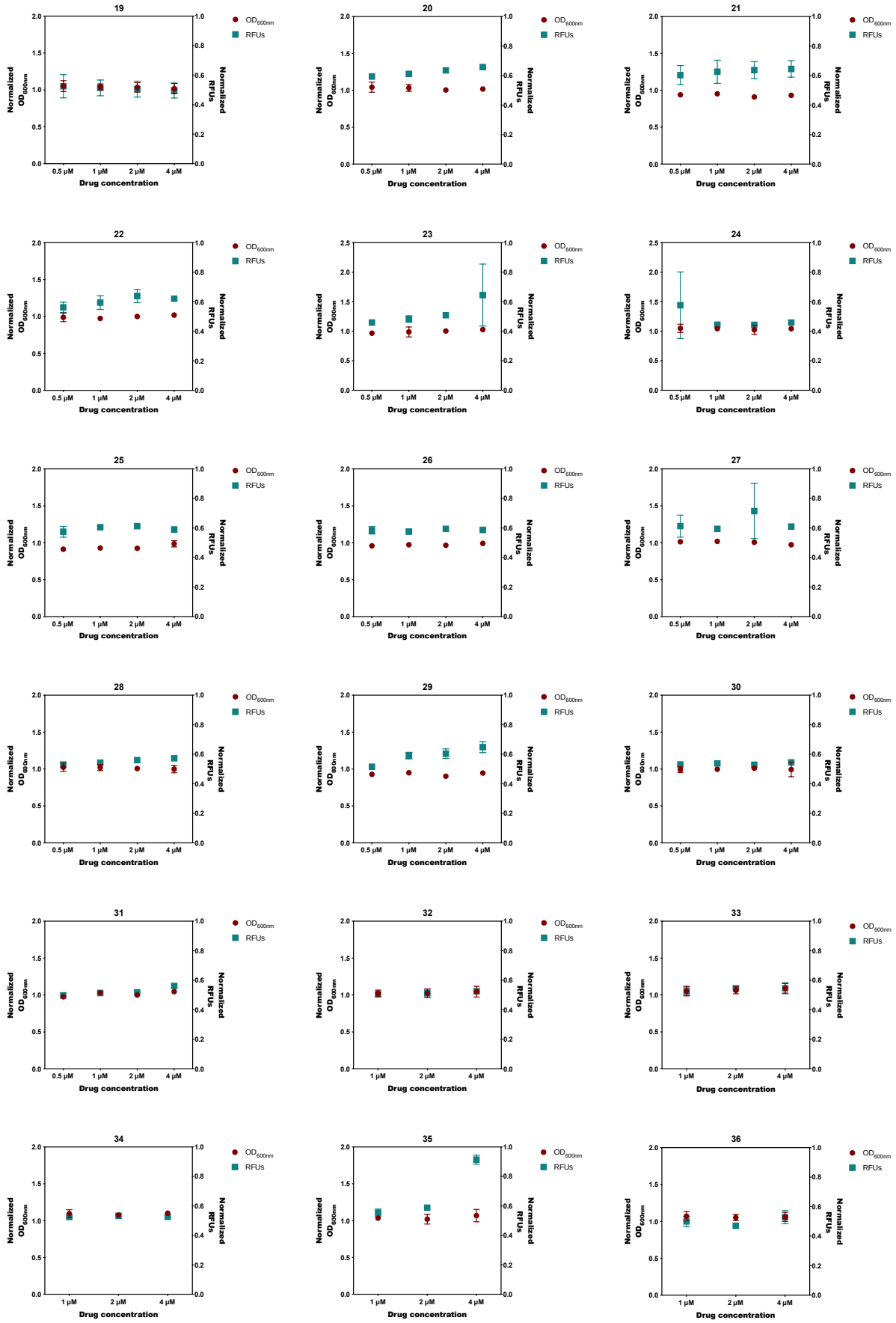
19
20
21
22
23
24
25
26
27
28
29
30
31
32
33
34
35
36
OD600nm
RFUs
Normalized OD600nm
Normalized RFUs
Drug concentration
0.5 µM
1 µM
2 µM
4 µM

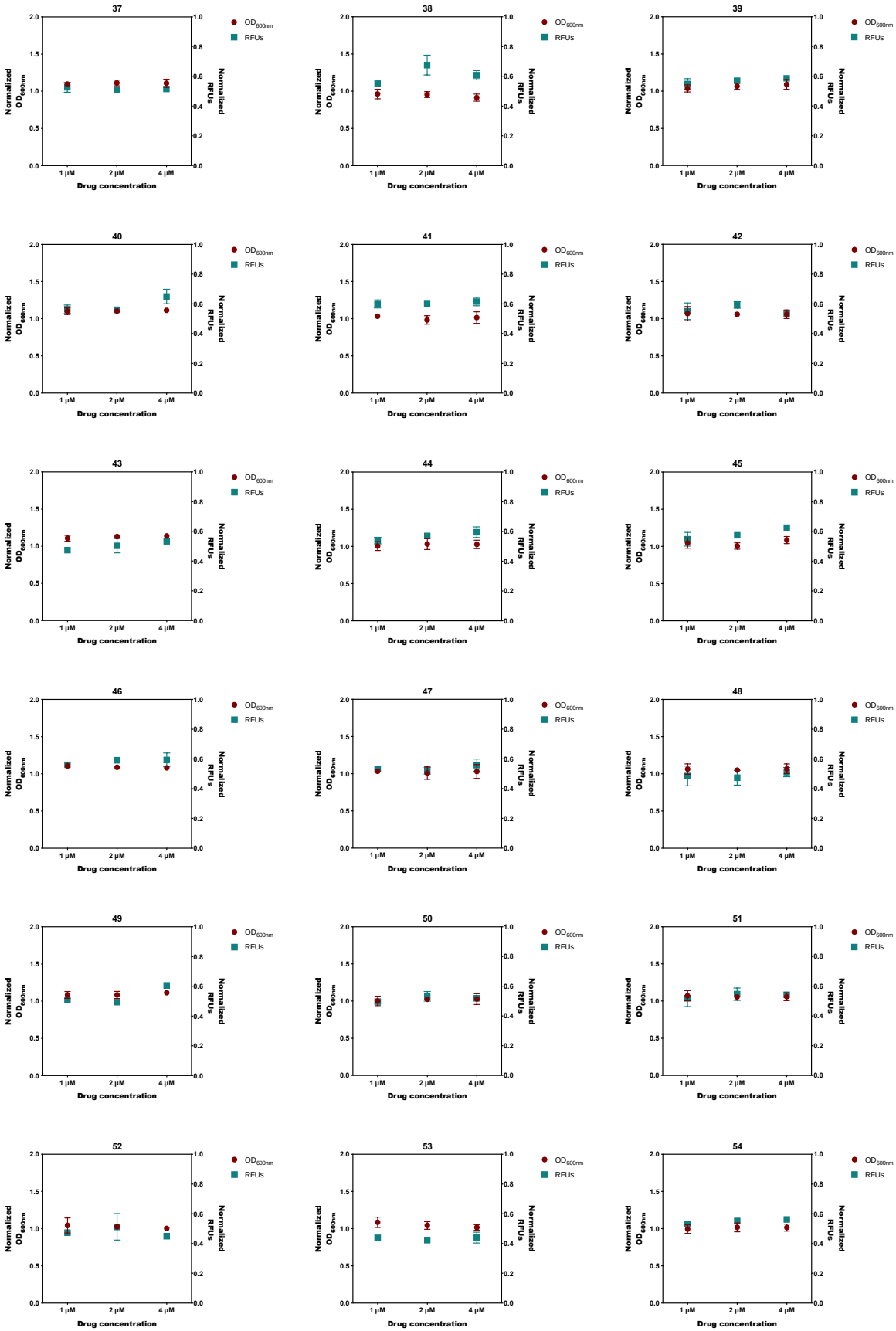
37
38
39
40
41
42
43
44
45
46
47
48
49
50
51
52
53
54
OD600nm
RFUs
Normalized OD600nm
Normalized RFUs
1 µM
2 µM
4 µM
Drug concentration

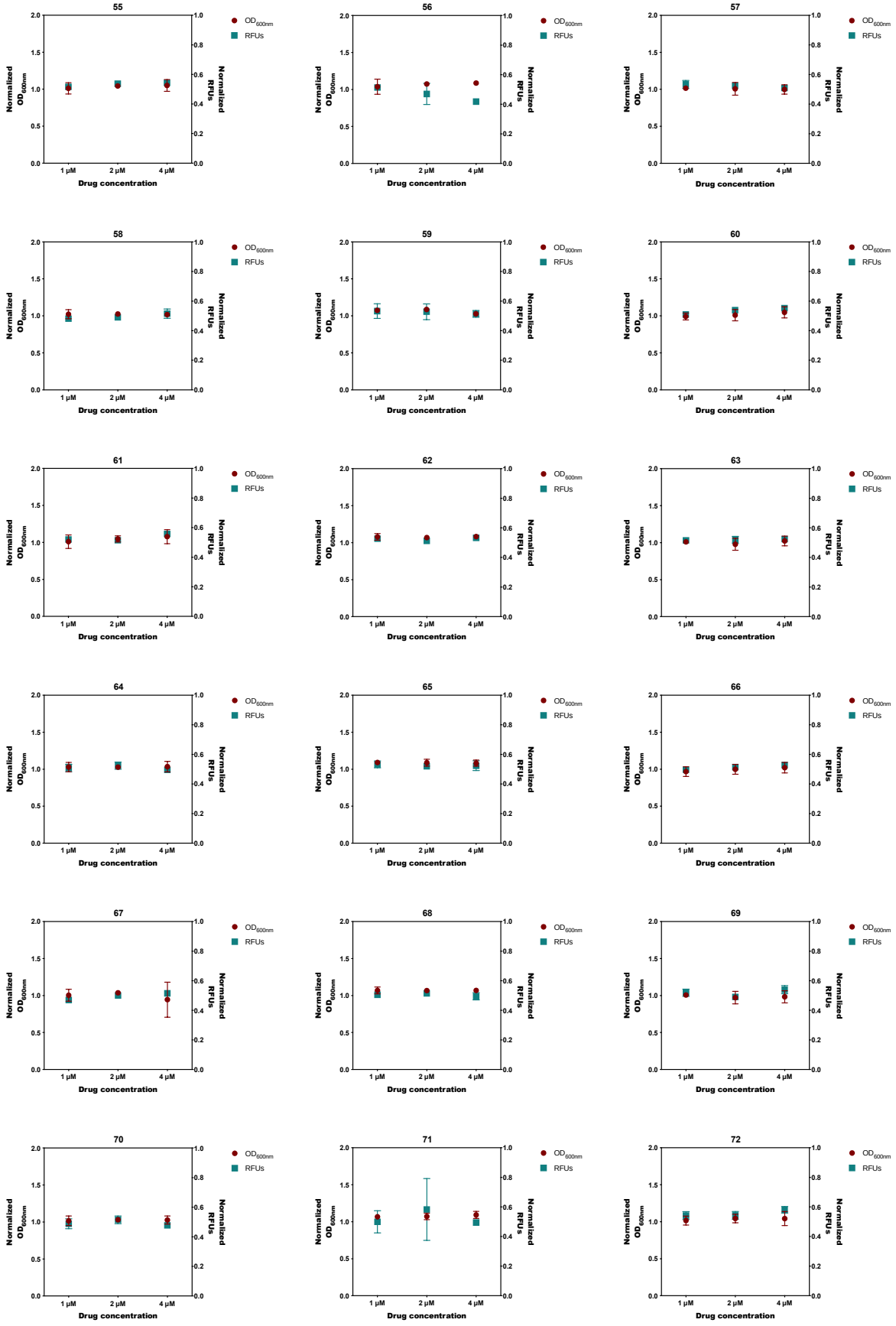
55
56
57
58
59
60
61
62
63
64
65
66
67
68
69
70
71
72
OD600nm
RFUs
Normalized OD600nm
Normalized RFUs
Drug concentration
1 µM
2 µM
4 µM

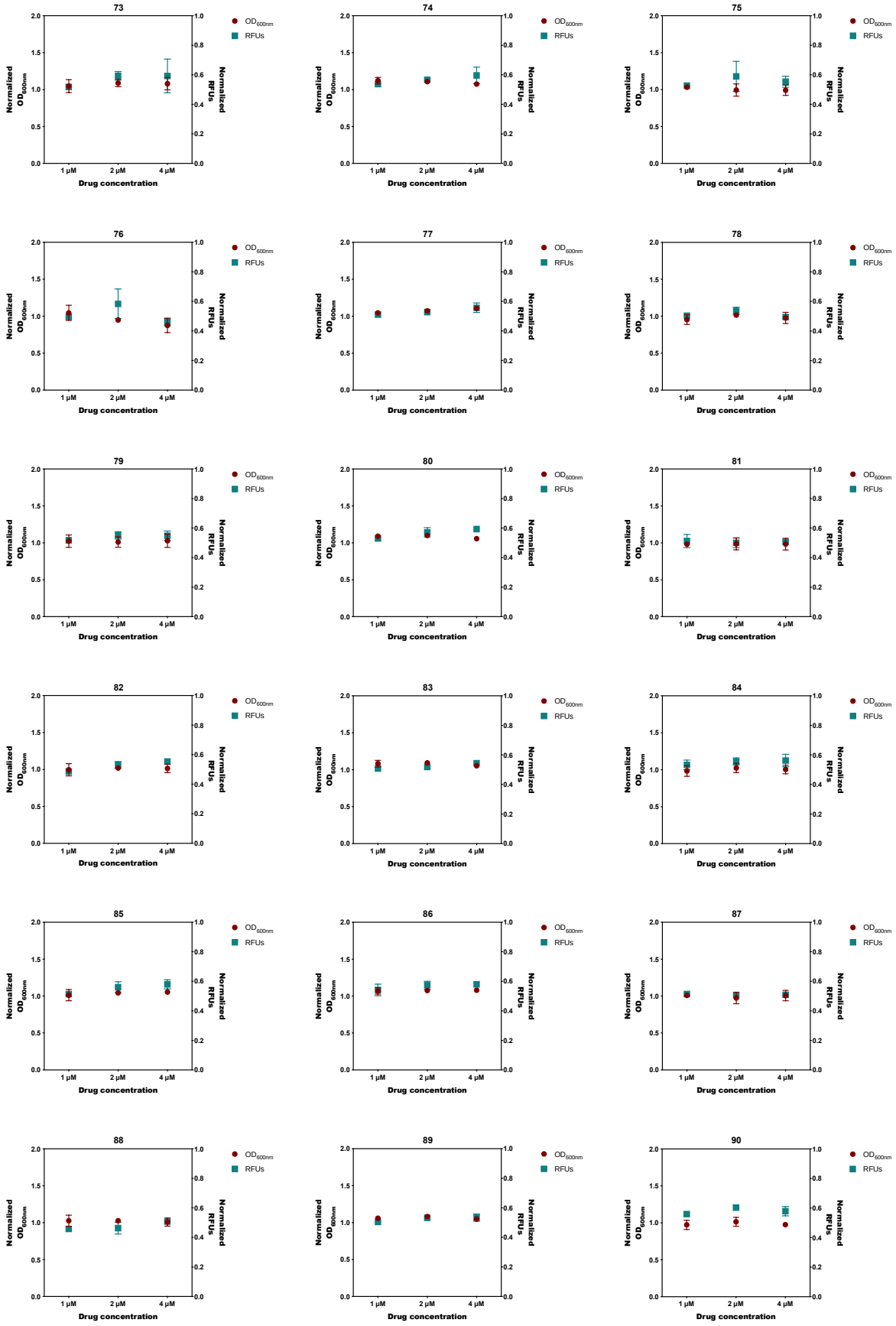
73
74
75
76
77
78
79
80
81
82
83
84
85
86
87
88
89
90
OD600nm
RFUs
Normalized OD600nm
Normalized RFUs
Drug concentration
1 µM
2 µM
4 µM

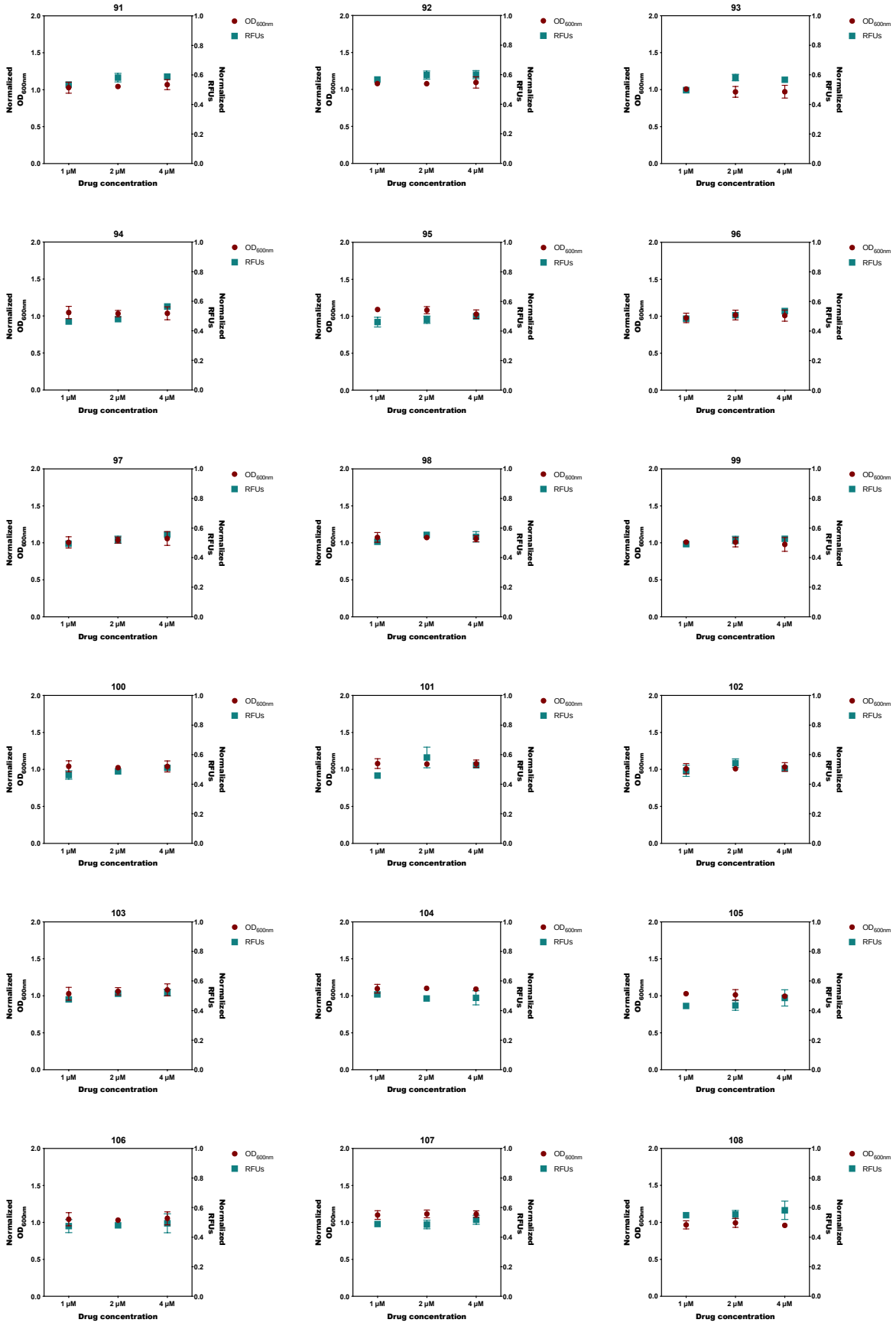
91
92
93
94
95
96
97
98
99
100
101
102
103
104
105
106
107
108
OD600nm
RFUs
Normalized OD600nm
Normalized RFUs
1 µM
2 µM
4 µM
Drug concentration

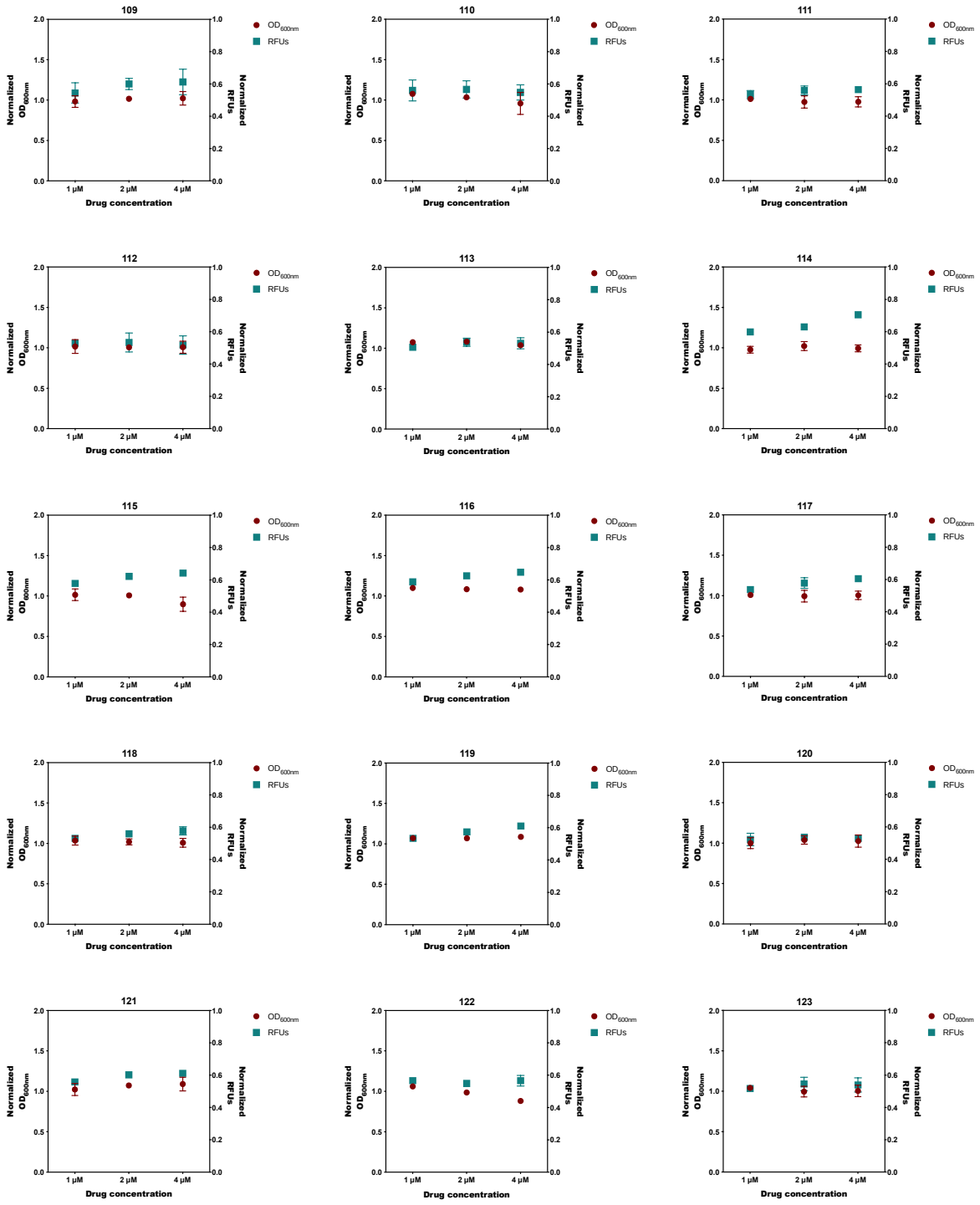

Figure S1 - 123 initial hit compounds for inhibiting the rhamnose at the bacterial surface were tested in dose-response assays, with concentrations ranging from 0.5 µM to 1 µM. Positive hits should be able to reduce the rhamnose at the bacterial surface without affecting the bacterial growth. Both OD_{600nm} and RFUs values were normalized with the negative control (*L. monocytogenes* EGD-e + DMSO). Circles represent the normalized OD_{600nm} and square represents the normalized RFUs. Error bars represent the standard deviation.

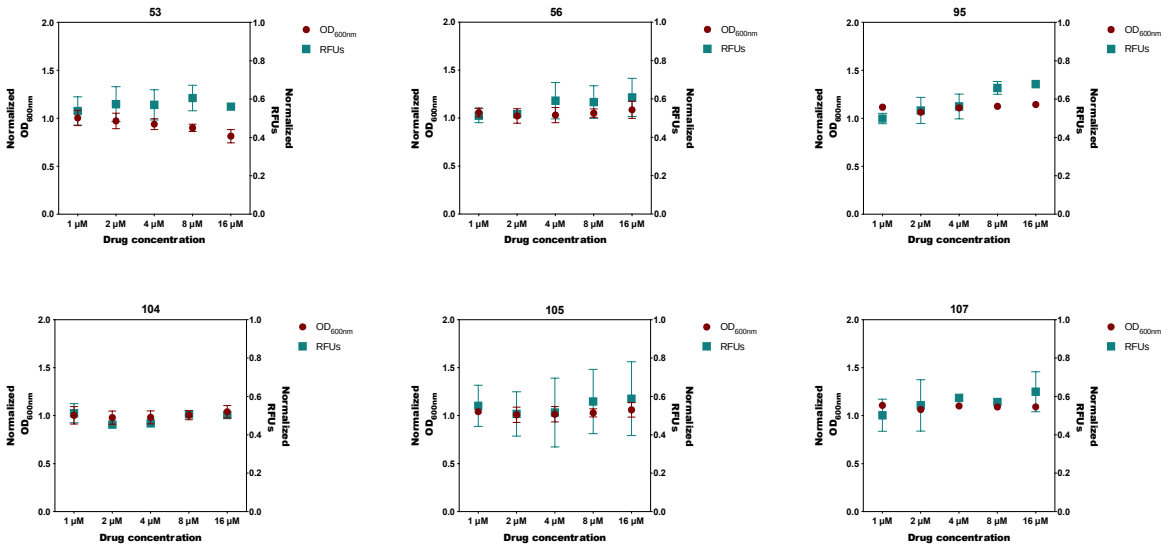

Figure S2 - The 6 hit molecules from the first dose-response were assayed again, this time with a concentration ranging from 1 µM to 16 µM. Positive hits should be able to reduce the rhamnose at the bacterial surface without affecting the bacterial growth. Both OD_{600nm} and RFUs values were also normalized with the negative control (*L. monocytogenes* EGD-e + DMSO). Circles represent the normalized OD_{600nm} and squares represent the normalized RFUs. Error bars represent the standard deviation.

1

A

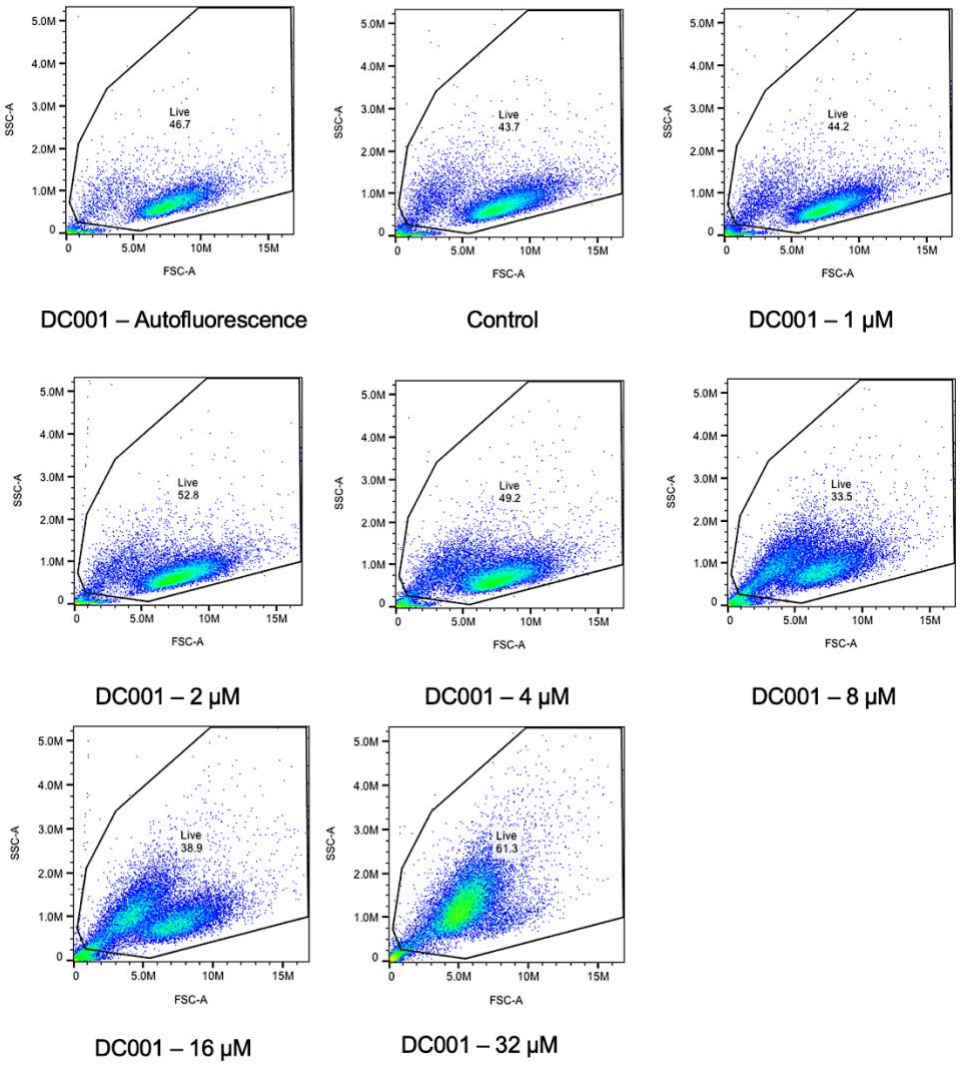

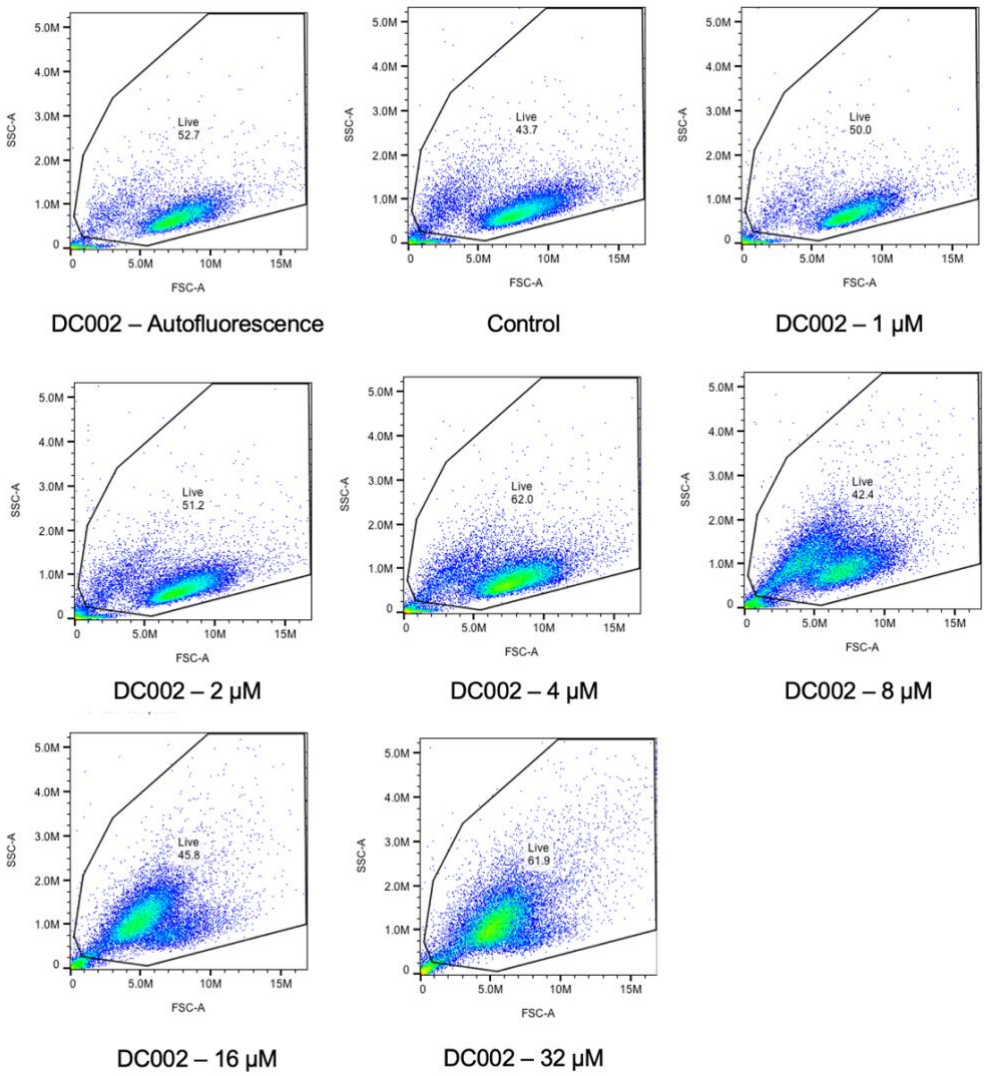
Live
52.7
DC002 – Autofluorescence
Live
43.7
Control
Live
50.0
DC002 – 1 µM
Live
51.2
DC002 – 2 µM
Live
62.0
DC002 – 4 µM
Live
42.4
DC002 – 8 µM
Live
45.8
DC002 – 16 µM
Live
61.9
DC002 – 32 µM
SSC-A
FSC-A

B

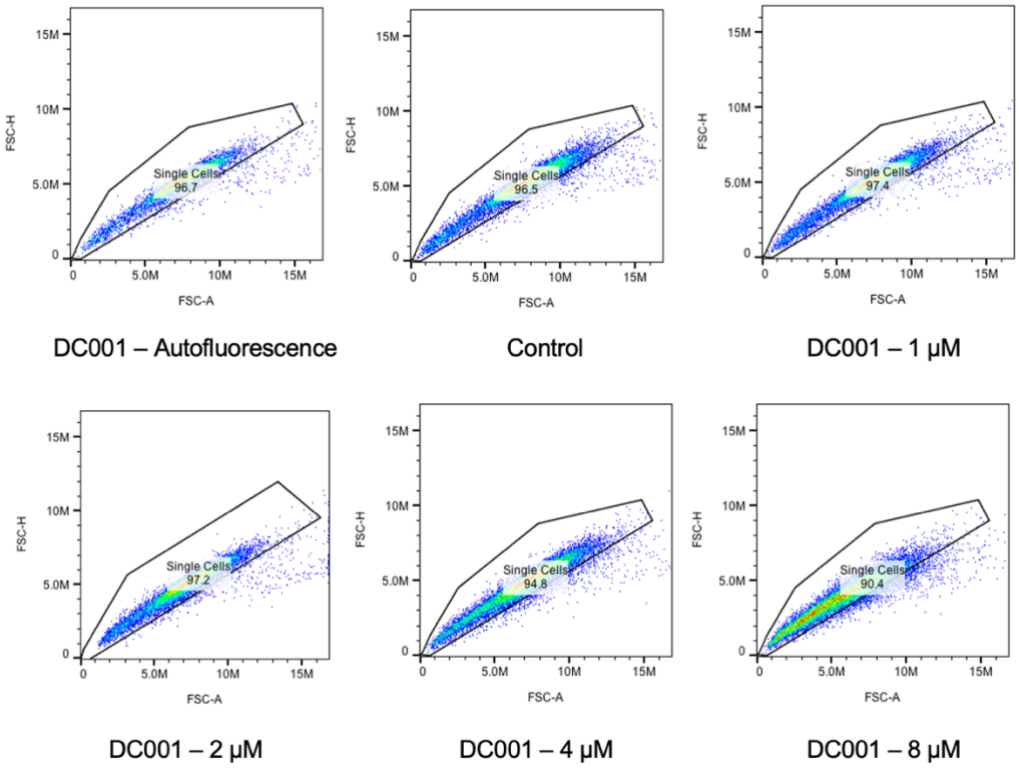
Single Cells
96.7
DC001 – Autofluorescence
Single Cells
96.5
Control
Single Cells
97.4
DC001 – 1 µM
Single Cells
97.2
DC001 – 2 µM
Single Cells
94.8
DC001 – 4 µM
Single Cells
90.4
DC001 – 8 µM
FSC-H
FSC-A

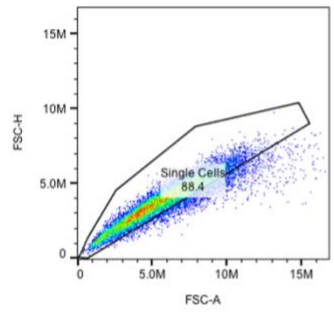

DC001 – 16 µM

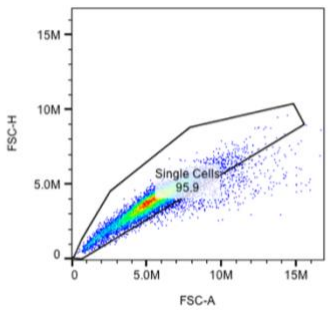

DC001 – 32 µM

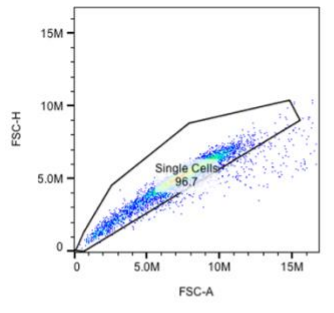

DC002 – Autofluorescence

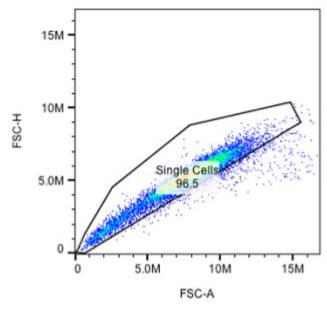

Control

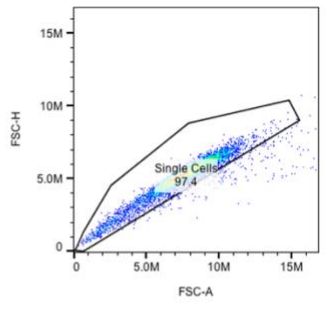

DC002 – 1 µM

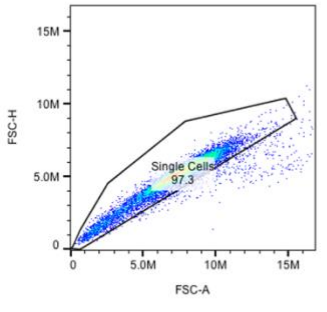

DC002 – 2 µM

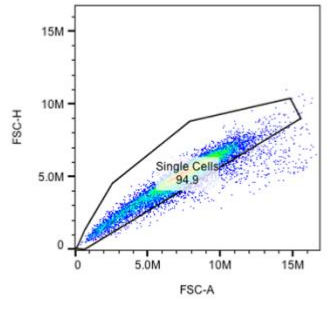

DC002 – 4 µM

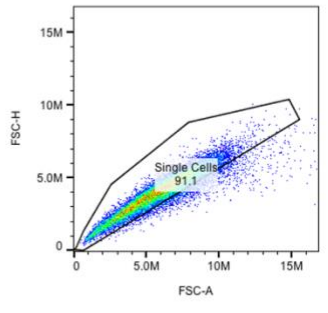

DC002 – 8 µM

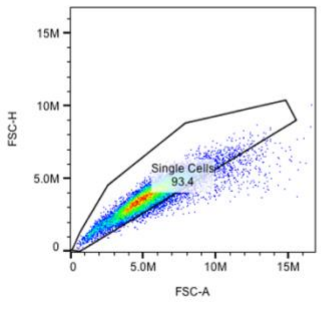

DC002 – 16 µM

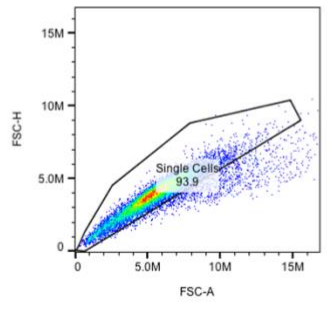

DC002 – 32 µM

C

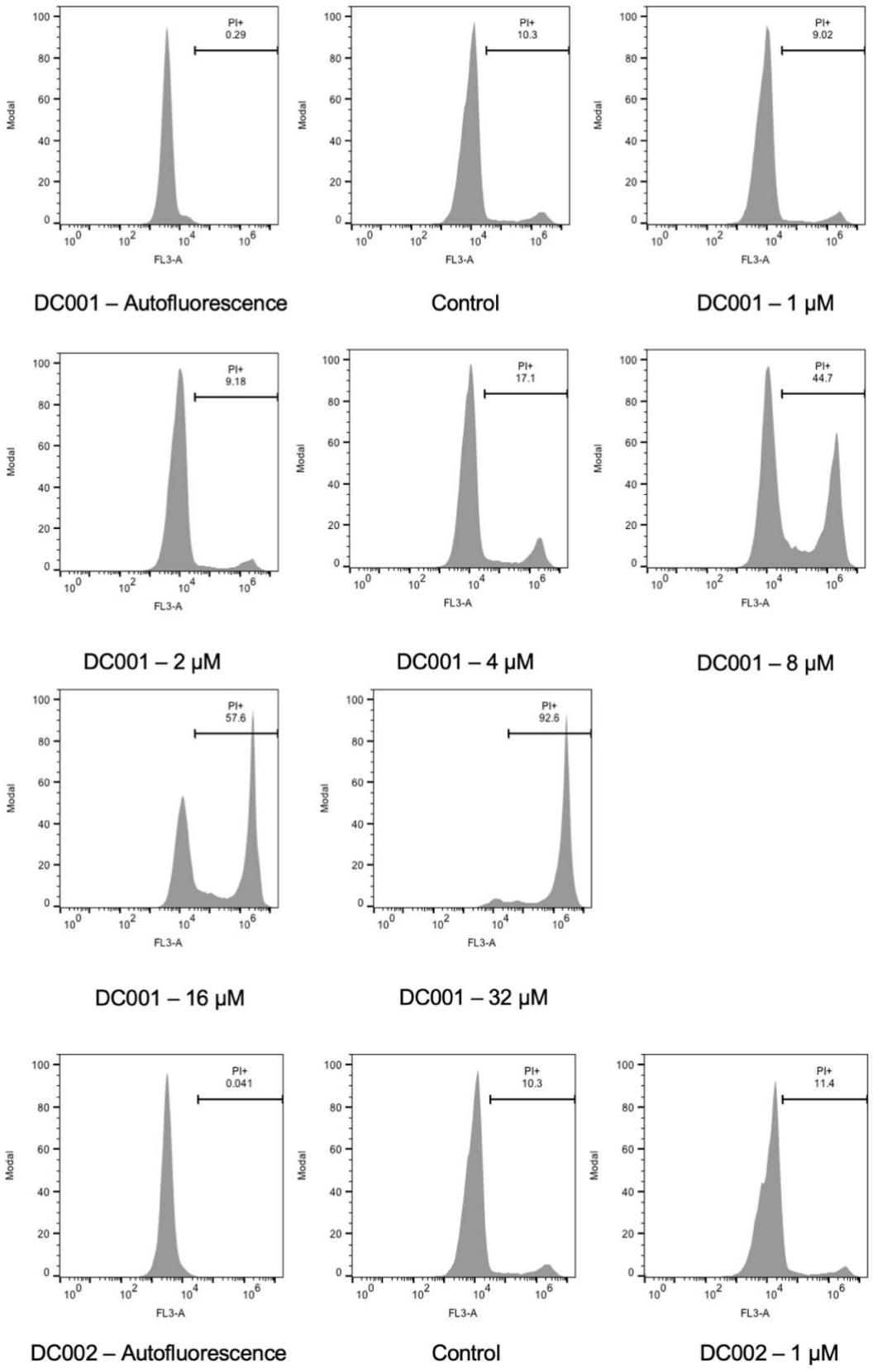
PI+
0.29
Modal
FL3-A
DC001 – Autofluorescence
PI+
10.3
Control
PI+
9.02
DC001 – 1 µM
PI+
9.18
DC001 – 2 µM
PI+
17.1
DC001 – 4 µM
PI+
44.7
DC001 – 8 µM
PI+
57.6
DC001 – 16 µM
PI+
92.6
DC001 – 32 µM
PI+
0.041
DC002 – Autofluorescence
PI+
10.3
Control
PI+
11.4
DC002 – 1 µM

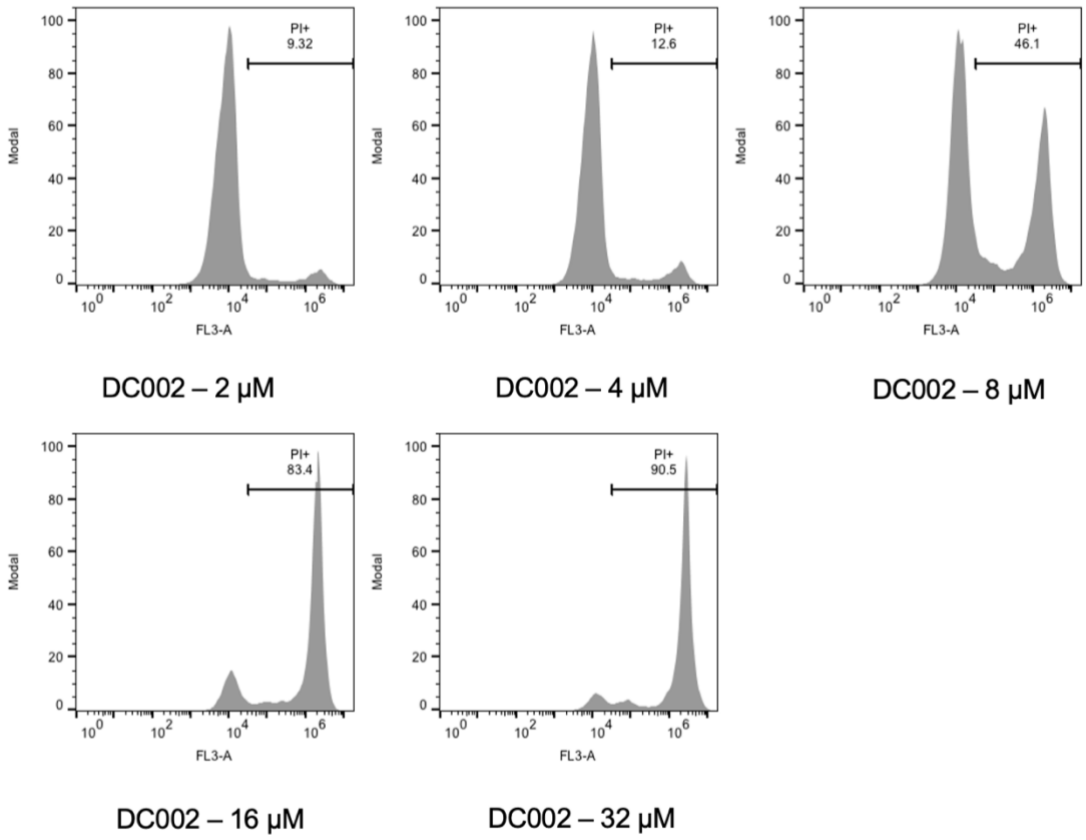
PI+
9.32
PI+
12.6
PI+
46.1
PI+
83.4
PI+
90.5
Modal
FL3-A
DC002 – 2 µM
DC002 – 4 µM
DC002 – 8 µM
DC002 – 16 µM
DC002 – 32 µM

2

A

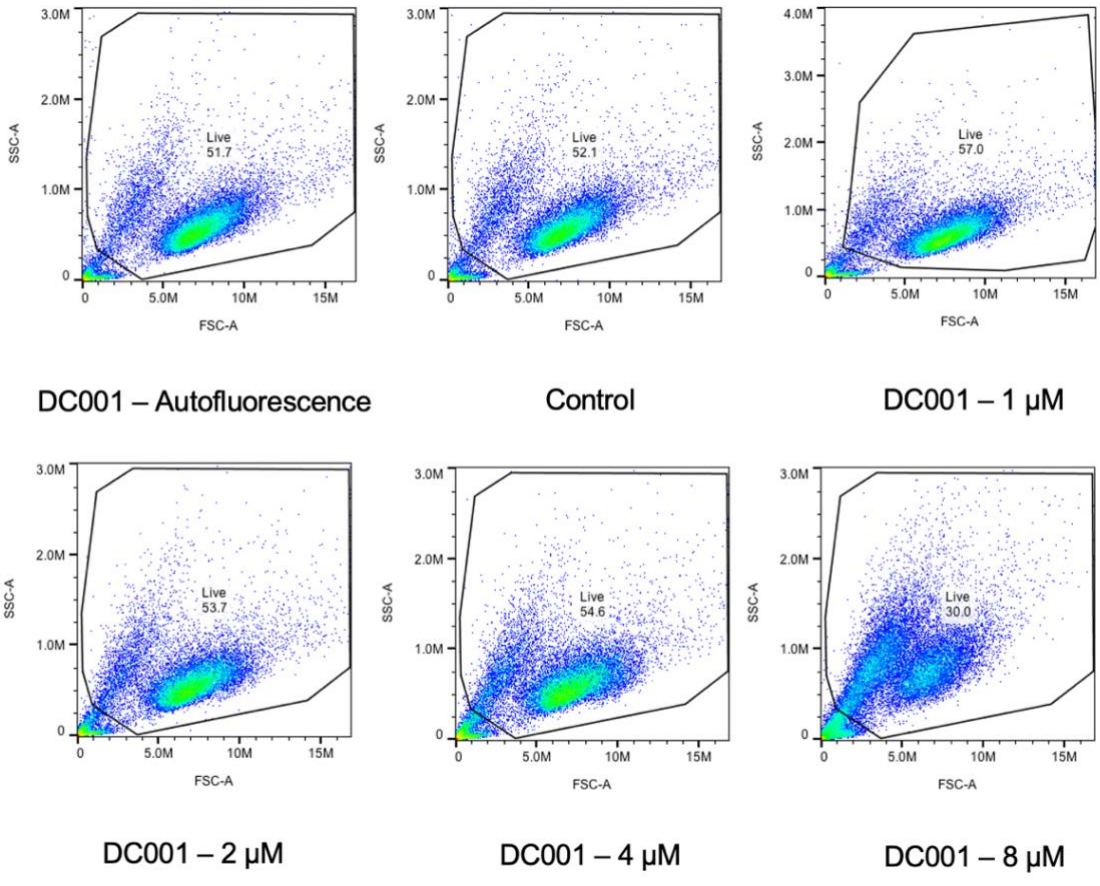
Live
51.7
Live
52.1
Live
57.0
Live
53.7
Live
54.6
Live
30.0
SSC-A
FSC-A
DC001 – Autofluorescence
Control
DC001 – 1 µM
DC001 – 2 µM
DC001 – 4 µM
DC001 – 8 µM

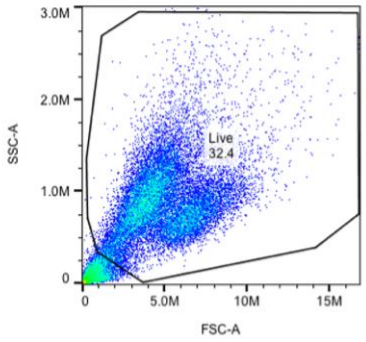

DC001 – 16 µM

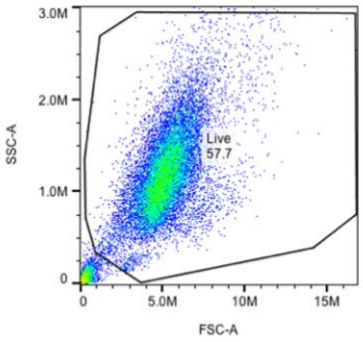

DC001 – 32 µM

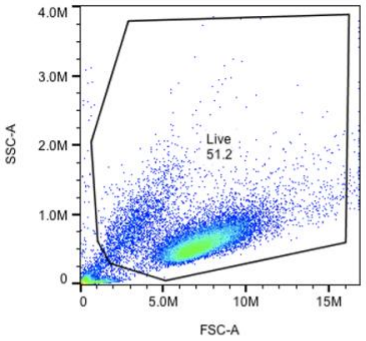

DC002 – Autofluorescence

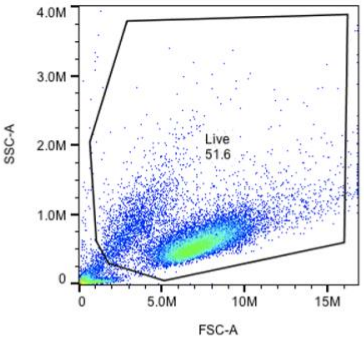

Control

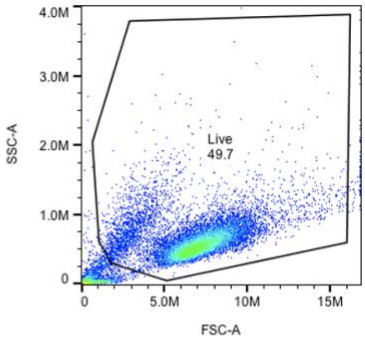

DC002 – 1 µM

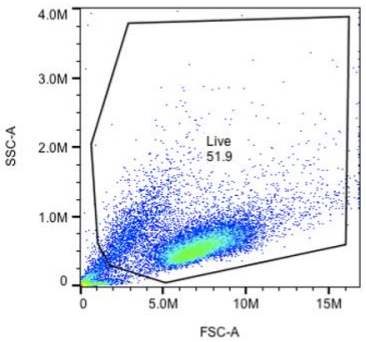

DC002 – 2 µM

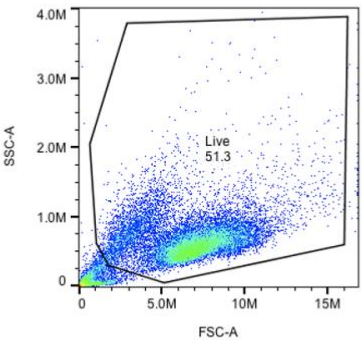

DC002 – 4 µM

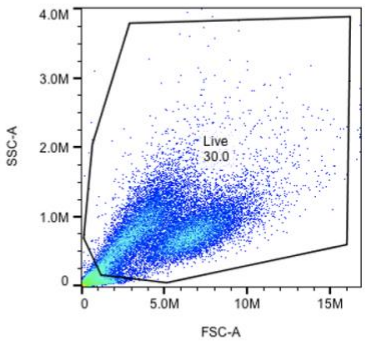

DC002 – 8 µM

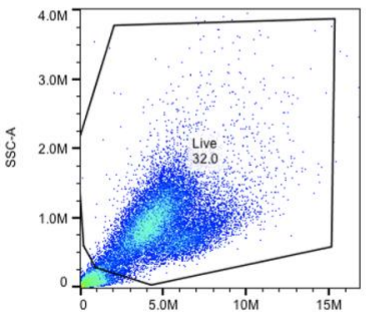

DC002 – 16 µM

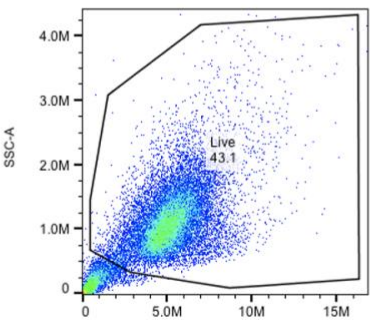

DC002 – 32 µM

B

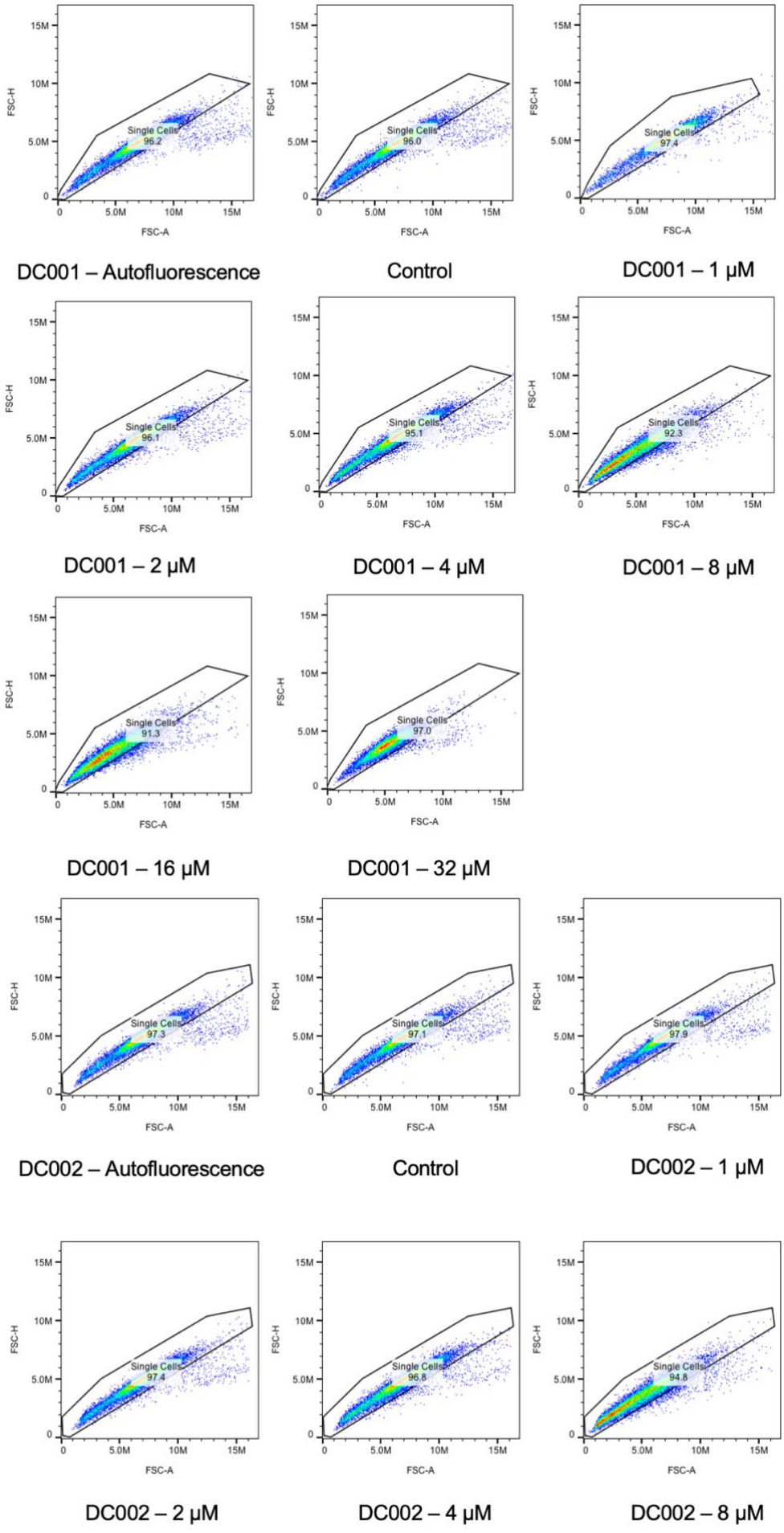
FSC-H
FSC-A
15M
10M
5.0M
0
5.0M
10M
15M
Single Cells
96.2
DC001 – Autofluorescence
Single Cells
96.0
Control
Single Cells
97.4
DC001 – 1 µM
Single Cells
96.1
DC001 – 2 µM
Single Cells
95.1
DC001 – 4 µM
Single Cells
92.3
DC001 – 8 µM
Single Cells
91.3
DC001 – 16 µM
Single Cells
97.0
DC001 – 32 µM
Single Cells
97.3
DC002 – Autofluorescence
Single Cells
97.1
Control
Single Cells
97.9
DC002 – 1 µM
Single Cells
97.4
DC002 – 2 µM
Single Cells
96.8
DC002 – 4 µM
Single Cells
94.8
DC002 – 8 µM

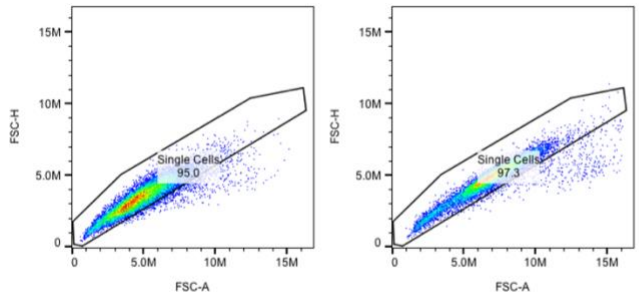

DC002 – 16 µM DC002 – 32 µM

C

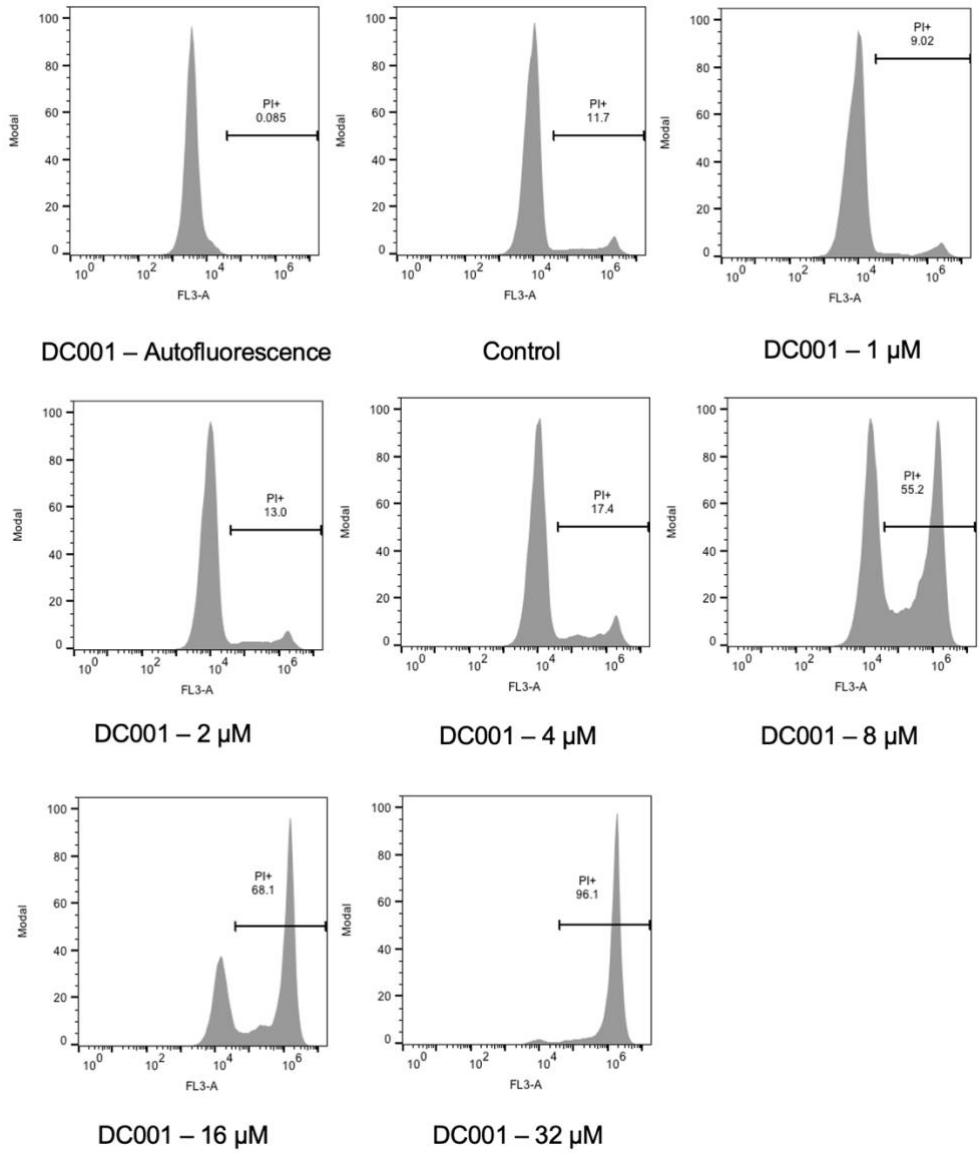

DC001 – Autofluorescence Control DC001 – 1 µM

DC001 – 2 µM DC001 – 4 µM DC001 – 8 µM

DC001 – 16 µM DC001 – 32 µM

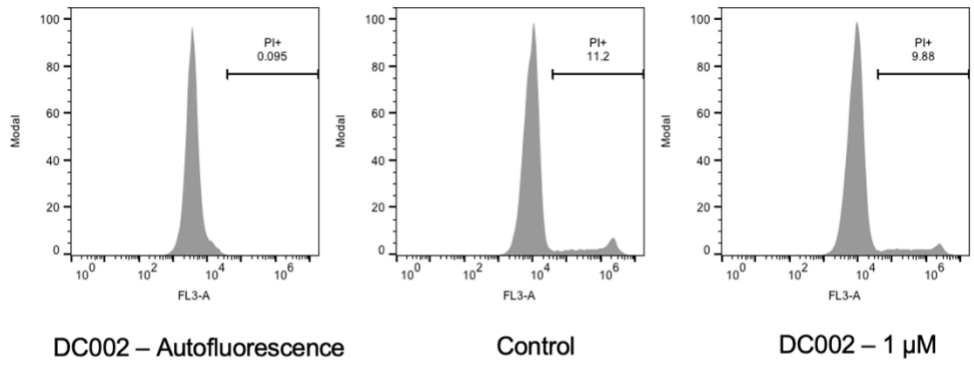

DC002 – Autofluorescence

Control

DC002 – 1 µM

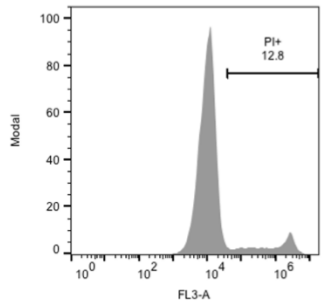

DC002 – 2 µM

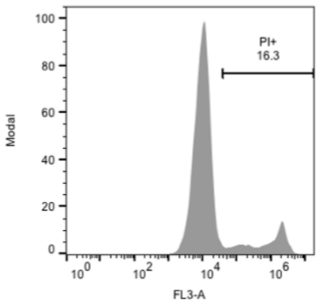

DC002 – 4 µM

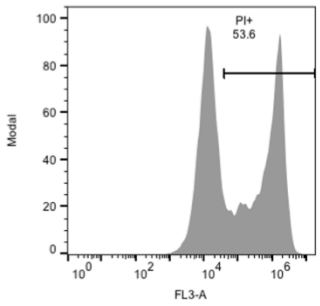

DC002 – 8 µM

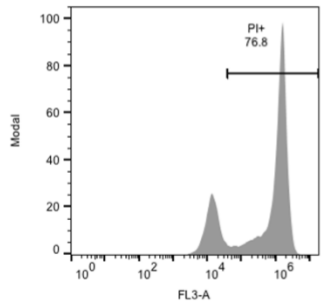

DC002 – 16 µM

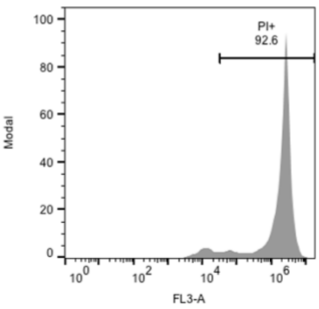

DC002 – 32 µM

3

A

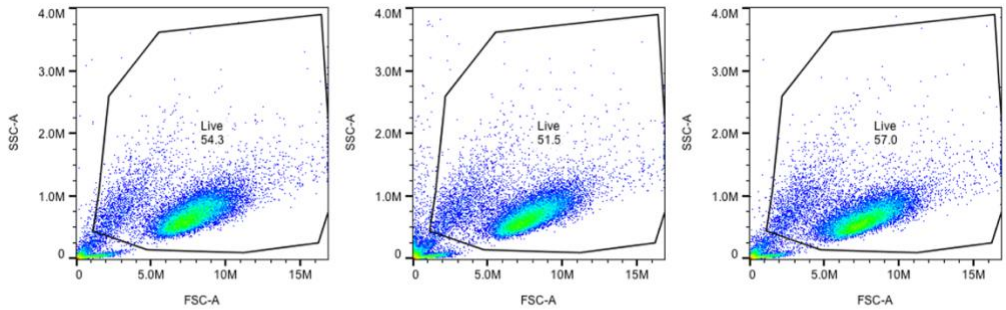

DC001 – Autofluorescence

Control

DC001 – 1 µM

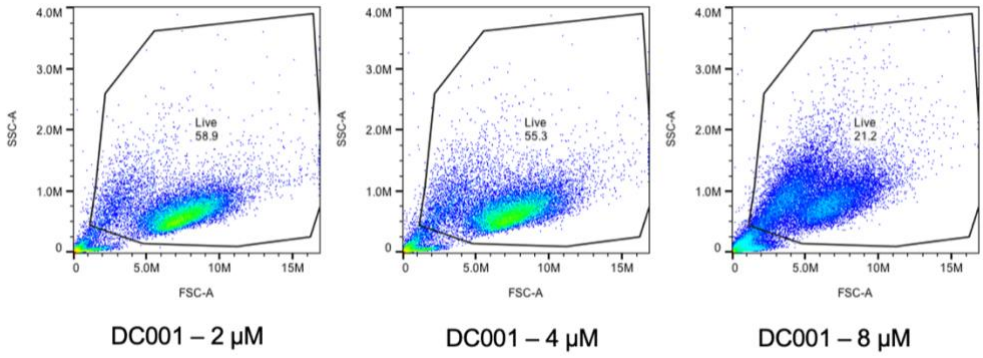

DC001 – 2 µM DC001 – 4 µM DC001 – 8 µM

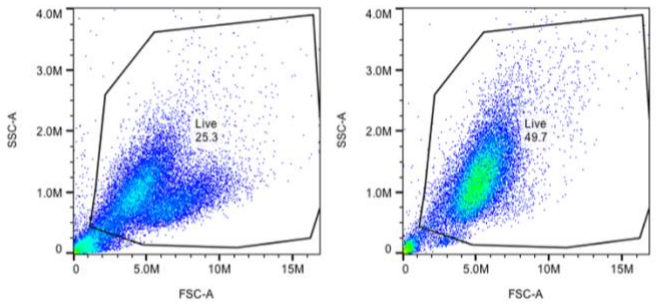

DC001 – 16 µM DC001 – 32 µM

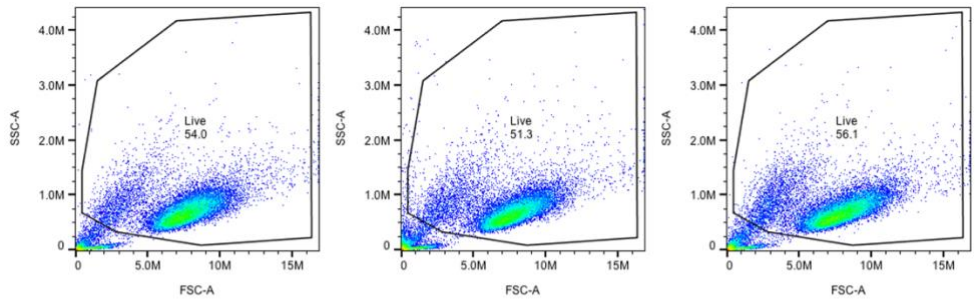

DC002 – Autofluorescence Control DC002 – 1 µM

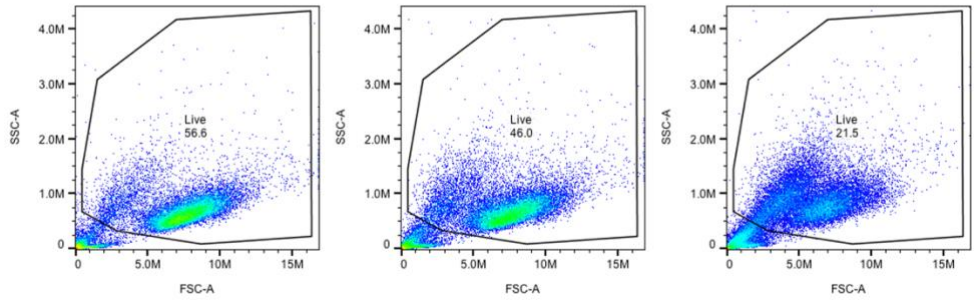

DC002 – 2 µM DC002 – 4 µM DC002 – 8 µM

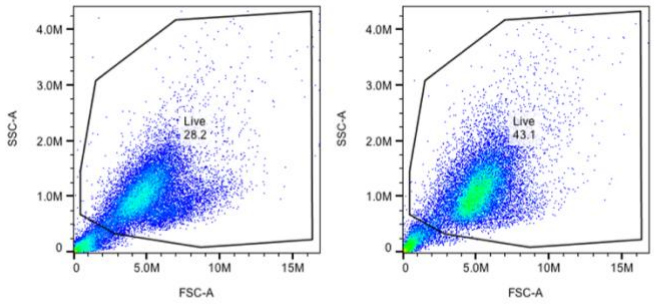

DC002 – 16 µM DC002 – 32 µM

B

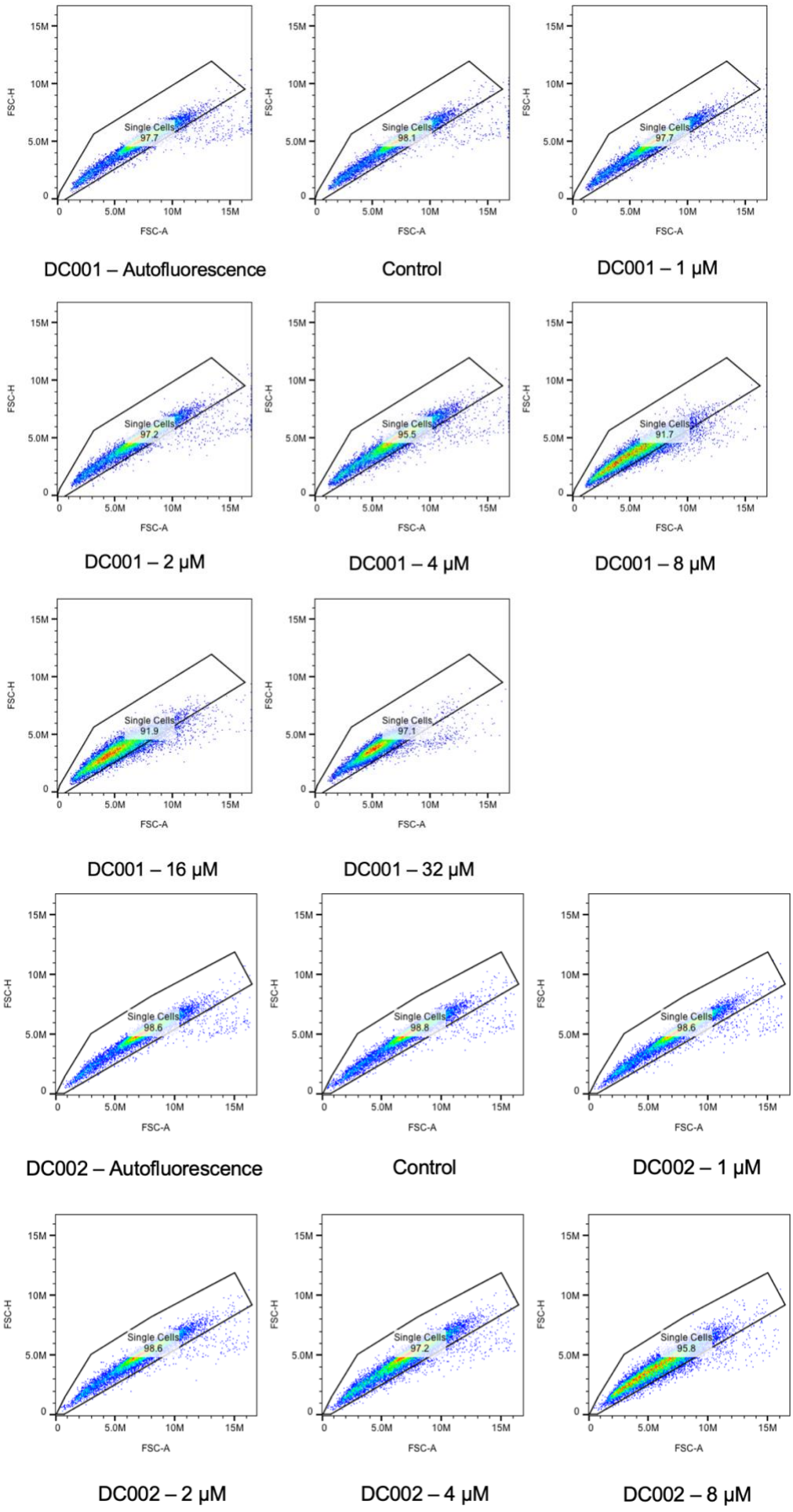
FSC-H
FSC-A
Single Cells
97.7
DC001 – Autofluorescence
98.1
Control
97.7
DC001 – 1 µM
97.2
DC001 – 2 µM
95.5
DC001 – 4 µM
91.7
DC001 – 8 µM
91.9
DC001 – 16 µM
97.1
DC001 – 32 µM
98.6
DC002 – Autofluorescence
98.8
Control
98.6
DC002 – 1 µM
98.6
DC002 – 2 µM
97.2
DC002 – 4 µM
95.8
DC002 – 8 µM

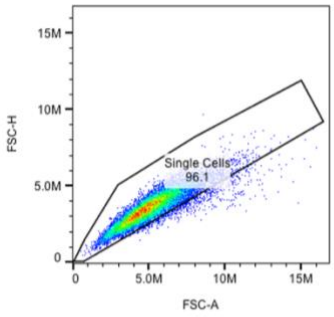

DC002 – 16 µM

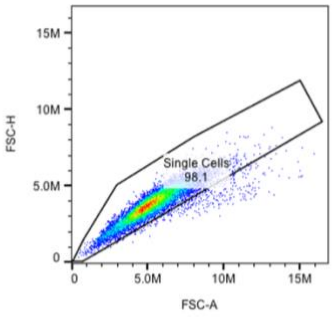

DC002 – 32 µM

C

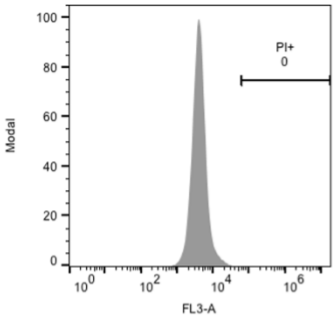

DC001 – Autofluorescence

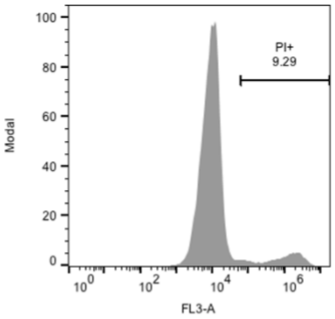

Control

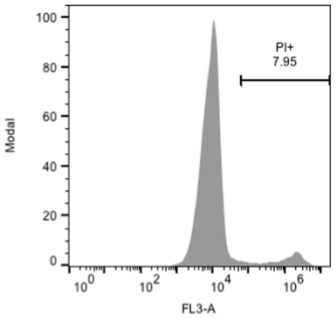

DC001 – 1 µM

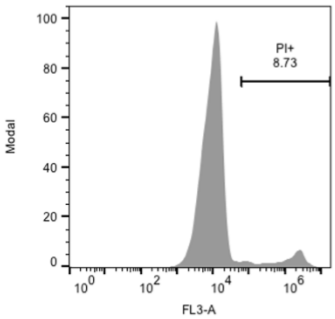

DC001 – 2 µM

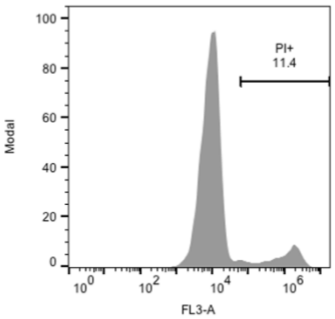

DC001 – 4 µM

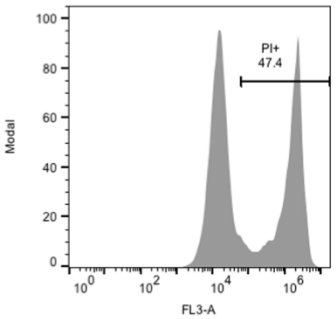

DC001 – 8 µM

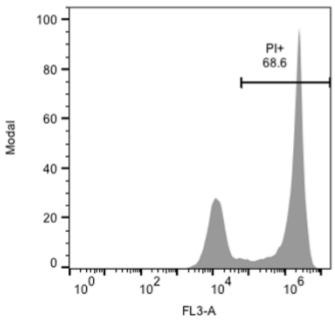

DC001 – 16 µM

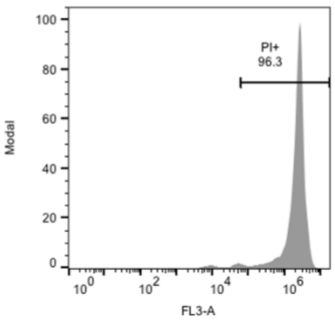

DC001 – 32 µM

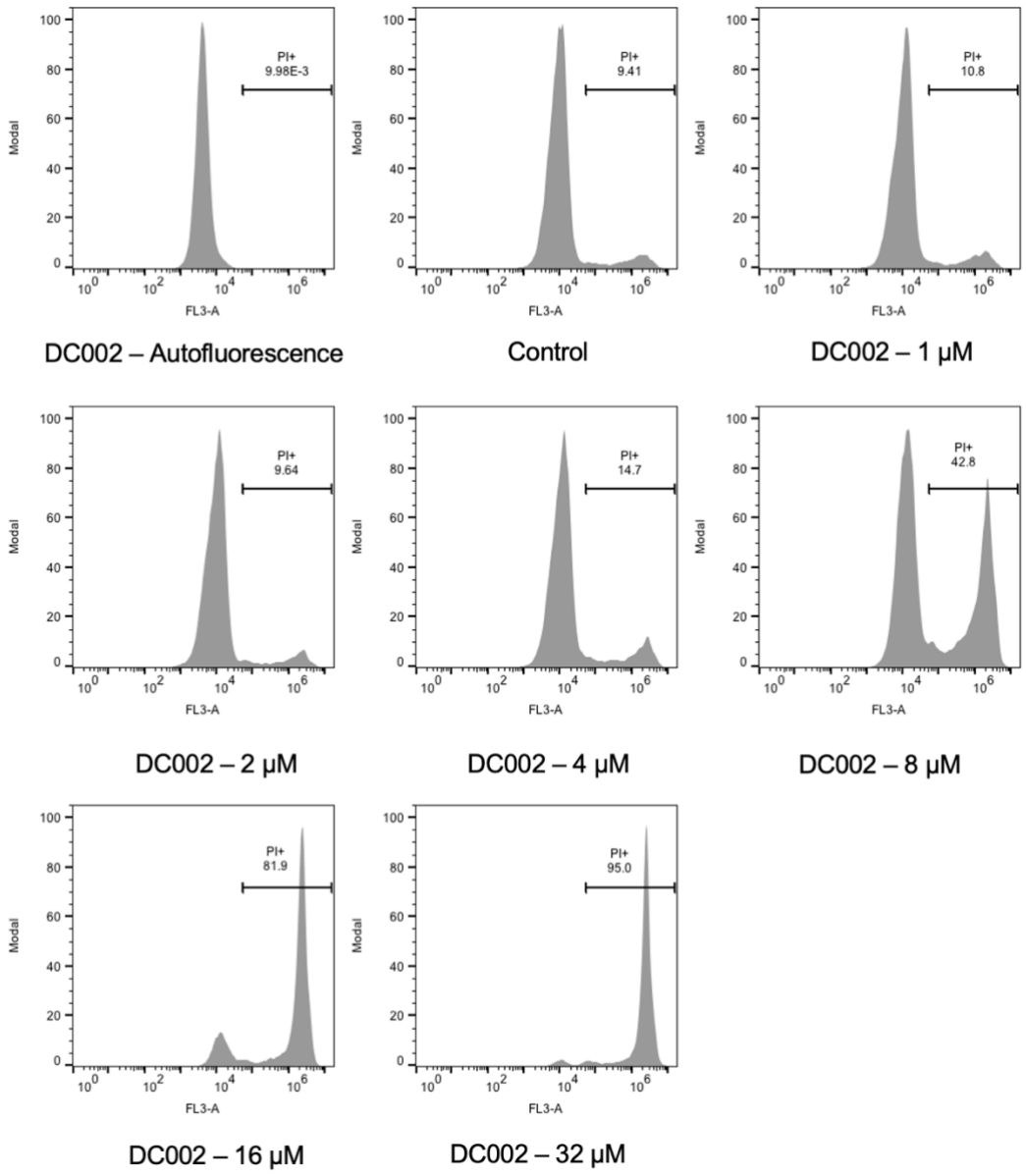

Figure S3 - Flow cytometry analysis of HeLa cells treated with DC001 and DC002. HeLa cells were incubated with several concentrations of the compounds for 16 hours in a 24-well plate and cells viability was measured by PI exclusion staining in three independent assays. **1** - Results from the first assay**; 2** - Results from the second assay**; 3** - Results from the third assay**.** (**A**) Live cells gated to remove the cell debris by creating a gate on the FSC versus SSC plots; (**B**) Live cells gated to remove doublets with FSC-A versus FSC-H plots, with singlets clustered diagonally; (**C**) Cells analyzed for PI fluorescence.